NOVEL REMEDIATION FOR BURIED PIPELINES UNDER GROUND DEFORMATION

By

Eziolu Ilozumba

A thesis submitted in partial fulfillment of the requirements for the degree of

Master of Science

in

Structural Engineering

Department of Civil and Environmental Engineering
University of Alberta

ABSTRACT

Buried pipeline systems often transverse regions with a wide variety of soil types, geological conditions, or regions of varying seismicity, exposing these buried infrastructures to severe geohazards that pose a significant amount of risk to their structural and mechanical integrity. The performance of these buried pipelines is a crucial engineering consideration in the oil and gas industry because its failure can cause severe risks to public safety and properties. Although pertinent efforts have been made to curb these pipeline incidents caused by abrupt ground movements, the existing solutions are deemed costly or inefficient.

This study focused on the development of an efficient mitigation method expected to address high construction or upgrade costs for buried pipelines undergoing ground deformation. This study proposed a novel mitigation technique that involves altering the boundary condition of buried pipelines with adjacently installed special geomaterial blocks (SGB). The proposed geomaterial involves a set of EPS geofoams and lightweight polypropylene squared plastic boxes designed to act as voids between the EPS geofoam blocks. The SGB was oriented such that the orthotropic mechanical property of these SGB allows the pipe to move laterally, accommodating a significant amount of ground deformation without developing significant reactions while reducing the ground-induced forces on the pipe. Firstly, the mitigation technique is first presented, followed by the experimental test program developed to evaluate the beneficial effects of the SGB on the local pipe response when subjected to lateral and oblique displacements. In addition, a simplified spring-based analytical modelling approach was proposed for predicting the force-displacement response of the pipe-SGB-soil assembly with emphasis on the interaction between the pipe and soil under the new boundary condition. The analytical model is validated using the experimental test data.

Secondly, six full-scale experimental test programs were developed to evaluate the beneficial effects of the SGB on the pipe response when subjected to lateral and oblique displacements; following these tests, a simple yet efficient finite element model was proposed to numerically simulate the pipe -SGB -soil interaction under lateral soil displacement. The result of the numerical model was validated using the data obtained from the experimental tests. The results of laboratory testing and numerical simulations confirm the efficiency of the proposed remediation technique in improving the structural integrity of buried pipelines.

PREFACE

All the research work presented for this thesis forms part of a research collaboration between the University of Alberta and ALFA Upgrades Inc. Edmonton, Alberta, Canada, with Dr. Ali Imanpour being the lead collaborator at the University of Alberta, and Dr.Ali Fathi being responsible for facilitation and acquisition of research funding at ALFA Upgrades Inc. Edmonton, Alberta, Canada.

The two introductory chapters in this thesis, i.e., Chapter 1 (Introduction) and Chapter 2 (Literature Review), are all my original work and include appropriate references as required.

The subsequent chapters (Chapter 3 and Chapter 4) are derived from research articles submitted for publication in the selected journal. Chapter 3 is derived from a paper submitted to the Journal of Pipeline Systems - Engineering and Practice: Ilozumba, E., Imanpour, A., Adeeb, S. and Fathi A. 2021. Novel Remediation For Buried Pipelines Under Ground Deformation: Cross-Sectional Testing And An Analytical Modelling Approach, Journal of Pipeline Systems - Engineering and Practice (under review). Chapter 4 is derived from a research article submitted to the Journal of Pipeline Systems - Engineering and Practice: Ilozumba, E., Imanpour, A., Adeeb, S. and Fathi A. 2021. Novel Remediation For Buried Pipelines Under Ground Deformation: Large-Scale Laboratory Testing And Numerical Modelling, Journal of Pipeline Systems - Engineering and Practice (under review).

I was the led investigator for the research conducted herein and, therefore, responsible for the data collection and analysis and manuscript composition. A. Fathi and I were responsible for the concept formulation. As the corresponding authors, A. Imanpour and S. Adeeb, were involved in concept improvement and manuscript editing. The authors included in this study provided extensive and resourceful technical input for methodology formulation and result validation.

E. Ilozumba

Dedicated with Love

To

My beautiful family; Dad, Mum, & my lovely siblings.

ACKNOWLEDGMENTS

To begin, I will like to thank the Almighty God, the maker of heaven and earth, the one who gives me life. Thank you, my heavenly father. It is only by Your grace, favour, and mercy that I achieved this feat. May all glory, honour, and adoration be ascribed unto Your Holy Name.

My deepest gratitude goes to my supervisor, Dr. Ali Imanpour, for his invaluable and consistent support, motivation, mentorship, and continuous availability to guide my steps throughout this academic journey. Sir, I am extremely grateful to you for your complete support, which has encouraged me always to strive to exceed expectations. I have been able to learn a lot under your supervision and tutelage. You made every problem and challenge seem easy, owing to your unending indomitable disposition. Thank you for your excellent mentorship in my academic and career endeavours, and thank you for always being so kind, understanding and patient.

In addition, my sincere appreciation also goes to Prof. Samer Adeeb for his intelligent direction, research insight and for investing his time and effort into making this research a success.

I would also like to appreciate the efforts of the industrial collaborator Dr. Ali Fathi for his technical advice, mentorship, and graciously encouraging me to produce a better version of this research work, which went a long way towards improving the quality of the academic publications produced from the study.

My sincere acknowledgement also goes to Dr. Onyekachi Ndubuaku of Stantec for his invaluable technical advice and guidance during the early stages of my research work.

Further thanks go to all my professors in the Structures group, Professor Robert Driver, Dr. Mustafa Gul, Dr. Carlos Cruz-Noguez, Dr. Yong Li and Dr. Douglas Tomlinson, whose masterly tutelage and invaluable academic insight have immensely contributed to my current academic achievements and, undoubtedly, to my future career accomplishments.

Many thanks also go to the highly cooperative and wonderful technicians at the I.F. Morrison Structural Engineering Laboratory, Greg Miller and Cameron West, for their constructive technical guidance and assistance, which enabled me to successfully carry out my series of laboratory tests, most especially the large-scale tests.

The research would not have been possible without the Natural Sciences and Engineering Research Council (NSERC) of Canada and ALFA Upgrades' financial supports. I am very grateful for funding my studies.

My heartfelt gratitude goes to all my friends and colleagues: Joshua Omolewa, Dominique Anekwe, Obumneke Okeke, Christopher Ilogu, Ikenna Aniobodo, Babalola Olabode, Oghenekioja Abele, Rajesh Kumar, Dilyara Tulegenova, Sylvester Agbo, Afaque Siddique, Palizi Mehrdad, Vahab Esmaeili, for all the happy conversations, joyful moments, moral and academic support you all were ever-willing to share.

I am also utterly thankful to my siblings; Chinasa Okafor, Usochi Ilozumba, Dr. Odichi Obodo, Mmadili Ilozumba and Ebubechukwu Ilozumba, for their encouragement, emotional and spiritual support. For your unending prayers and countless words of encouragement, I am very grateful.

Last but not least, to my ever-loving and ever-supportive parents, Arc. and Mrs. Callistus Ilozumba. You have invested all your time, sweat, and resources to provide me with the opportunities that have undoubtedly made it possible for me to be in this position. You held nothing back to ensure my siblings and I were given the best education and training. I can never thank you enough, and God knows I will forever be indebted to both of you for your endless love, care, constant prayers and dedication. I hope this degree makes you proud.

TABLE OF CONTENTS

LIST OF TABLES

LIST OF FIGURES

1 INTRODUCTION

1.1 INTRODUCTION

Buried steel pipeline systems are a preferable means to transport natural oil and gas and other materials from source to various consumption locations. A significant number of pipelines are installed such that they traverse a wide variety of soil types with varying geological conditions and seismicity. Due to these soil variations, pipeline networks may be exposed to geohazards, which pose a significant amount of risk to their structural and mechanical integrity, particularly in geological areas prone to landslides (or slope instabilities), fault fracture, earthquake-induced ground movements, urban excavation, soil liquefaction, and excessive ground settlement (Choo et al. 2007, Zhao et al. 2010). Fig. 1-1 shows an illustration of seismic faults and translational landslides that can affect pipeline networks.

(a)

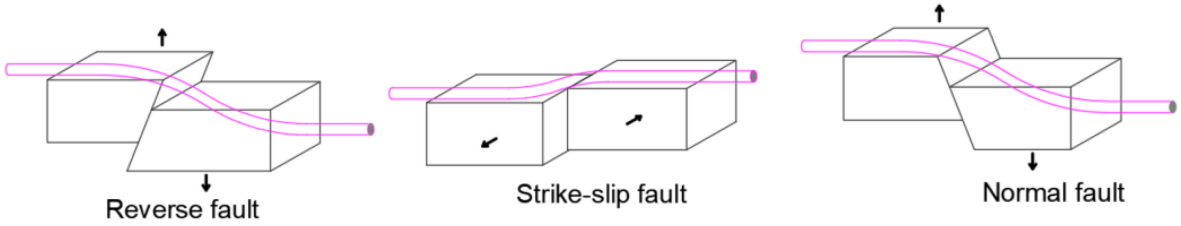

(b)

Figure 1- 1: (a) Seismic faults, (b) Slope instability or translational landslide (Highland & Bobrowsky 2008).

Transmission pipelines that traverse the regions susceptible to geohazards may experience large longitudinal bending strains caused by differential soil movement and plastic circumferential strain when the pipeline's alignment changes (Kennedy et al. 1977). This effect can be particularly troublesome because longitudinal strain concentrations near ground rupture zones strongly influence the yielding and post-yielding performance of buried pipelines. The strains generated by the ground movement are dependent upon several parameters, including the soil type, properties and geometry of the pipeline, soil-pipe interaction, properties and geometry of the backfill, differences in the properties between the backfill and the native soil, variability of the soil properties along the pipeline route, conditions of the pipe-soil interface, the orientation of the pipe to the differential soil movement and rate of loading between the pipeline and the soil (Choo et al. 2007, Han et al. 2012).

Modern pipeline design methods are primarily driven by the need to construct pipelines in the arctic regions, deep-water offshore, and other areas with a high probability of extensive ground motion. The loads imposed by these large ground motions due to landslides and seismic fault movement often exceed all other types of loads the pipeline may experience throughout its entire

lifecycle. In many cases, these ground movements induce large circumferential and axial strains in the pipe, which often may result in appreciable tensile stresses or compressive stresses, thus causing pipe wall local buckling or wrinkling on the compression side of the buckled pipe (Mahdavi et al. 2008, Wang et al. 2008, Zhang et al. 2017). Examples of pipe local buckling and tensile rupture are shown in Figs. 1-2a and 1-2b. Moreover, where the pipelines are subjected to concentrated ground movements such as those expected at the margins of a landslide or fault crossing (Fig. 1-1), a fracture can occur in the pipe due to high tensile or shear stresses (O'Rourke and Liu 1999).

Local buckling involves the deformation of a pipe cross-section, usually characterized by different features such as kinking and localized wall wrinkling. Karamanos et al. (2007) noted that local buckling (Fig. 1-2a) significantly reduces the fatigue resistance of the pipe due to the likelihood of high strain concentration around the buckled area. Following these wrinkles, pipelines may still be able to withstand all operational stresses and perform their transportation function adequately, provided that the pipeline possesses an adequate amount of residual ductility and no crack has been developed from the excessive wrinkling of the pipe walls. In the presence of high strain concentrations in the buckled areas, repeated loadings such as a change in the pipeline internal pressure can further reduce the fatigue resistance and burst capacity of pipelines (Ndubuaku 2019). Also, in the event of significant and drastic ground movements, the loads from such abrupt ground movements develop large plastic strains in the pipeline, sufficient to cause a tensile fracture, possibly leading to pipe leakage or rupture. Pipelines may also be subjected to high longitudinal stress or strain due to tension or bending or a combination of both. Under tensile longitudinal stress or strain, the primary integrity concern is the pipe girth weld's ability to withstand such significant stress or strain. If the tensile strain demand is higher than a girth weld's strain capacity, a leak or

rupture may occur at the girth weld's junction, as shown in Fig. 1-2b. The tensile strain capacity of onshore pipelines is typically controlled by the ability of the pipe girth welds to resist fracture when subjected to tensile stress and strains caused by geo-environmental loads (Agbo 2020).

(a) (b)

Figure 1- 2: a) Severe pipe local buckling formed at zero internal pressure, b) Girth weld tensile rupture (Wang et al. 2017).

Several cases of pipeline damage due to ground movements have been recorded around the world every year. For instance, the 1971 San Fernando earthquake caused by thrust faulting resulted in extensive damage to buried oil and gas lines, water mains and sewer lines (Vazouras et al. 2012). The pipelines were buried along the Glenoaks Boulevard at an angle with an active fault, and as the fault moved, the pipelines were subjected to an axial compression which led to pipe wall buckling and collapse of the buried lines. The San Fernando earthquake damaged three hundred miles of a 16 inch-diameter steel pipeline. Lam (2015) stated that 7% of pipeline failures in Canada are caused by earth movements, leading to intense explosions and loss of lives. In Europe, European Gas Pipeline Incident Data Group reported that from 2004 to 2013, slope instabilities

accounted for 85.2% of the geological disaster, which led to 13% of gas pipeline accidents (EGIG 2013).

Ground movements are sometimes slow-moving, which can be monitored and mitigated before a catastrophic failure. Otherwise, they can, however, be challenging to predict. Failure of onshore oil and gas pipelines can cause severe consequences, which in most circumstances, may lead to gas explosions resulting in loss of human life, industrial facilities, environmental damage, leading to significant economic losses due to the repair and replacement of failed pipelines (Farhadi and Wong 2014). In terms of property damage, Lockey and Young (2012) reported the cost of a 20 year-trend pipeline incidence in the United States. Their records indicated that between 2001 and 2020, the cost of significant pipeline incidents resulted in over 9.8 billion dollars in economic loss. Several techniques have been proposed in the past to mitigate the effects of ground movements on buried pipelines. These techniques include using a wide trench with soft backfill, the use of pipes with a lower diameter to thickness (D/t) ratio, slope stabilization, and periodic excavation and backfilling of pipes under slow but steady ground movement (Honegger et al. 2010). However, in developing the appropriate procedures to curb the hazards caused by these ground movements, the designer should consider the geotechnical conditions of the site, historical experiences, and tolerance levels of stresses and strains in the pipe welds.

1.2 PROBLEM STATEMENT

Buried pipelines transverse various geotechnical areas that involve seismic activities, landslides, adjacent earthworks, thaw settlement of permafrost, frost heave, or slope instabilities, which can create ground movements and, in turn, result in large lateral displacements on the pipe. As the soil moves relative to buried pipelines, the pipe is subjected to tensile or compressive stresses, causing excessive plastic deformations or local damages. Soil movement due to geological instability

typically occurs over time - ranging from a few hours to thousands of years - and dependent upon several factors, including soil stress level, environmental conditions, construction activities such as dredging and hydraulic forces such as waves (Lee 2012).

Approximately 50% of buried pipelines in Canada are laid in high-risk areas of unstable geological conditions to reduce the length of the pipeline route, and the construction costs Lam (2015). Each year, ground movements are responsible for a large number of pipeline failures in Canada and around the world as the pipes subjected to severe ground movements typically experience high longitudinal or circumferential strains, leading to pipe compressive buckle or tensile rupture. Various monitoring and mitigation techniques have been proposed and implemented to reduce the detrimental effects of ground movements on buried pipelines. These techniques include but are not limited to rerouting or relocation of pipelines around areas susceptible to severe ground movements, slope stabilization, use of high ductile steel (Choo et al. 2007, Highland and Bobrowsky 2008). However, these techniques may not necessarily offer a cost-effective and efficient solution for the majority of pipelines currently in service. For instance, the direct cost of relocating a 26 in-diameter natural gas pipeline subjected to landslide hazards was estimated to be 1 million dollars (Lam 2015). Additionally, the use of dredged material such as sand has been employed as a cost-efficient solution for backfilling pipelines. However, regardless of the type of material used as a backfill, the material stiffness between cohesive natural soil and backfilled material is highly significant, which may exacerbate the pipeline response when subjected to large ground movements (Paulin 1998). In view of a large number of cases where pipeline failures occur due to ground movement and its respective fatalities and economic losses, there is an urgent need to develop novel methods to effectively and economically mitigate displacements resulting from ground movements.

1.3 RESEARCH OBJECTIVES

This M.Sc. research project introduces a novel mitigation technique to improve the stability performance of buried pipelines when subjected to ground movements. The primary objective of this research is to develop a state-of-the-art remediation technique using adjacent-installed Special Geomaterial blocks (SGB) that target economic and efficient means of improving the stability response of buried pipelines when subjected to large lateral deformations caused by severe ground movements such as landslides or unstable slopes. The specific objectives of this research are:

- To understand the beneficial effects of using the SGB adjacent to the pipe.
- To evaluate the local response of pipe-SGB assembly consisting of a typical cross-section of a pipe and the SGB and quantify the influential effects on the SGB response.
- To analytically predict the response of pipe- SGB assembly.
- To assess the global response of buried steel pipelines equipped with the SGB to curb the horizontal ground displacements.
- To propose a simplified finite element approach to predict the response of buried steel pipelines equipped with the SGB.
- To propose design guidelines for the improvement of buried steel pipelines using the SGB.

1.4 RESEARCH METHODOLOGY

The objectives of this research project are achieved in six phases that are described below:

- The first phase involved a literature survey of the pre-existing mitigation techniques and discovering their existing shortcomings to form the basis for this research work.
- The second phase involved conducting a set of 25 cross-sectional tests involving a typical pipe cross-section and an SGB to evaluate the local response and interaction between pipe and soil

under the modified boundary condition. Various parameters, including the loading configurations and the interface frictional force between the SGB and sand, were studied. The loading configuration included transverse lateral and two oblique loadings with inclination angles of –27 and 27 degrees. Five different cover configurations were varied to assess the interface frictional force. The results were then used to determine the most efficient parameters for the SGB.

- Furtherance to the second phase, a simplified analytical model was developed to predict the force-displacement response of a pipe- SGB assembly. The model was then used to investigate the effects of different geometrical configurations of the SGB on the system response.
- A numerical finite element model of the pipe-SGB-soil was developed in the finite element program to evaluate the pipe response with and without the adjacent SGB. The results were then used to design the large-scale experimental test program and propose a simplified mathematical approach to predict the response of buried steel pipelines equipped with the SGB.
- The fifth phase involved six full-scale tests of an 8-in 6-m length of a non-pressurized steel pipe. The test programs were carried out to replicate pipelines located in an area subjected to lateral, upslope, and downslope landslide movements. The loading configurations mimicked the cross-sectional test described in Phase 2.
- The last phase involved developing guidelines for pipeline engineers to implement the new mitigation technique and numerically model pipelines equipped with the SGB.

1.5 ORGANIZATION OF THESIS

This thesis consists of five chapters. Chapter 1 provides an introduction to the thesis, including the background, problem statement, research objectives and methodology. Chapter two performs a

review of the literature on different failure modes due to ground movements, various types of landslides, common hazard scenarios caused by landslides, existing mitigation measures employed to mitigate ground movements in pipeline networks, and exiting numerical techniques for the soil-pipe interaction. Chapter three (first journal article) presents the cross-sectional test program along with the analytical formulation to determine the local response of a typical cross-sectional pipe when interacting with the soil and the SGB. Chapter four (second journal article) presents the large-scale experimental test program and the results obtained from the finite element analysis of the test specimens under lateral loading conditions. Furthermore, the benefits of applying the proposed mitigation technique and guidelines on the implementation of the mitigation technique in practice are provided. Chapter 5 provides a summary and conclusions of this research program and highlights recommended areas for further research works.

Chapters three and four include the main findings of the research project and have been submitted for publication as follows:

1) Ilozumba, E., Imanpour, A., Adeeb, S. and Fathi A. 2021. Novel Remediation For Buried Pipelines Under Ground Deformation: Cross-Sectional Testing And An Analytical Modelling Approach. ASCE Journal of Pipeline Systems - Engineering and Practice
2) Ilozumba, E., Imanpour, A., Adeeb, S. and Fathi A. 2021. Novel Remediation For Buried Pipelines Under Ground Deformation: Large-Scale Laboratory Testing And Numerical Modelling. ASCE Journal of Pipeline Systems - Engineering and Practice.

2. LITERATURE REVIEW

2.1 INTRODUCTION

This literature survey aims to report previous research works carried out on the effects of ground-induced actions on buried pipelines and provide the necessary background knowledge to guide this research. This review will cover failure modes of pipelines due to ground movements, pipeline design criteria, existing finite element simulation techniques for pipe-soil interactions, the key properties of geofoams and their applications, types of landslides, and existing mitigation techniques for buried pipelines.

2.2 PIPE FAILURE MODES DUE TO GROUND MOVEMENTS

The risks posed on buried pipelines are proportionally significant, especially pipelines which run transversely or parallel to unstable slopes or landslides, tectonic rupture, geotechnically active zones, or faults. The surrounding ground movements may significantly induce excessive deformations on pipelines, leading to a significant amount of strains in the pipe walls (Ferreira 2016, Ndubuaku et al. 2019, Cheng et al. 2019). Depending on the pipeline's relative orientation with respect to the ground movement, the failure modes of a continuous steel pipe with welded joints may involve combined axial tension and bending or axial compression and bending. These combined effects may ultimately lead to a pipeline failure either in the form of buckle or wrinkle caused by high compressive stresses, as shown in Fig. 2-1. In the presence of severe buckling of the pipe walls, post-buckling tensile rupture of the pipe wall (Fig. 1-2b) may also occur, especially at the welded regions resulting in oil and gas leakage and other environmental hazards (O'Rourke and Liu 1999). The key failure modes of buried pipelines expected due to ground movements are outlined below.

2.2.1 Compressive buckling

Past research studies on the buckling behaviour of oil and gas pipelines highlighted the harmful consequences that ground movements of surrounding soil medium may have on the mechanical and structural integrity of buried pipes. These movements are associated with unfavourable geological actions such as landslides, fault movements, slope failure, and tectonic rupture (Fathi and Cheng 2011). The structural instability of buried pipelines is evaluated based on their buckling behaviour which constitutes a more complex structural phenomenon, directly linking to its stiffness and the state of stress under which it is subjected (Ndubuaku 2019). Buckling failure is characterized by the loss of structural stiffness, which may occur before the onset of the material plasticization or in the plastic range of the material. When the compressive strain on the pipe wall exceeds the critical buckling strain, its instability occurs in the form of wrinkling or local buckling in the pipe wall. These resulting high compressive strains and curvatures in the pipe wall may often lead to circumferential cracking of the pipe walls and eventually leakage. As shown in Fig. 2-1a, local buckling is defined as a diamond-shaped inward and outward deformation of a pipe wall usually caused by a combination of bending, axial and torsional loads. In contrast, a pipe wall wrinkling, as shown in Fig. 2-1b, involves a smooth sinusoidal-shaped inward and outward deformation of a pipe's diameter over a finite arc of the pipe circumference (CSA Z662 2019).

(a) (b)

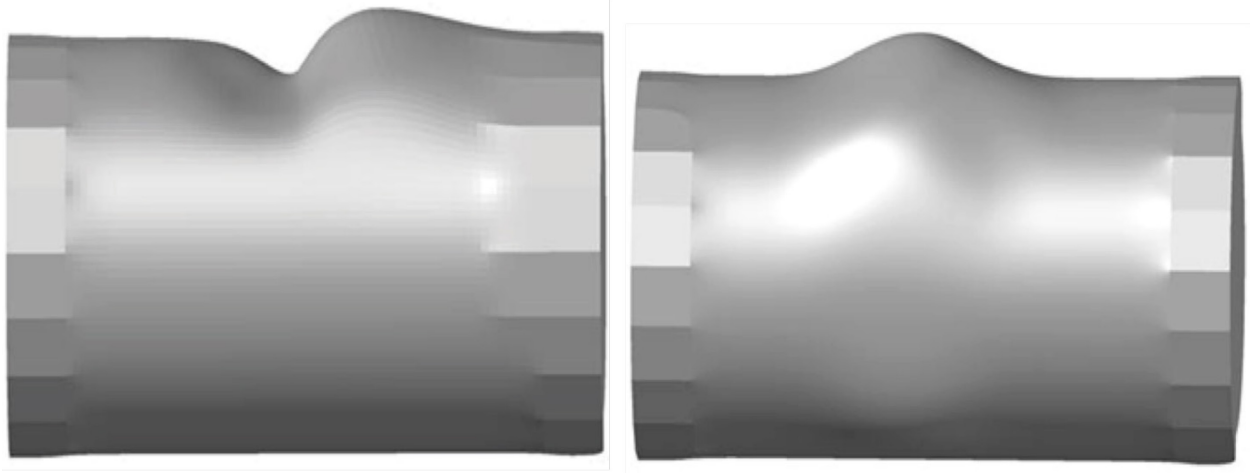

Figure 2- 1: a) Pipe buckle, b) Pipe wrinkle (CSA Z662 2019).

Local buckling is categorized as either a serviceability limit state or an ultimate limit state, depending on the buckling mode and the nature of the induced ground movement. However, it can progress to the global buckling of a pipeline due to excessive plastic deformation. Extensive research into axial compression and bending of steel pipes demonstrated that compressive strain limits for steel pipes depend on several factors, such as the presence of external or internal pressure, pipe yield stress, diameter-to-thickness ratio, *D/t,* as well as the initial imperfections and residual stresses. The Canadian design standard for Oil and gas pipeline systems CSA Z662 (CSA Z662 2019) considers a local buckle as a serviceability limit state at the start of the pipe deformation, which may progress to an ultimate limit state. As such, the code requires the critical local buckling compressive strains due to primary or secondary loads be limited to ε_c^{crit} initially proposed by (Gresnigt 1986):

$$\varepsilon_c^{crit} = \left\{ 0.5\,\frac{t}{D} - 0.0025 + 3000\left(\frac{f_p\,\sigma_y}{E}\right)^2 \right\} \qquad \text{if } f_p < 0.4 \qquad (1)$$

$$\varepsilon_c^{crit} = \left\{ 0.5\ \frac{t}{D} - 0.0025 + 3000\ \left(\frac{0.4\sigma_y}{E}\right)^2 \right\} \qquad \text{if}$$

$$f_p \geq 0.4 \tag{2}$$

in which f_p is the pressure fracture and can be obtained as follows:

$$f_p = \frac{(p_i - p_e)\, D}{2t\sigma_y} \tag{3}$$

σ_y is the material yield stress, t is the pipe wall thickness, D is the external pipe diameter, E is Young's modulus of the pipe material, p_i and p_e are internal and external pressure.

2.2.2 Tensile Failure

Modern pipeline design methods are primarily driven by the need to construct pipelines in the arctic regions, deep-water offshore, and other areas with a high probability of extensive ground motions. Pipelines subjected to these extreme ground motions may experience high longitudinal tensile or compressive stress/strains. The primary integrity concern in the design of a pipeline under tensile failure is the ability of the girth welds to resist fracture when subjected to a significant amount of axial tension and bending caused by operational and environmental loads. In turn, these loads may lead to the development of tensile strains in pipeline walls and even tensile fracture due to the excessive post-buckling formation of the wall segments of the pipe in the areas under large curvature due to bending caused by ground movements, as shown in Fig 2-2. The behaviour of girth weld flaws and the capacity of the girth weld determines the tensile strain limit to be considered in the design. Pipe tensile rupture is categorized as an ultimate limit state since it can lead to product or human losses. CSA Z662-19 aims at preventing this mode of pipeline failure by limiting the longitudinal tensile strain due to primary or secondary loads or a combination of both to the minimum strain requirement as follows:

$$Ø_{\varepsilon t}\ \varepsilon_t^{crit} \geq \varepsilon_{tf} \quad (4)$$

where $Ø_{\varepsilon t}$ is the resistance factor for tensile strain, ε_t^{crit} is the ultimate tensile strain capacity of the pipe wall or weldment, and ε_{tf} is the factored tensile strain in the longitudinal or hoop direction. The ultimate tensile strain capacity of the pipe wall or weldment ε_t^{crit} should be determined through full-scale testing.

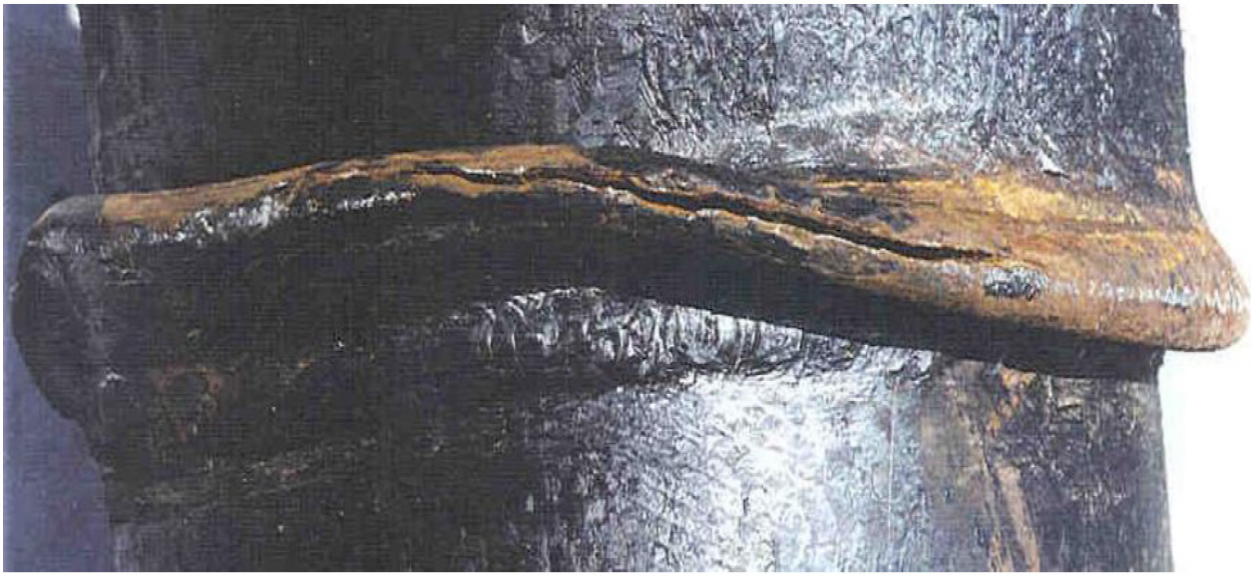

Figure 2- 1:Wrinkle formation near a girth weld and the resulting cracking of pipe wall at the apex of the wrinkle (Wang et al. 2017).

2.3 DESIGN OF BURIED PIPELINE SYSTEMS

With the increasing world populations and need for the production of products from oil and gas, pipeline networks are expected to expand, and the existing pipelines need to be upgraded and maintained for safe transportation of oil and gas. Therefore, many such pipelines inevitably transverse or will transverse regions that are geographically unstable or prone to seismic activities, landslides, ground subsidence or fault movements. Most modern design standards account for the

effects arising from such diverse conditions, which typically exceed the forces or deformations due to other types of loadings, such as operational loads that the pipeline may experience over its entire life cycle.

Most modern pipeline design codes use the concept of allowable stress limit, which aims to limit both the circumferential and longitudinal stresses in pipelines caused by either load-controlled or displacement-controlled loading conditions, which is an example of the loading conditions due to ground movements to a specified minimum yield strength of the pipe material (Liu et al. 2009, Ndubuaku et al. 2019). However, it is impractical to meet the allowable stress limit in conventional pipeline design because large ground movements can cause high longitudinal plastic strain deformation in the pipe beyond the strain range permitted by the allowable stress limits (Kan et al. 2018). Therefore, a strain-based design approach has been adopted by various pipeline design standards such as CSA Z662-19 in Canada and API RP 1111 (API RP 1111 2015) in the U.S. as a more realistic design approach that can well represent the anticipated response of the pipe under the applied displacements. The reason being ground movements are expected to induce high longitudinal plastic strains in the pipe, which the allowable stress design methodology may not well represent.

A strain-based design approach following the limit state design methodology or reliability-based design method can be considered for steel pipelines where the longitudinal strains induced under displacement-controlled conditions are evaluated and compared to the pipe strain capacity determined through full-scale testing. The key advantage of the strain-based design over the conventional allowable stress limit is the room for effective use of the pipeline longitudinal strain capacity rather than the stresses and allowing the pipe to plastically deform while maintaining the relevant ultimate and serviceability limit state considerations. To design for these limit states, it is

important to evaluate the magnitude of strain demands and strain capacity. The strain demand is the strain imposed on the pipeline by its operational and environmental conditions, while the strain capacity is the tolerable strain limit level beyond which a failure condition is reached.

For the design of pipelines expected to experience high longitudinal plastic strains caused by displacement-controlled environmental conditions, various pipeline design standards (e.g. ABS 2006, DNV-OS-F101 2010, API RP 1111 2015, CSA Z662 2019) require applying strain-based design as a complementary tool to the more conventional allowable stress design procedure because the former provides a more systematic approach to account for the effects of high longitudinal strains (Wang et al. 2014). The key design requirement of the strain-based design approach is to ensure the probability of failure is reduced to the nearest minimum between the pipe strain demand and strain capacity (Gioielli et al. 2007, Macia et al. 2010). The estimation of the strain demand in pipelines involves a rigorous and complex process that inclusively requires factors related to the pipe's mechanical properties, the variability of underneath soil properties and all other environmental conditions. The level of complexity in predicting the strain demand may range from a relatively simple deterministic approach that involves a conservative estimate of the strain demand to a full reliability-based design approach. However, the evaluation of the strain capacity is essentially based on the pipe's mechanical resistance (Ndubuaku et al. 2019). Finally, the ultimate and serviceability limit state design should be carried out to ensure that the pipeline remains safe against any factors such as pipe buckling or rupture that may hinder its proper operation.

2.4 NUMERICAL SIMULATION OF SOIL-PIPE INTERACTION

Over the last few decades, several numerical and analytical studies have been undertaken to investigate the response of buried pipelines subjected to ground movements. Some of the key studies performed to predict the response of pipes subjected to ground motions are summarized here.

2.4.1. Newmark and Hall (1975)

Newmark and Hall's pioneering work was the first to develop the procedure to analyze the effect of fault movements on a pipeline. They developed a simplified analytical model for calculating the tensile strains on pipelines with the assumption that the most critical situation would arise when the pipe is predominantly subject to tensile force under large displacement due to fault movements. In the method, the small deflection theory was used for estimating the strains along the pipe length by relating the soil slip friction on the pipe to the passive soil pressure at rest, which is uniformly distributed around the pipe perimeter. Consequently, the pipe was modelled as a cable in which the pipe bending stiffness and the lateral interaction are ignored. This model assumed that the pipeline would be subjected to direct tension due to the fault motion and hence assumes failure from tension. They found that resistance of the buried pipeline to relative fault movement depends on the soil characteristics, crossing angle, slip length, and pipe ductility. This model is only suitable for buried pipelines subjected primarily to only tensile strains, and the lateral resistance of the soil was ignored.

2.4.2. Kennedy et al. (1977)

Kennedy et al. extended the work by Newmark and Hall (1975) to determine the capacity of a pipe to resist fault movement by considering the uniform passive soil pressure and the concept of large deflection theory. They took into account soil-pipe interaction in the transverse and longitudinal directions. A schematic diagram of the buried pipe movement resulting from horizontal fault displacement used in this work is shown in Fig. 2.3. It was assumed that the pipe would deform between an anchorage point and the point of relative ground offset for simplicity and that the pipe segment near the abrupt ground deformation deformed in the form of a flexible cable into a single constant curvature with no flexural resistance, thus leading to the overestimation of the bending strains of pipelines. In this model, lateral forces on the pipe were supported by axial tension acting

through the longitudinal pipe curvature. Therefore, the pipeline can accurately be analyzed as if it has only axial stiffness. They also analyzed the relationship between axial force and bending moment and concluded that the concept of constant curvature is required to determine the axial force in a pipe segment, provided that the bending strain is less than 80% of the axial strain. In their model, when evaluating the longitudinal strain effects due to fault movement, the pipe curvature remains essentially constant throughout the zone of relative displacement, and only axial tensile force at the inflection points is considered for equilibrium. Ramberg-Osgood relationship (1943) was used to account for material nonlinearity (Equation 2.5).

$$\varepsilon = \left(\frac{\sigma}{E}\right)\left[1+\left(\frac{n}{r+1}\right)\left(\frac{|\sigma|}{\sigma_y}\right)^{r}\right] \qquad (2\text{-}5)$$

Where σ is longitudinal stress at any point, ε is longitudinal pipe strain, σ_y is yield stress of pipe material, and r are Ramberg- Osgood coefficients.

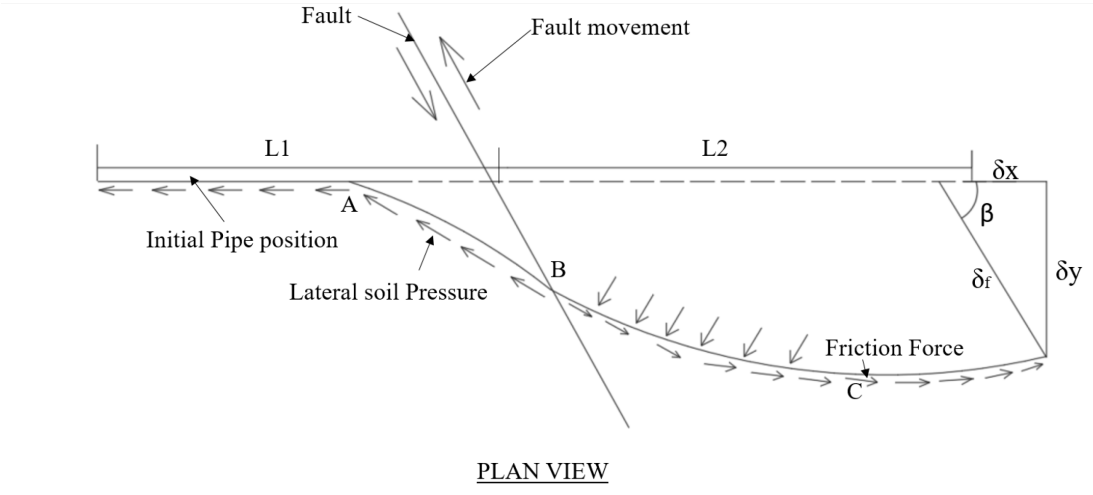

Figure 2- 2:Schematic diagram of buried pipe movement due to horizontal fault motion (modified from Kennedy et al. 1977).

2.4.3. Wang and Yeh (1985)

Wang and Yeh (1985) improved this model proposed by Kennedy et al. (1977) for any buried pipeline across any strike-slip fault that may cause tension or compression failure of a pipeline. They incorporated the shear stiffness at the point of inflection of the curved pipe crossing the fault zone and the bending stiffness of the pipe segment closest to the abrupt ground displacement. The concept of a semi-infinite beam on an elastic foundation was incorporated in this model. A schematic representation of their model is shown in Fig. 2-4. The pipe segments (CB and DE) away from the abrupt ground deformation are modelled based on the concept of beams on an elastic foundation, while the pipe segments (AB and AD) within the fault crossing zone are assumed to behave as a cable with constant curvature. To satisfy the force equilibrium concept, bending moments and shear forces transmitted from the pipe segments away from the fault were considered. Notwithstanding, the flexural rigidity of the pipe segments and the nonlinearity of the pipe material within the fault crossing zones were considered in the model. It was found that the critical locations are the segments within the fault zone. Moreover, bending strains were underestimated due to the unfavourable contribution of axial forces on the flexural rigidity of the pipeline.

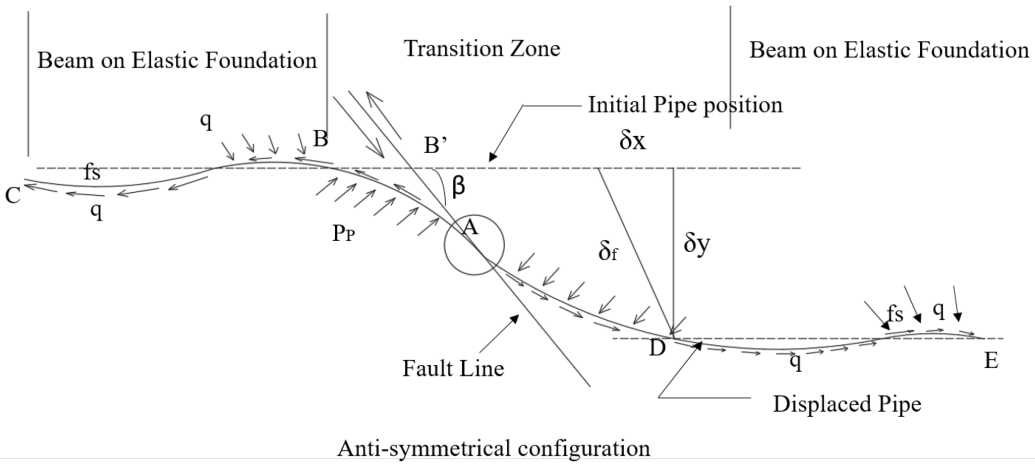

Figure 2- 3: Analytical model for buried pipeline subjected to large strike-slip fault movement (modified from Wang and Yeh 1985).

2.4.4. Karamitros et al. (2007)

Karamitros et al. (2007) refined the methodologies presented above by proposing an analytical method for computing the pipeline axial force and bending moments. In this model, the equations proposed by Kennedy et al. (1977) were employed to evaluate the effect of axial force on the pipeline curvature. Furthermore, as proposed by Wang and Yeh (1985), the pipeline was divided into four segments, and a beam on an elastic foundation was used to analyze the pipe segments away from the abrupt ground deformation to determine shear and bending in the pipe. These researchers considered the material nonlinearities and second-order (or geometrical) effects calculated based on the constant curvature assumption for the pipe segment within the fault zone for relatively large pipe deformations. Compared to previous analytical methods, the actual stress-strain distribution at a pipe cross-section was accounted for in this model by quantifying the interaction of the axial-bending strain.

Given the limitations of the simplified analytical solutions and the advancement of computational simulations in the past years, numerous numerical finite element modelling techniques have been employed to investigate the stability response of buried pipelines when subjected to large ground-

induced actions by considering the nonlinear soil behaviour and the interaction between the surrounding soil and pipe. A three-dimensional (3D) finite element was developed by Karamitros et al. (2007). The model is shown in Fig. 2-5a accounts for the pipe-soil interaction using a set of axial and transverse nonlinear soil springs to model the surrounding soil and shell elements. The proposed predictive model was then compared with other existing methodologies and finite element models. The result of the comparison on the axial strain of the pipe is shown in Fig. 2-5b, which confirms that the analytical model can well predict pipe strains.

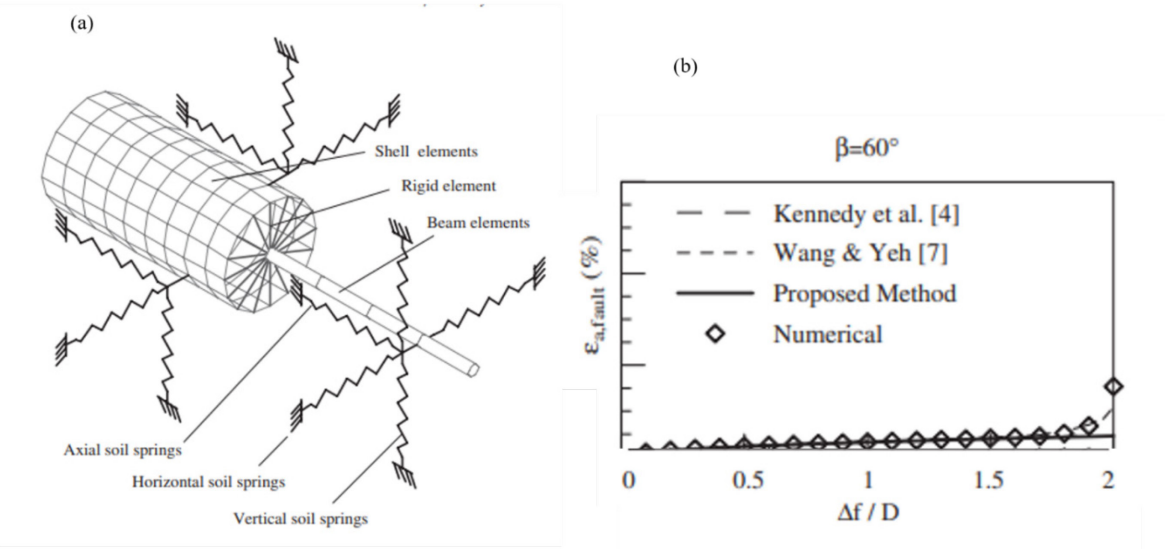

Figure 2- 4: a) 3D finite element model; b) comparison of the result of axial strain with existing models (Karamitros et al. 2007).

2.4.5. Liu et al. (2008)

Following the simplified 2D models used in the existing analytical expressions, Liu et al. (2008) employed a 3D finite element simulation model to capture the cross-sectional deformation behaviour of buried pipelines resulting from induced ground displacement. They investigated the effect of fault intersection angle on a pipe's axial strain. A total of 100-m pipe segments at the fault trace was modelled using the commercial ABAQUS software. The pipe was modelled with 24 sets

of bi-linear shell elements around the pipe circumference. The surrounding soil medium around the pipe was modelled using a set of spring elements defined in axial, horizontal, and vertical directions. The fault movement was applied at the free end of the soil springs. Their investigation concluded that the fault movement creates a localized axial strain around the pipe segment close to the fault zone. Also, it was found that the pipe is under tension at a low intersection angle, and the pipe compressive strain becomes maximum at the 90°intersection angle.

2.4.6. Fathi et al. (2018)

Fathi et al. (2018) used the Abaqus finite element program to simulate the pipe behaviour under large compressive deformations. Their model aimed at developing a new approach to reduce the compressive axial force on buried pipelines while enabling the pipeline to fail under a stable global buckling mode. The pipe body was modelled using beam elements PIPE31. The internal pressure applied in the pipe was equal to 40% of the pipe SMYS (specified minimum yield strength). The loads and boundary conditions used in the model are shown in Fig. 2-6. Conventional soil springs and OBF elements were defined to simulate the lateral stiffness based on the average measurement collected from their cross-sectional test. The OBF elements have an orthotropic mechanical property that enables them to resist the backfill weight while accommodating axial deformations due to lateral pipe movement. The OBF elements were then incorporated in the design to modify the pipe boundary condition as it undergoes a full global buckling mode by maintaining the compressive strain of the pipe under the critical buckling strain along the entire deformed pipe length. The model used to validate the global compression tests was extended to simulate pipe-soil-OBF element interactions under different pipe sizes and backfill conditions. The result showed that under the modified boundary condition, the pipe compressive strain could potentially reach 0.4% - 0.5% while remaining stable throughout the entire length.

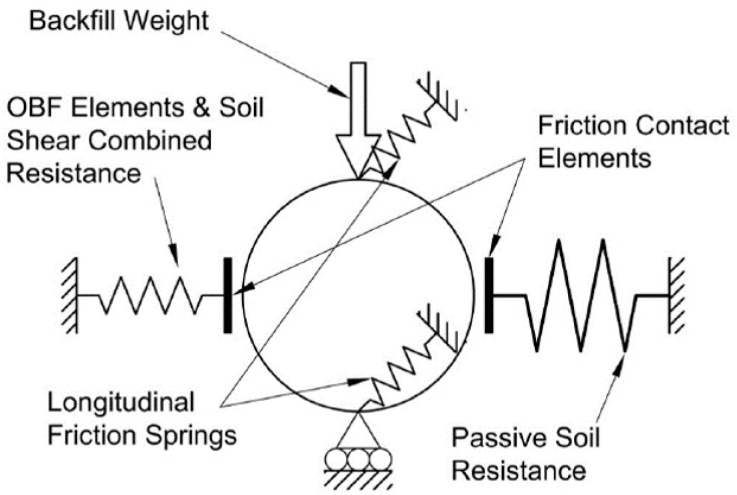

Figure 2- 5: Cross-section of proposed pipe model by Fathi et al. (2018).

2.5 GEOFOAMS: MECHANICAL PROPERTIES AND APPLICATIONS IN THE PIPELINE INDUSTRY

An innovative element referred to as Special Geomaterial Blocks (SGB) is proposed in this study to be used adjacent to the pipe to mitigate displacements induced in buried pipelines by ground movements. This section is devoted to the mechanical properties and application of geofoams used in the proposed SGB.

The SGB encased in a corrugated plastic sheet comprises a set of Expanded PolyStyrene (EPS) geofoam and polypropylene squared plastic boxes shown in Fig. 2-7. The EPS geofoams, which are the primary source of the load-bearing capacity of the SGB system, are a low-density lightweight plastic cellular geosynthetic material (Athanasopoulos et al. 1999, Lingwall 2011). A finite amount of resin basin is first produced through a polymerization process that involves pentane and a fire retardant, forming a modified resin basin during the manufacturing process of EPS geofoams. The modified resin basins are then pre-puffed by the injection of steams that softens the polymers. The second process involves block moulding some amounts of pre-puff beads by steam heating in a tightly closed steel-walled mould. The heating steam further causes the beads to expand and fuse to

form EPS geofoam blocks. These blocks are manufactured following the specifications of ASTM D6817 (ASTM D6817 2013). The standard density of EPS geofoams typically range from 11 to 48 kg/m^3. The density of EPS in kg/m^3 is used as the designation of the geofoam block. For instance, EPS19 represents EPS geofoam with a nominal density of 19 kg/m^3.

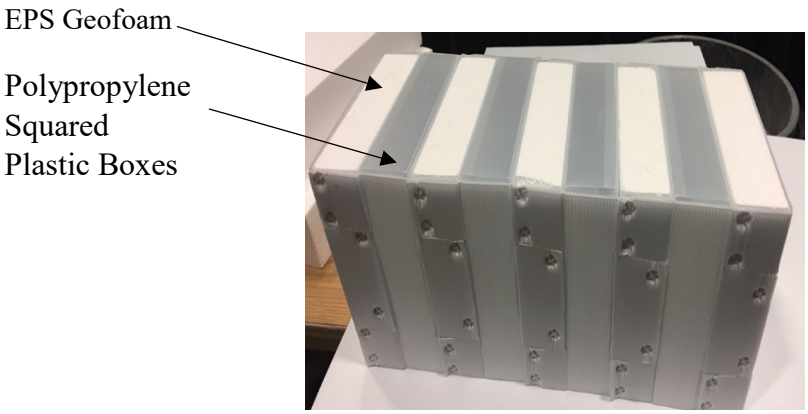

Figure 2- 6: Special Geomaterial Blocks (SGB).

Extensive laboratory testing on the material properties of EPS geofoam has been investigated. Hazarika (2006) studied the stress-strain properties of EPS geofoam for large-strain applications. A series of unconfined compression tests were performed on different sizes of EPS geofoam with two different nominal densities of 16 and 20 kg/m^3. It was shown that the behaviour of EPS geofoam blocks in compression is a function of the strain rate, specimen size, and density of the EPS geofoam block. The stress – strain response of the geofoam blocks shown in Fig. 2-8 shows that EPS geofoam is highly nonlinear with a small elastic range of approximately 0 to 2% of the compressive axial strain. Negussey (2006) found that the Young's modulus of EPS geofoam is approximately 10 MPa for ESP19 and is greater for higher EPS densities.

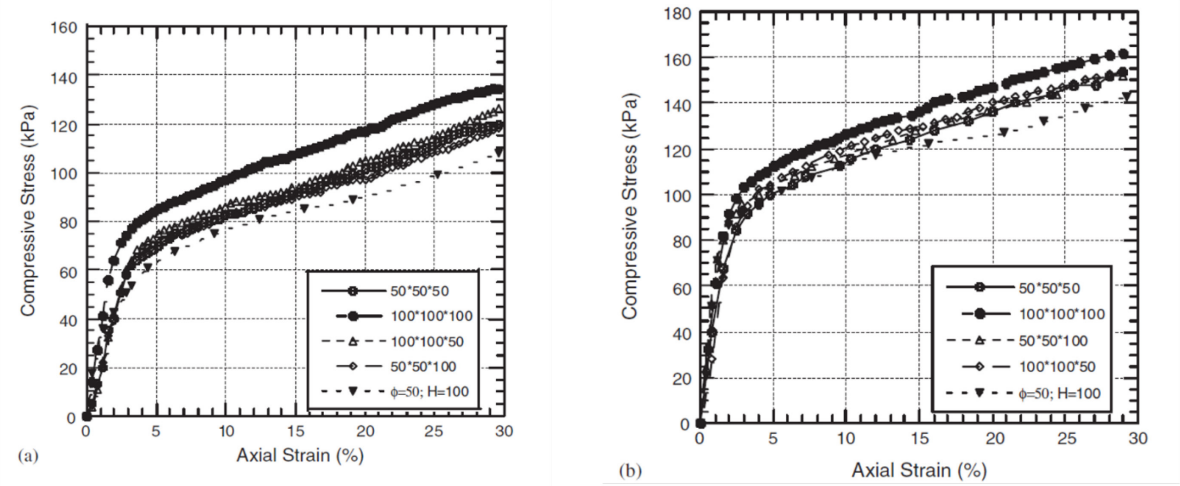

Figure 2- 7: Stress – strain behaviour of geofoams: a) EPS16; b) EPS 20 (Hazarika 2006).

EPS geofoam blocks have been receiving increasing attention in civil engineering construction projects due to their low density and lightweight properties. It has been used in various civil infrastructure projects as shown in Fig. 2-9, such as slope stabilization, earth retaining structures, and abutments to reduce the vertical and horizontal stresses induced on buried structures such as pipelines and culverts (Horvath 1997, Sheeley et al. 2001, Hazarika 2006, Lingwall 2011, Beju and Mandal 2017). The first use of EPS geofoam started as far as 1975 in Norway and has been adopted worldwide. The first geofoam application in Norway was undertaken to reconstruct road embankment projects adjacent to a bridge (Aabøe 1996, D. Negussey 2006). Furthermore, this lightweight fill has been used to reduce the settlements caused by geotechnical loads and its potential damage to adjacent structures. Due to its extremely lightweight, which is approximately 1% the weight of soil, and cellular nature, EPS geofoam blocks are not significantly compressible under typical geotechnical loads encountered in most field applications. Thus, making the geofoam blocks suitable for use as a compression inclusion.

(a) (b)

(c) (d)

Figure 2- 8: Applications of EPS geofoam: a) buried pipelines; b) abutment backfill; c) stadium and theatre seating; d) roadway construction (EPS Industry Alliance 2012).

The interface frictional properties for geofoam-soil and geofoam-structure interactions have been investigated by Athanasopoulos et al. (1999) and Sheeley et al. (2001). Very little research has been carried out to investigate the use of ESP geofoam as a mitigation technique for reducing stresses induced on a buried pipeline by ground movements. Yoshizaki and Sakanoue (2003), Choo et al. (2007), and Bartlett and Lingwall (2014) investigated the application of EPS geofoams as a cover system to control the lateral force induced in buried pipelines under a given displacement

when subjected to fault movements. Full-scale experimental tests were conducted on a 100mm steel pipeline under horizontal pipe displacements in a deep trench box using conventional sand cover and geofoam cover systems. No geofoam was placed along the pipe sides; rather, it was placed as a lightweight cover to reduce vertical loads. The pipe was horizontally displaced at a maximum displacement of 150 mm using a hydraulic jack, and the force – displacement response was measured to evaluate the soil-pipe interaction in the horizontal direction (Yoshizaki and Sakanoue 2003). The peak horizontal force was reduced by approximately 33 to 60% for the geofoam cover systems compared with a typical sand cover (Fig. 2-10).

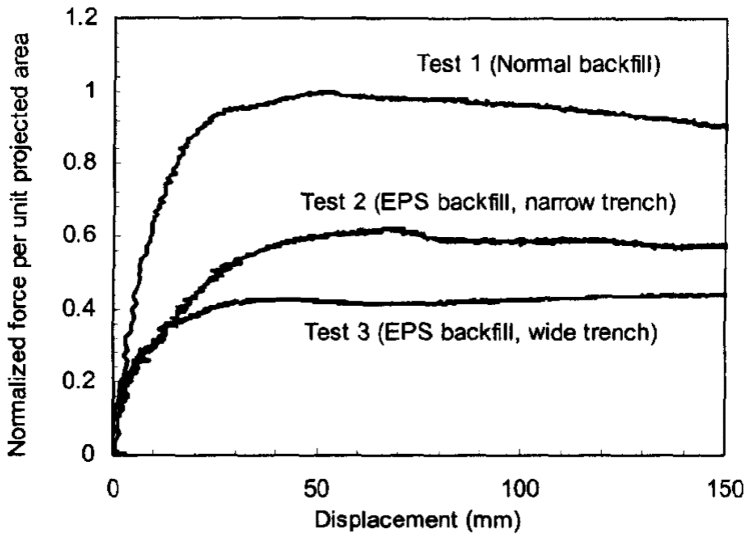

Figure 2- 9: Normalized force – displacement response for pipe undergoing horizontal displacement (Yoshizaki and Sakanoue 2003).

Choo et al. (2007) performed 12 centrifuge testing to evaluate the benefits of reducing stresses on high-density polyethylene (HDPE) pipe undergoing vertical offset using EPS geofoam. They varied the pipe orientation to the fault line to examine various horizontal offsets (Fig. 2-11). The remediation strategy was intended to reduce the lateral soil – structure interaction force attracted

by the pipe. This study showed the benefits of using EPS geofoam for lightweight cover application, but the compressible inclusion effects of geofoam cover in reducing pipe stresses were not explicitly studied. However, the peak lateral force at the soil-pipe interface was reduced by 80 – 90%, depending on the placement of the geofoam block with respect to the fault line. The reduction in the lateral force led to a 45 – 60% reduction in the bending strain and a 30% reduction in axial strain when compared to the systems without EPS remediation.

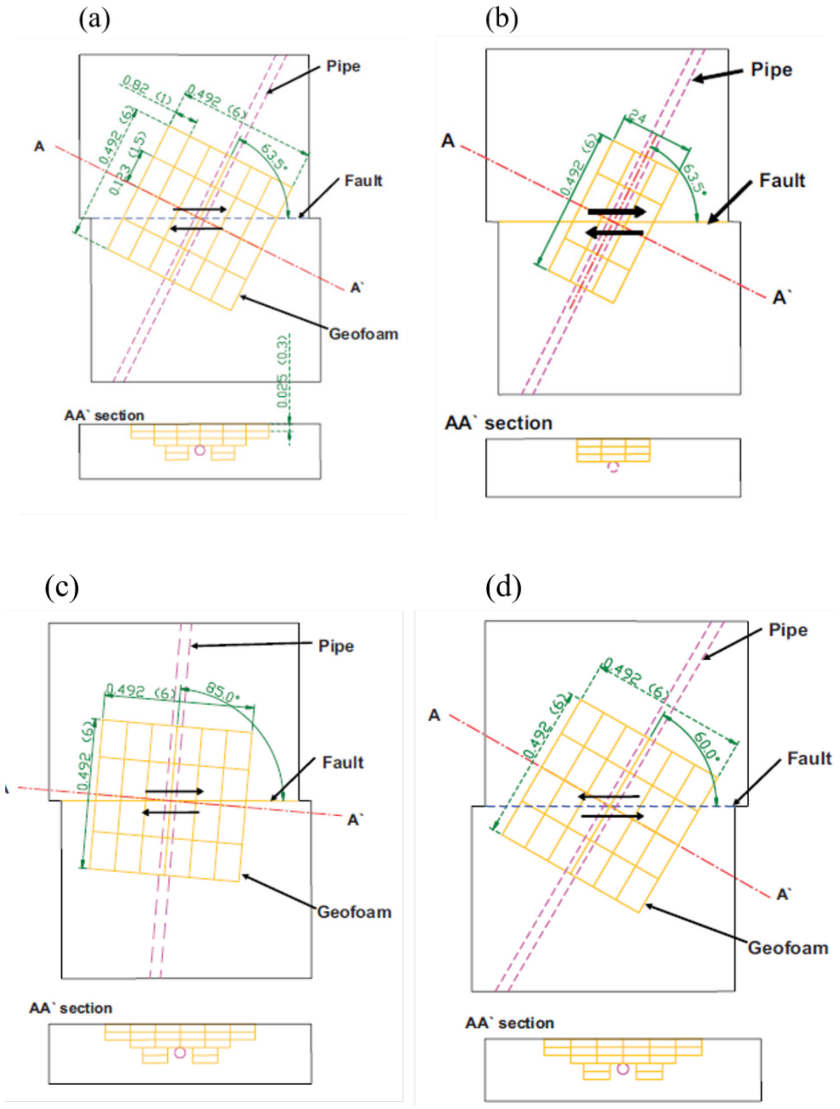

Figure 2- 10: Variation of pipe orientation to a fault line (Choo et al. 2007).

Bartlett and Lingwall (2014) carried out two full-scale tests to investigate the lightweight and compressible nature of EPS geofoam in reducing the vertical forces on buried steel pipelines that could potentially undergo vertical offset caused by normal faulting (Fig. 2-12). The first test was carried out using EPS29 as a lightweight cover placed lengthwise atop the steel pipe, while the second test was done with only sand fill. A 6.1m X42 steel grade pipe with an outside diameter (OD) of 324 mm and a wall thickness of 6.5 mm was used for the test. The pipe was slowly pushed up using an 850kN-crane to simulate the vertical offset. As shown in Fig. 2-13, the results confirmed that the geofoam cover system reduced the peak uplift force on the pipe to 136 kN at a displacement of 136mm compared to the sand cover test with a peak uplift force of 520 kN at a displacement of 70mm. Thus, it was found that the EPS geofoam can reduce the peak force by approximately a factor of 4. The results also confirmed that about 2.75 times more displacement was required to mobilize the peak uplift resistance.

Figure 2- 11: Photograph of the end of the trench, pipe, EPS block after the uplift test (Bartlett and Lingwall 2014).

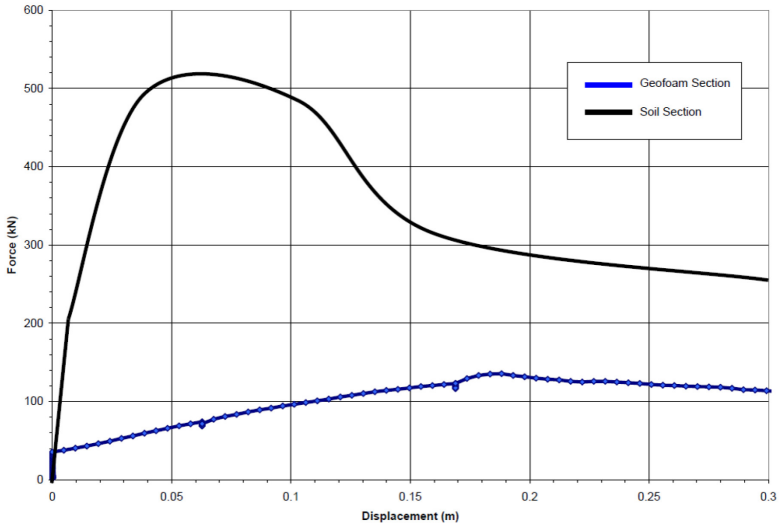

Figure 2- 12: Force-displacement plots for pipe uplift test (Bartlett and Lingwall 2014).

2.6 LANDSLIDES

Engineers, geologists, and other professionals have a unique and slightly different interpretation of landslides. Its complex nature reflects appreciable disparities associated with understanding and interpreting landslides phenomena across many disciplines. Its complexity comes from the fact that there are numerous types and combinations of landslides, varied and complex geologic environments in which landslides occur, and various causes and sizes of landslides (Cruden and Varnes1996, Highland and Bobrowsky 2008). However, in all simplicity, the term landslide refers to any gravitational movement of a soil mass, rock, or debris down a mountainous slope, which are initiated by the influence of intense or prolonged rainfall, seismic activities, river undercutting, freeze-thaw processes, human activity or any combination of these factors. Fig. 2-14 shows the various features of landslides.

A landslide occurs when the downslope components of forces (i.e., driving forces) that act on a slope exceed the shear resistance of the underlying materials (i.e., soil). One of the main reasons landslides occur is due to natural factors like wildfires or human-made factors such as indiscriminate deforestation and haphazard constructions. Driving forces can be increased through

changes to the geometry of the slope or increased slope loadings (e.g., earthquake shaking). Simultaneously, the resisting forces of the materials underlying the slope can be reduced through mechanical and chemical weathering (West et al. 2020). Regardless of the exact definition used under discussion, understanding the essential parts of a typical landslide is instructive, allowing various parties to communicate effectively regarding landslides.

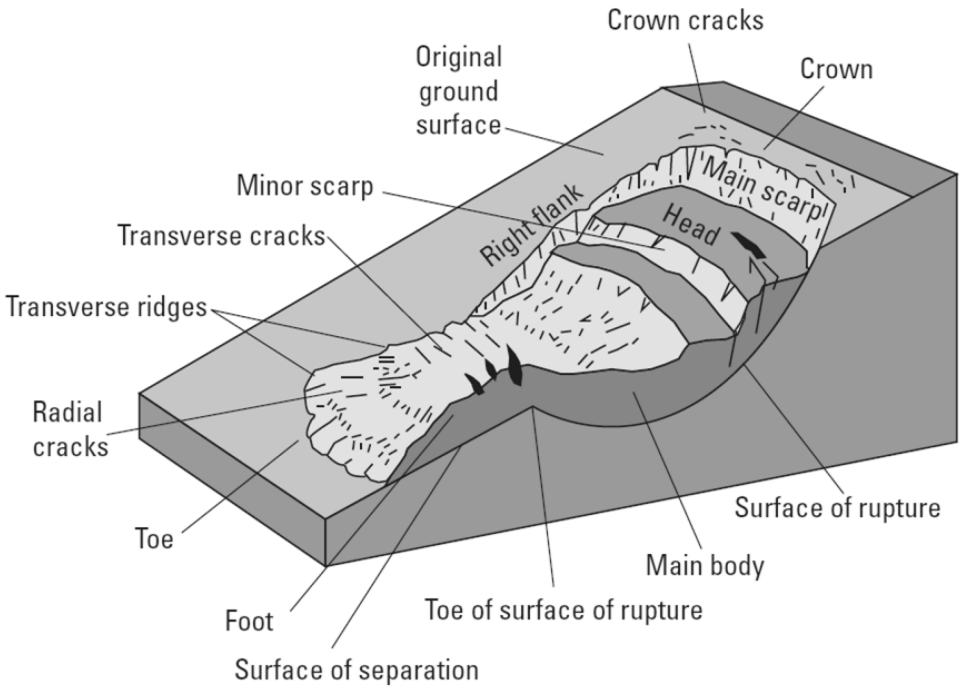

Figure 2- 13: Features of landslides (Highland & Bobrowsky 2008).

A landslide may be shallow or deep and can occur too rapidly, in seconds, minutes, hours, or even years. However, human activities such as deforestation or excavation of slopes for building sites or roads have become the significant triggers of landslide movements (Varnes 1978, Leinala 1999). The term landslides are classified into various types depending on the type of material involved (e.g., rock debris, earth, rock) and the movement type, which describes the actual internal mechanics of how the landslide mass is displaced (e.g., topples, spreads, flows, slides, and falls). Landslides are generally categorized as rockslides and debris flows. The rockslides are a type of

translational landslide caused by rock failure in which a part of the bedding failure plane passes through the path of compacted rocks. While debris flows refer to a rapidly moving mixture of soil, rocks, water, and other debris, which are accelerated downhill by gravity and tend to follow steep mountain channels. According to Highland and Bobrowsky (2008), in the U.S., Canada, and Mexico, the landslides that commonly affect pipelines include rotational and translational slides, earth flow, debris flow, and rockfall.

Understanding the essential types of landslides and their accompanied geohazards is useful when adopting an appropriate mitigation approach to reduce the risks of loss and damage caused by these slope movements. The type of landslide determines the potential spread of debris, the displacement volume, and their effects.

2.6.1 Slides

A slide is a downslope movement of a rock or soil mass that occurs on surfaces of rupture or thin zones of intense shear strain (Varnes, 1978). Slides usually occur as rotational or translational slides, or both known as compound slides. Rotational slides, referred to as slumps, are a type of landslide on which its curved surface of rupture is spoon-shaped, and the sliding movement rotates about an axis parallel to the contour of the sliding slope, as shown in Fig. 2-15a. Under certain circumstances, the displaced mass with little internal deformation moves a relatively coherent mass along the rupture surface. The head of the displaced material moves almost vertically downward while backwardly tilting the displaced material's upper surface towards the head scarps. The flow velocity of rotational slides varies from extremely slow (less than a foot per year) to moderately fast (5 feet per year) to rapid (6 feet per hour) (West, 2020). While in translational landslides shown in Fig. 2-15b, the rupture zone is relatively along a planer surface with little rotational movement

or tilting. This type of landslide is the most common type of landslide, which is found globally in all kinds of environmental conditions. Translational slides commonly fail along geologic discontinuities such as faults, joints, bedding surfaces, or the contact between rock and soil. They may progress over a considerable distance if the surface of rupture is sufficiently inclined. The materials in this type of slide may range from unconsolidated loose soils to extensive slabs of rocks or a combination of both. Unlike the rotational slides, the flow velocity of translational slides ranges from prolonged (5 feet foot per month) to moderately fast (5 feet per day) to extremely rapid (10 miles an hour).

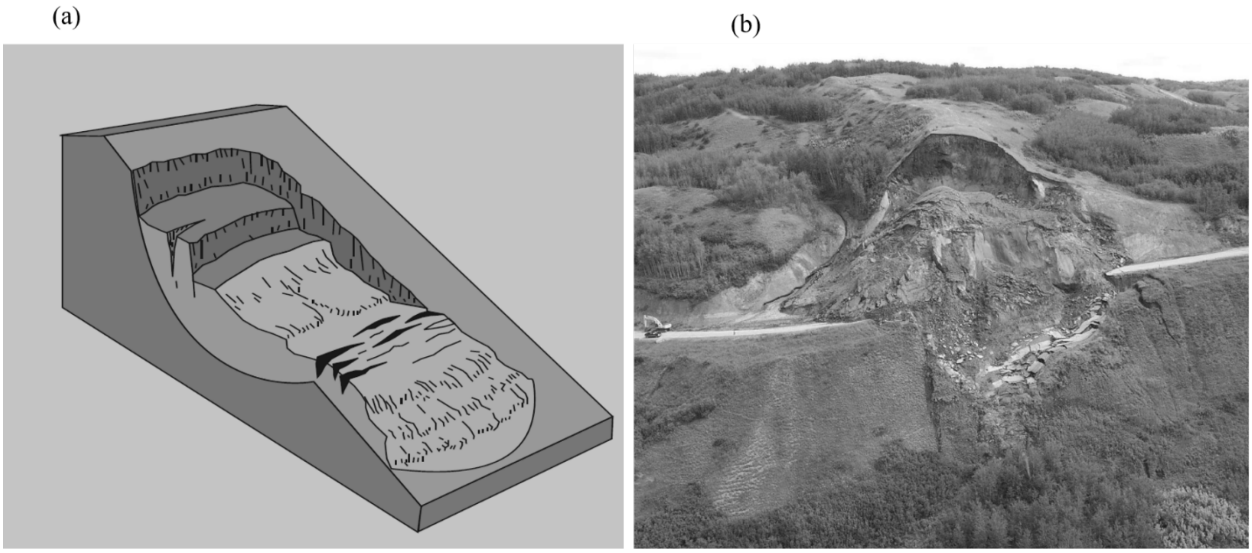

Figure 2- 14: a) A schematic of a rotational landslide; b) A translational landslide, Beatton River Valley, British Columbia, Canada, 2001 (Highland and Bobrowsky 2008).

2.6.2 Debris Flows

As shown in Fig. 2-16, a debris flow is a rapidly moving mass of loose soil, rock, and sometimes organic matter combined with water to form a slurry that flows downslope under gravity. As rotational or translational slides gain more velocity with their internal mass losing cohesion, it may evolve into a debris flow. In terms of size, this type of flow can be thin and watery or thick with

sediments. Debris flow can be extremely deadly as they occur at a high velocity (35 miles per hour or 56 km per hour) without any prior warning (Highland & Bobrowsky 2008).

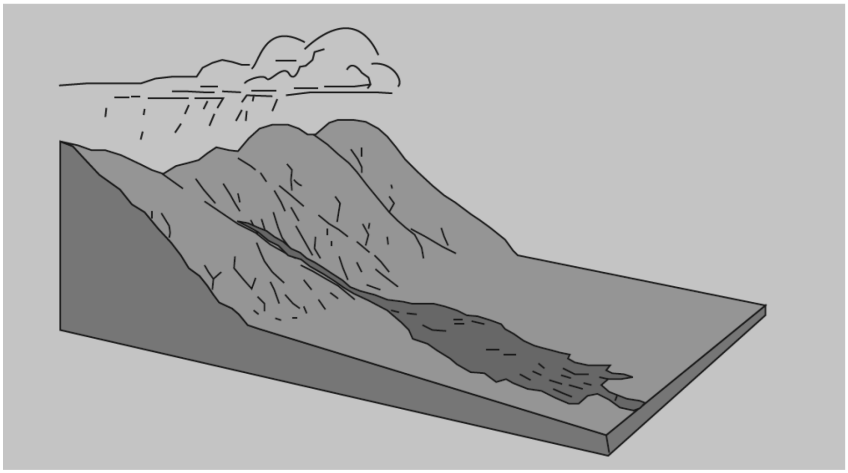

Figure 2- 15: A schematic of a debris flow (Highland & Bobrowsky 2008).

2.7.3 Rock Fall

A fall involves the detachment or collapse of soil or rock from a steep slope along a surface with little or no occurrence of shear displacement, resulting in debris collection near the base of the slope. After the collapse, the material subsequently descends mostly through the air by free-falling, bouncing or rolling (Varnes 1978). A schematic representation of a rockfall is shown in Fig. 2-17. Fall landslides usually happen due to earthquakes, shaking, human activities such as excavation during road building, differential weathering, and gravity forces. Fall landslides are reported to be usually very rapid to extremely rapid. In a situation where the landslide displacements occurred in waves, a swift flow of debris, commonly referred to as rockfall avalanches, is experienced.

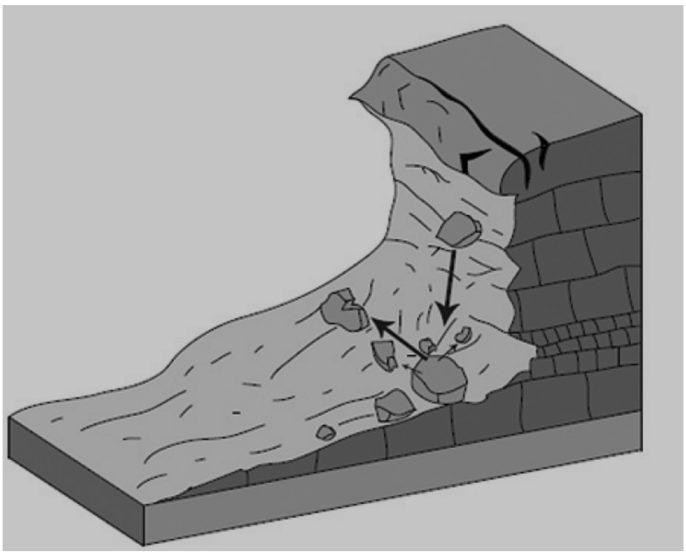

Figure 2- 16: A schematic of a rockfall (Highland & Bobrowsky 2008).

2.8 LANDSLIDES DAMAGES TO BURIED PIPELINES

When pipelines transverse through hazardous terrain, they can become vulnerable to the effects of landslide-induced soil loadings. The extent of vulnerability depends on the pipe burial depth, wall thickness, grade of steel, quality of welds, and the geometry of the pipe trench, material properties of the trench backfill (Wang 2017). Previous studies have shown that the common failure scenarios of pipelines subjected to landslide-induced loadings are connected to the pattern and the angle at which the pipeline transverses the landslide (Liu et al. 2009, West 2020). There are three generally encountered pipeline-landslide interaction scenarios as described here.

As shown in Fig. 2-18, when the landslide moving mass is parallel to the pipeline longitudinal axis, the pipe is mainly subjected to a frictional force, impacting tensile stress on the portion of the pipeline near the leading edges of the landslides, while compressive stresses are induced on the toe of the landslides.

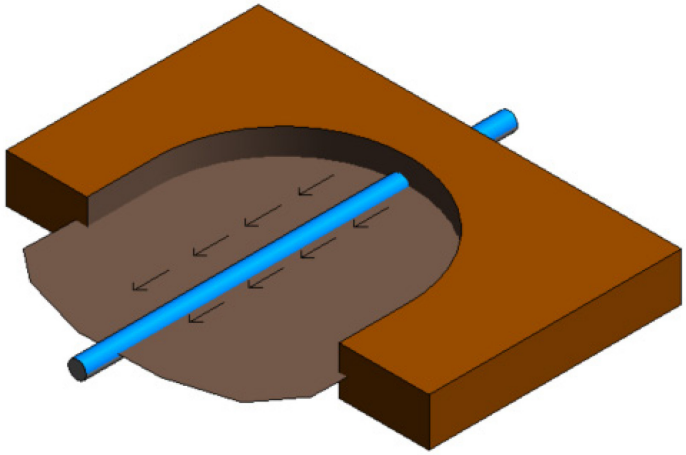

Figure 2- 17: Deformation of the pipeline passing parallel through the landslide.

For landslides that transverses perpendicular to the longitudinal axis of the pipe (Fig. 2-19), the pushing force from the sliding mass puts the pipeline under bending, and shear stresses at the lateral edges of the landslide. Moreover, the pushing force from the soil may put the pipe in tensile and compressive stresses as the landslide mass extends downslope, depending on the nature of the movement.

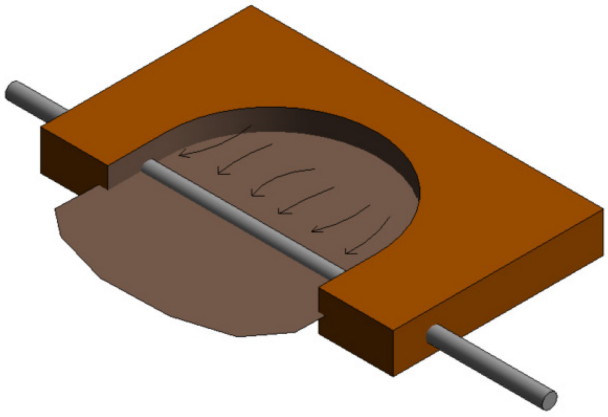

Figure 2- 18: Deformation of the pipeline passing perpendicular through the landslide.

As shown in Fig. 2-20, when the pipeline is obliquely oriented across the landslide mass, the landslide-induced loading on the pipeline would depend on the oblique movement's skew angle relative to the pipeline. The pipeline is expected to experiences lateral, shear, and axial stresses.

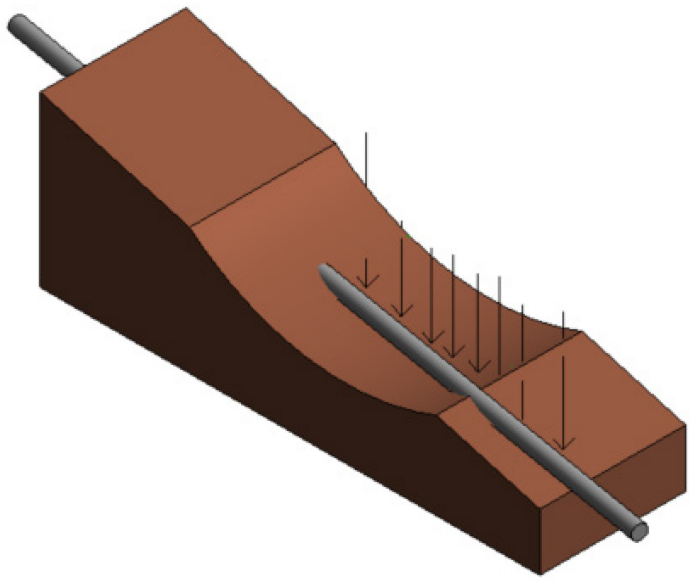

Figure 2- 19: Deformation of the pipeline passing oblique through the landslide.

2.9 LANDSLIDE MANAGEMENT

Landslide management refers to the process of identifying, characterizing, and mitigating any landslide-induced risks. In recent years, the use of powerful "Remote Sensing" and Geographic Information System (GIS) technologies to identify potential hazards in hot spot areas is one of the key techniques employed by engineers and geologists in carrying out risk management assessment of landslides. With these modern technologies, engineers or pipeline operators can map out the possible landslide hazards along a particular area, which is made possible using high-resolution aerial photography and terrain models (Andersson et al. 2013, Wang et al. 2017). The results

obtained from using this mapping software help reveal inconsistencies with hazard records and provide vital information for hazard prevention and mitigation purposes.

There are three-phased approaches commonly employed by qualified and experienced geoscientists and geotechnical engineers to identify, classify, and evaluate potential hazards that threaten pipeline integrity (Sancio et al. 2020). These phases allow for a successful, more detailed investigation to be employed. The first phase involves an office-based regional screening assessment where the owner/operator provides information regarding the topographic, geology, and any available data regarding the study area is gathered to identify potential geologic hazards that may affect the pipeline system. An aerial reconnaissance usually accompanies this first phase to confirm the in-office assessment (Nyman et al. 2006). The second phase involves a site-specific, non-intrusive field geologic and geomorphic reconnaissance mapping to verify the existence and levels of threats from previously identified hazardous features and identify those features that may require the Phase 3 investigations. During Phase 3 reconnaissance, the information and data collected provide a more detailed and site-specific understanding of the location, nature, and extent of the hazard and its potential threat to the pipeline. The information compiled in this phase is entered into a GIS database, updating the Phase 1 assessment data. The final step involves both office and field-based site-specific investigations that focus on the confirmed hazards from phase three reconnaissance. This phase commonly investigates the detailed surface and subsurface geologic and geotechnical site characterization to support appropriate mitigation designs and develop and implement the appropriate mitigation and monitoring programs.

In today's present world, monitoring and mitigation of landslides are one of the logical steps taken by pipeline operators and owners to investigating and providing viable solutions towards the potential adverse effects a ground movement may have on a pipeline system. When a mitigation

approach has been designed and implemented, the performance of such measure must be monitored to ensure that it continues to function correctly and offers the relevant protection to the pipeline system for which it was intended.

Recent studies have shown that landslide mitigation measures implemented alone or in combination to improve the response of pipelines when subjected to ground displacements can take many forms, which include avoiding the landslide area by rerouting the pipelines' right-of-way, slope stabilization, improving the strain capacity of the pipe through the use of high ductile steel. The selection of a particular approach depends on factors that vary with the location, topographic constraints, construction costs, constraints, ability to procure necessary right-of-way access, and the need to avoid existing subsurface structures and utilities (Choo et al. 2007, Bartlett and Lingwall 2014, Fathi et al. 2018).

Modifying the alignment of the buried pipeline adjacent and around potential areas prone to ground displacement can significantly reduce the pipe strains. The aim of pipeline alignments or re-alignments is generally to minimize the exposed length of pipeline to ground displacement, eliminate points where loads generated by soil can concentrate along the pipeline, and maximize the flexibility of the pipeline to accommodate imposed deformations (Sancio et al. 2020).

Modifications to the material or geometrical properties of pipelines, such as the application of high ductile materials and increased wall thickness, can significantly improve the structural integrity of the pipe. Sancio et al. (2020) noted that increasing the wall thickness tends to increase the allowable longitudinal compression strain while increasing the pipe bending and axial strength relative to the surrounding soil.

The capacity of buried pipelines to withstand ground displacements can also be enhanced by minimizing the longitudinal, lateral, and uplift soil resistance to pipe movements. These can be

achieved by using loose granular backfill materials with an internal friction angle of 35° or less such as sand or gravel, which offers less resistance to pipe movement than compacted cohesive backfill materials.

Replacing the soil backfill with either expanded polystyrene (EPS) or extruded polystyrene (XPS) geofoam has been extensively used to reduce the axial, lateral, and upward vertical soil loads. Geofoam is a rigid cellular plastic foam used as a low-density backfill for construction over weak or compressible soils. Yun woo Choo et al. (2007) and Lingwall and Bartlett (2014) investigated the use of low-density materials in reducing the effect of soil loads on buried pipelines. They reported that the induced pipe stresses and strains due to soil loads could be reduced by replacing the wedge of soil backfill using low-density materials.

In addition, a novel mitigation technique referred to as the installation of Special Geomaterial Blocks (SGB), consisting of a set of expanded polystyrene (EPS) geofoam and polypropylene squared plastic boxes (referred to as voids) adjacent to a steel pipeline, has been developed with the objective of effectively enhancing the performance of buried pipelines underground deformation (Ilozumba et al. 2021). The novel remediation technique involves uttering the boundary conditions of buried pipelines by placing the SGB adjacent to the pipe before backfill. The lower boundary stiffness of the SGB would enable the pipeline to endure large lateral displacements by distributing its deformation over a longer length while achieving a minimal lateral force. However, there is a need to validate the method's efficiency using lab testing and develop numerical modelling techniques for pipeline engineers taking advantage of the method.

3. CROSS-SECTIONAL TESTING AND ANALYTICAL MODELLING

3.1.ABSTRACT

This paper proposes a novel mitigation approach to improve the safety and structural integrity of buried steel pipelines subjected to ground deformation. This method involves altering the boundary condition of buried pipelines with adjacently installed special geomaterial blocks (SGB) consisting of a set of expanded polystyrene geofoam and polypropylene squared plastic boxes. The proposed SGB allows accommodating ground deformation while significantly reducing the ground-induced forces on the pipe. The mitigation technique is first presented, followed by the experimental test program developed to evaluate the beneficial effects of the SGB on the pipe response when subjected to lateral and oblique displacements. Furthermore, a simplified spring-based analytical modelling approach is proposed for predicting the force-displacement response of the pipe-SGB-soil assembly with emphasis on the interaction between the pipe and soil under the new boundary condition. The analytical model is validated using the experimental test data. The results of the experimental test confirm the efficiency of the proposed remediation and feature the relationship between the applied displacement and dissipated force in the SGB. Furthermore, it is found that the proposed analytical model can appropriately predict the expected nonlinear response of the reaction of the pipe equipped with the SGB.

Keywords: Buried pipelines, Geohazards, Ground deformation, Geomaterial, Experimental testing.

3.2 INTRODUCTION

Buried pipeline systems are extensively used worldwide to transport natural oil, gas, or other materials from source to various consumption locations. Given the appreciable length of the

transportation line, the majority of buried pipelines run across mountainous regions with various environmental and geotechnical conditions. Therefore, these pipelines may be subjected to large lateral and longitudinal displacements due to permanent ground movement arising from landslides, moving slopes, earthquake-induced faulting, urban excavation, soil liquefaction, and excessive ground settlement (Choo et al. 2007, Agbo et al. 2019). Under such large ground displacements, the pipelines may experience significant bending and axial strains, thus causing pipe fracture due to high tensile strains or pipe wall wrinkle or buckle due to large compressive forces (Mahdavi et al. 2008, Wang et al. 2008, Han et al. 2012, Zhang et al. 2017). These failures can potentially compromise the entire pipeline's functionality, resulting in significant economic losses or even fatalities.

A large number of pipeline damage cases due to ground movements (e.g., landslides and slope failure) have been recorded in the past. For example, as European Gas Pipeline Incident Data Group (EGIG 2013) reported that landslides accounted for 85.2% of the geological disaster in Europe from 2004 to 2013, leading to 13% of gas pipeline accidents. In Canada, 40% of pipeline incidents recorded in 2018 were caused by both geotechnical and environmental activities (Government of Canada 2018). In 2013, Enbridge, Canada, reported a heavy rainfall that triggered ground movement at a slope near the Cheecham Alberta pipeline's right of way. This incident led to approximately 1,300 barrels of light synthetic crude oil leaked from the damaged pipeline, causing a temporary suspension of service and large financial losses (Enbridge 2013). In 2016, Husky Energy reported on the pipeline incident failure caused by ground movements, which was triggered by heavy rainfall and unstable soil conditions. The pipeline failure caused approximately 225,000 litres of heavy crude oil spillage into the North Saskatchewan River and 90 million dollars in financial loss (MacPherson 2016). The pipeline incidents can therefore cause dangerous,

catastrophic failures that have significant consequences felt by the population, environment, industrial facilities, and pipeline operators (Fathi et al. 2018).

Several mitigation measures have been proposed in the past to improve the structural integrity of buried steel pipelines that may be susceptible to damage due to ground movement. Some of those techniques include rerouting pipelines around sites susceptible to severe ground movement, stress-relief, slope stabilization, using a wide trench with soft backfill, using pipes with a lower D/t ratio where D is the pipe outside diameter and t is the wall thickness, and the application of fibre-reinforced wraps (Choo et al. 2007, Honegger et al. 2010, Mokhtari and Nia 2014, West 2020). When the axial strain dominates pipeline response, the use of high ductile materials with a large pipe wall thickness has been argued to improve the resistance of the pipeline against ground movements (O'Rourke and Liu 1999). Moreover, the application of low-density materials was found beneficial in reducing the effect of soil loads on buried pipelines (Choo et al. 2007, Bartlett and Lingwall 2014, Bartlett et al. 2015). Some of these methods are summarized below.

The application of expanded polystyrene (EPS) geofoam cover system to protect the pipelines undergoing vertical displacements due to fault movement was evaluated through large-scale field testing (Bartlett and Lingwall 2014; Bartlett et al. 2015). In this mitigation method, the lightweight, compressible nature of EPS geofoam was used as a trench cover to reduce the vertical, bending and shear forces induced on steel pipelines, especially when undergoing vertical offset caused by normal faulting. The results showed an approximately 73% reduction in the peak uplift force of the geofoam cover system when compared to traditional soil backfill materials.

Choo et al. (2007) performed a series of 12 centrifuge tests using EPS geofoam blocks as low-density backfill to reduce the soil-pipe interaction on high-density polyethylene (HDPE) pipelines. The beneficial effects of this remediation technique were confirmed for pipes under flexure and

axial tension, but unfavourable results were observed for pipes subjected to a combination of axial compression and bending. Additionally, it was found that EPS geofoam blocks can result in an approximately 85% reduction in the peak lateral force at the soil-pipe interface, depending on the geofoam block's placement with respect to the fault line. The reduction in the lateral force led to a 50% reduction in the bending strain and a 30% reduction in axial strain when compared with the pipeline systems without the EPS remediation.

The response of the pipes equipped with internal flexible joints having a large expansion and contraction capabilities was examined using a three-point bending experiment with the objective of reducing the strains developed under transverse displacements (Melissianos et al. 2017). This method led to reducing the risk of pipe failure by concentrating the strains at the joint locations while leaving the rest of the pipe relatively unstressed. It is worth noting that this mitigation method is intended to only address vertical offset due to fault movement and not horizontal ground displacement caused by landslides or unstable slopes.

Although several remediation techniques have been proposed in the past to address the detrimental effects caused by ground movement on buried pipelines, these techniques may not necessarily provide an effective and cost-efficient solution in practice. For instance, rerouting a pipeline may result in a longer pipeline length, leading to higher construction costs and the inability to procure a necessary right–of–way. Rukovansky et al. 1985 reported the one million dollars direct cost of relocating a 365-m length of a pipeline subjected to landslide geohazards. Further, the variations in the soil medium's geomechanical properties and pipe's embedment conditions can increase the backfill resistance against the pipe movement. Finally, pipelines are typically subjected to relatively large forces induced by ground movement when the available mitigation techniques are employed. To address high construction or upgrade costs and achieve a more efficient mitigation

method, there is an urgent need to develop novel mitigation techniques to effectively improve the integrity of buried pipelines subjected to ground deformation.

3.3 RESEARCH OBJECTIVES AND METHODOLOGY

This paper introduces a new mitigation technique to improve the performance of buried steel pipelines exposed to the lateral displacement induced by ground movement. The proposed technique involves the installation of special geomaterial blocks (SGB), which consists of a set of expanded polystyrene (EPS) geofoam and polypropylene squared plastic boxes adjacent to a steel pipeline. The application of the SGB aims to enhance the integrity of buried pipelines by altering their boundary conditions. This novel technique would enable the pipe to effectively distribute the induced lateral soil displacements within a longer distance while reducing the backfill resistance against pipe movement.

Herein, the methodology employed is to perform a series of laboratory tests on a typical cross-section of a pipe placed adjacent to the SGB. Three different loading angles are considered to investigate various displacement angles induced by ground movement. Four different SGB cover configurations are explored to examine the effect of the interface frictional force between the SGB and the sand fill on the behaviour of the proposed technique. Moreover, a simplified analytical procedure is proposed to analytically predict and gain insight into the local response between the pipe-SGB-soil assembly. The effect of the different SGB parameters, including the thickness of geofoams and the number of geofoam layers, are investigated using the proposed method. This analytical model is hypothesized to provide pipeline engineers with an efficient tool for the purpose of design.

The proposed mitigation approach, its key components and mechanism are first introduced. The cross-sectional test program is developed to assess the response of the pipe-SGB-soil assembly, verify the adequacy of the proposed analytical model and evaluate the influential effects, including

the loading angle and the interface frictional force between the SGB and sand, are then presented. The results of the experimental tests performed on the 25 SGB specimens are presented and discussed. A simplified yet efficient analytical model developed to predict the capacity of the SGB when interacting with the soil and pipe is described and validated against the experimental test data.

3.4 PROPOSED MITIGATION TECHNIQUE

3.4.1 Components of the SGB

The special geomaterial block (SGB) proposed in this study to mitigate ground movements in steel buried pipelines are shown in Fig. 3-1a. This element referred to as the SGB hereafter comprises a set of expanded polystyrene (EPS) geofoams and lightweight polypropylene squared plastic boxes encased in corrugated plastic sheets fabricated to act as voids between the geofoams. The squared plastic boxes are referred to as voids for simplicity. The EPS geofoams, which were primarily designed to resist the overburden pressure and lateral loads, are the low-density lightweight plastic cellular geosynthetic material. The EPS geofoams are commonly used in ground fill applications where the lightweight fill material is required to reduce stresses on underlying soils. They can also act as compression inclusion as well as thermal insulators. The EPS geofoams are designated with their density in kg/m^3. For instance, EPS15 represents an EPS geofoam with a nominal density of 15 kg/m^3. The standard density of EPS geofoams ranges between 11 and 46 kg/m^3. In this study, EPS39 is used to design the SGB.

The SGB has an orthotropic mechanical property, which increases the stiffness of the element in the directions laying on the plane of geofoam layers, while it is relatively flexible in the direction perpendicular to the plane of geofoam layers. The SGB, as shown in Fig. 3-1b, are to be placed adjacent to the cross-section of the pipe such that their flexible axis is oriented against the pipe to allow the pipe to move laterally along its cross-sectional plane without developing significant

reactions while resisting the weight from the soil overburden pressures acting on the top surface of the SGB. A stiff shell that protects the SGB from the in-situ lateral soil pressure is used at the end of the SGB when placed in a trench (Fig. 3-1b).

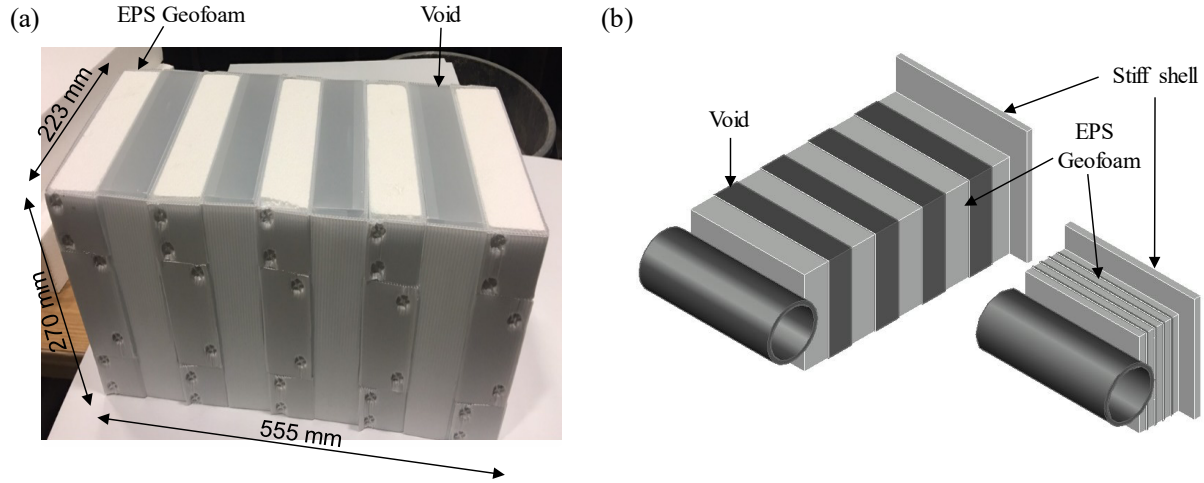

Figure 3- 1: a) Special Geomaterial blocks (SGB); b) The SGB response when interacting with pipe and soil before and after ground movement.

When the pipe is subjected to the lateral displacement caused by ground movement, the voids in the SGB are fully collapsed (Fig. 3-1b), and the pipe is moved towards the fixed end (i.e., stiff soil). In a pipeline network, a set of the SGB is installed adjacent to the pipe in the regions where ground movement is likely to occur (Fig. 3-2a). When the pipeline network is subjected to a lateral displacement (e.g., due to a landslide), the relative flexibility of the SGB allows the pipe to distribute the deformation to a longer length, as shown in Fig. 3-2b. As a result, the maximum pipe curvature at kinks significantly reduces, which results in lower longitudinal strain demands and a lower risk of subsequent pipe buckling or girth weld rupture. This improved response is expected, in turn, to contribute to significantly reducing the costs associated with the maintenance of pipeline networks in geohazard sites with slow and steady ground displacements.

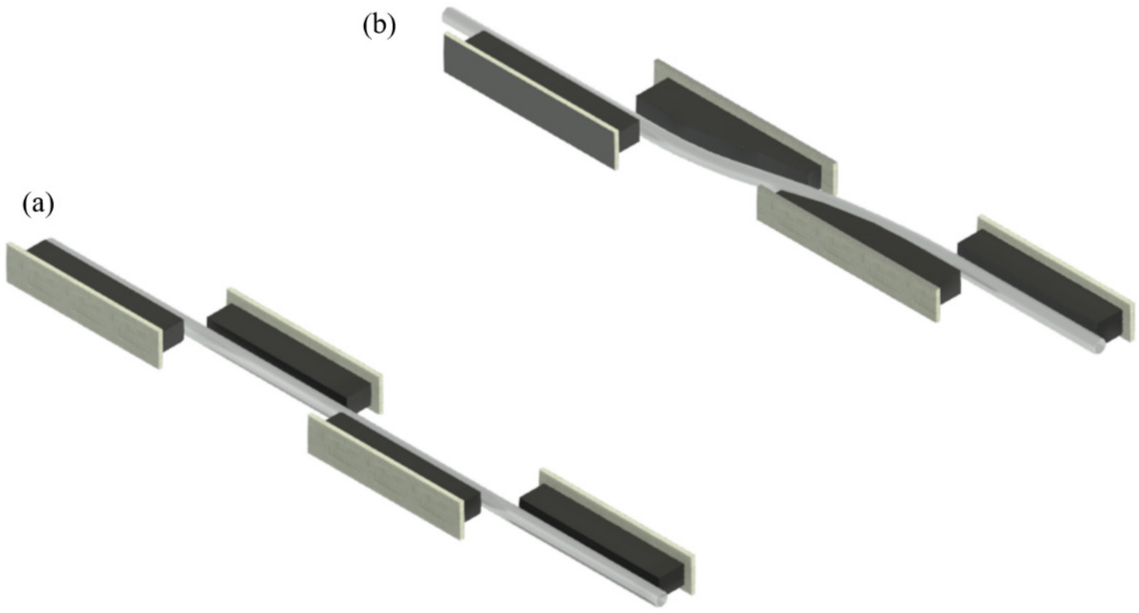

Figure 3- 2: Enhanced response of a pipeline network equipped with the SGB under lateral ground movement: a) before lateral displacement; b) after a lateral displacement.

3.4.2 The SGB Mechanism

Special Geomaterial blocks are fabricated to act as a set of relatively stiff (geofoams) and relatively flexible (void) springs in series. The mechanism of the SGB with one flexible and two stiff elements placed adjacent to a pipe and backfilled with the soil is shown in Fig. 3-3. The SGB is intact before the displacement is applied (Fig. 3-3a). Fig. 3-3b shows the onset of soil loading, where the EPS geofoams blocks are to remain undeformed while resisting the soil frictional forces. The expanded polystyrene (EPS) geofoams act as a set of stiff elements capable of transferring the interface soil frictional forces to the voids. As the lateral displacement increases, the void collapses as soon as the frictional forces develop between the soil and the SGB are achieved (Fig 3-3c). If there exists more than one void, which is anticipated to accommodate the anticipated lateral displacement, all the voids are expected to collapse stepwise. Once the void is completely closed, further lateral displacement engages the geofoam blocks (Fig. 3-3d), causing the blocks to gradually deform in the direction of the applied displacement until the geofoam blocks fail and no longer can resist lateral loads.

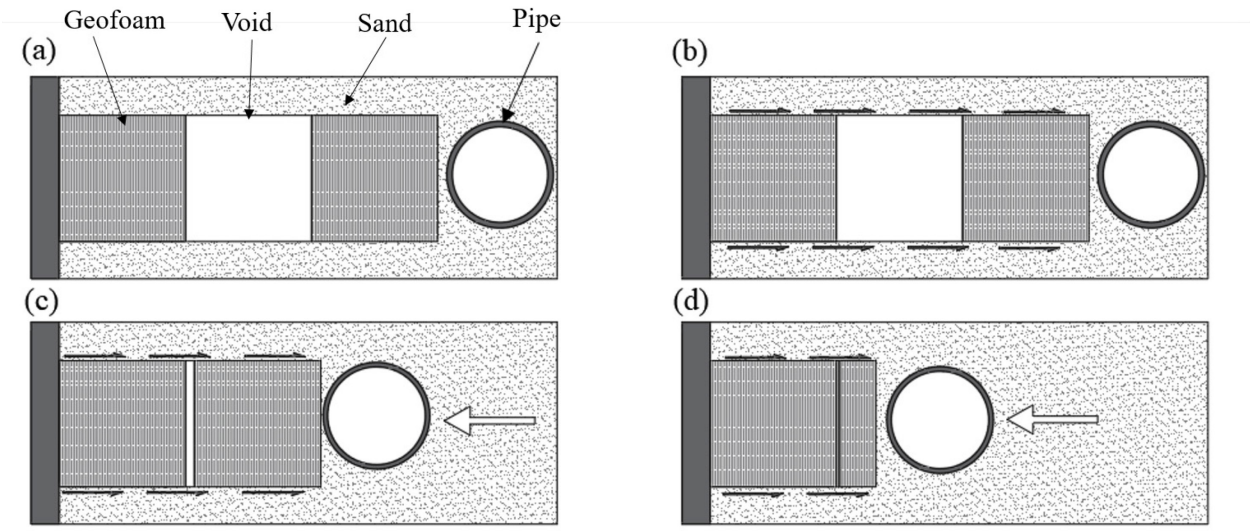

Figure 3- 3: The SGB mechanism under lateral movement: a) before the application of lateral movement; b) onset of loading; c) collapse of voids; d) geofoam deformations at large lateral movement (thicknesses and deformations magnified).

The set of geofoams and voids should be configured such that they accommodate the expected lateral displacement of the pipe through collapsing the voids and not the failure of the geofoams, which defines a minimum number of voids and therefore geofoams to be used for a given lateral displacement expected to induce on the pipe. This mechanism can efficiently control the deformation of the pipe by distributing the applied ground movement to a longer pipe length while significantly limiting the force induced in the pipe, reducing the likelihood of failure in the pipeline system. Furthermore, the thickness of geofoams and voids should be configured such that the assembly can safely carry the overburdened weight of the passive soil backfill without significant flexural deformation or even failure while taking into account the manufacturing considerations. The verification of the flexural strength and deformations or stability is particularly important for the void elements before the ground movement occurs. Finally, the engineer should consider the weight of the compacted soil or future site changes that may affect the overburdened weight used in the selection of the thickness of the void and geofoam.

3.5 EXPERIMENTAL PROGRAM

3.5.1 Test Setup

An experimental test program consisting of 25 cross-sectional tests was developed at the University of Alberta to evaluate the structural response of the SGB and pipe assembly backfilled with soil when subjected to lateral displacement representing ground movements. The tests also served to evaluate the beneficial effects of the SGB on the stability response of the pipe and determine the influential parameters affecting the capacity of these elements. The experimental test setup is shown in Fig. 3-4a. The test frame was designed as a self-balanced frame using aluminum members under sand gravity loads and the lateral load applied by the actuator following the CSA S157 (CSA S157 2017). A transparent Plexiglass was used to track the test progress while pushing the pipe with the electric linear actuator against the SGB. An electric linear actuator capable of producing up to 4000-pounds force with a stroke length of 1016 mm was mounted on a heavy-duty mounting bracket. The stroke end of the actuator was attached to a 2000-pound compression load cell. The actuator loads were transmitted through a 19mm-diameter drive shaft with one of its ends connected to the load cell and the other end attached to the center of the pipe through a linear ball bearing. The diameter of the pipe used in the test is 219 mm, and its nominal wall thickness is equal to 8.2 mm, resulting in a diameter-to-wall thickness ratio, $D/t = 27$. The pipe material conforms to G40.21-M350W steel with yield and tensile strength of 310 MPa and 450 MPa, respectively. The pipe was placed adjacent to the SGB as shown in Fig. 3-4b and backfilled with dimensions of 1.09 × 0.35 × 1.35 m.

(a)

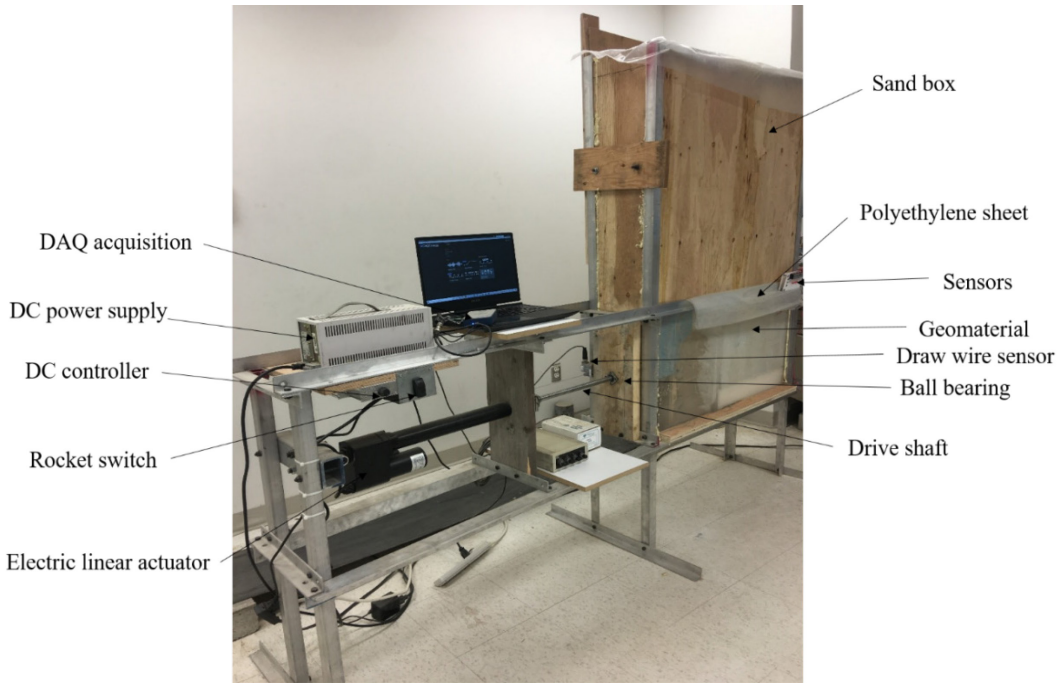

(b)

Figure 3- 4: a) Test setup components (horizontal loading shown); b) Pipe and the SGB assembly.

The linear actuator and the drive shaft were positioned using the D.C. speed controller. The centerline of the pipe was placed at a depth of 1.1 m, with a minimum of 245mm of sand placed beneath the pipe. An SGB was placed between the pipe and the test frame wall. The dimensions of the SGB are 555 × 223 × 270 mm (Fig. 3-1a). Polyethylene plastic sheets were placed in front and on top of the SGB to prevent sands from getting into the gap between the walls of the sand

container and the SGB specimen, which may otherwise affect the behaviour of the SGB. After placing the specimen in the test frame, approximately a $0.4m^3$ volume of 5 mm-sized dry sand with a density of $1551kg/m^3$ was moved into the sandbox without compaction.

3.5.2 Test Specimens and Procedure

In total, 25 SGB specimens were tested by varying the loading angle and the SGB cover configurations. Table 3-1 shows the experimental test matrix. Fig. 3-5 shows a schematic of the SGB cover configuration. The loading angle is measured with respect to the vertical plane passing through the pipe axis. The horizontal loading signifies the angle 90 degrees, while 27 and -27 degrees represent upward and downward loading, respectively. The geometry of the test frame was modified for each loading angle by changing the angle of inclination of the load actuator. Figs. 3-6a to 6c shows the test frames used to perform 90, 27 and -27 degrees loading cases, respectively.

Table 3- 1: Experimental test matrix.

Group	Specimen	Loading Angle	Loading Condition	Cover Configuration				
				First layer	Second layer	Third layer	Fourth layer	Fifth layer
I	C-G1	90^0	Faulty	Geofoam	Plastic Sheet	SGB	Plastic Sheet	Geofoam
			Faulty	Geofoam	Plastic Sheet	SGB	Plastic Sheet	Geofoam
			Faulty	Geofoam	Plastic Sheet	SGB	Plastic Sheet	Geofoam
			H1	Geofoam	Plastic Sheet	SGB	Plastic Sheet	Geofoam
			H2	Geofoam	Plastic Sheet	SGB	Plastic Sheet	Geofoam
			H3	Geofoam	Plastic Sheet	SGB	Plastic Sheet	Geofoam
II	C-G2	90^0	H4	-	Plastic Sheet	SGB	Plastic Sheet	Geofoam
			H5	-	Plastic Sheet	SGB	Plastic Sheet	Geofoam
			H6	-	Plastic Sheet	SGB	Plastic Sheet	Geofoam
			H7	Geofoam	-	SGB	-	Geofoam

III	C-G3	90^0	H8	Geofoam	-	SGB	-	Geofoam
IV	C-G4	90^0	H9	Geofoam	Teflon Pad	SGB	Teflon Pad	Geofoam
			H10	Geofoam	Teflon Pad	SGB	Teflon Pad	Geofoam
V	C-G5	27^0	D1	Geofoam	Plastic Sheet	SGB	Plastic Sheet	Geofoam
			D2	Geofoam	Plastic Sheet	SGB	Plastic Sheet	Geofoam
			D3	Geofoam	Plastic Sheet	SGB	Plastic Sheet	Geofoam
VI	C-G5	27^0	D4	-	Plastic Sheet	SGB	Plastic Sheet	Geofoam
			D5	-	Plastic Sheet	SGB	Plastic Sheet	Geofoam
			D6	-	Plastic Sheet	SGB	Plastic Sheet	Geofoam
VII	C-G6	-27^0	U1	Geofoam	Plastic Sheet	SGB	Plastic Sheet	Geofoam
			U2	Geofoam	Plastic Sheet	SGB	Plastic Sheet	Geofoam
			U3	Geofoam	Plastic Sheet	SGB	Plastic Sheet	Geofoam
VIII	C-G7	-27^0	U4	-	Plastic Sheet	SGB	Plastic Sheet	Geofoam
			U5	-	Plastic Sheet	SGB	Plastic Sheet	Geofoam
			Faulty	-	Plastic Sheet	SGB	Plastic Sheet	Geofoam

*C = cross-sectional test, G = specimen, H = Horizontal loading, D = Downward loading, U = Upward loading

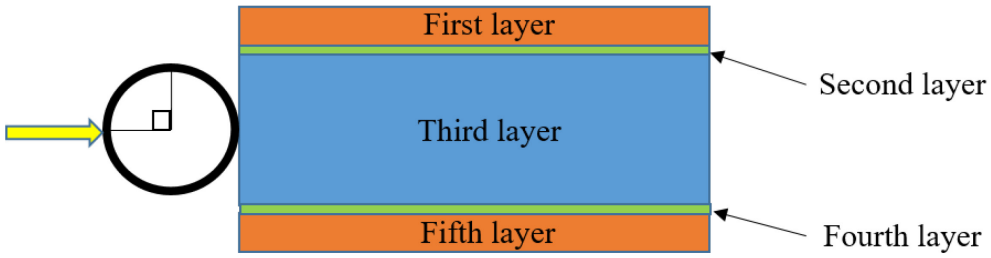

Figure 3- 5: Schematic representation for Group 1.

To perform the test, the pipe was pushed in a displacement-controlled mode against the SGB into the sandbox using the actuator until the target displacement of 250 mm was achieved. Though the loading condition applied in the test is different from what pipelines experience in the field, it would not affect the expected response of the pipe-SGB-soil assembly. As shown in Table 3-1,

four different cover configurations were tested by varying the contact surfaces between the SGB and the underlying layers of plastic sheets and geofoam blocks to explore the effects of the interface frictional force between the SGB and the sand fill. The tests performed using the plastic sheet with geofoam blocks (Group 1) served as a baseline to compare with the rest of the experimental specimen. The top geofoam block was used to uniformly distribute the soil loads on the SGB as the pipe pushes towards the SGB.

(a) (b)

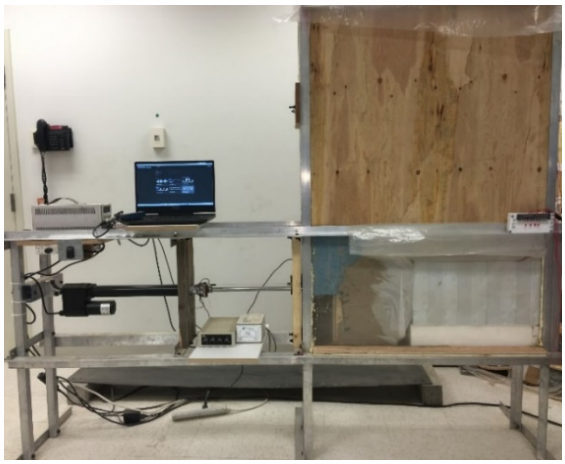

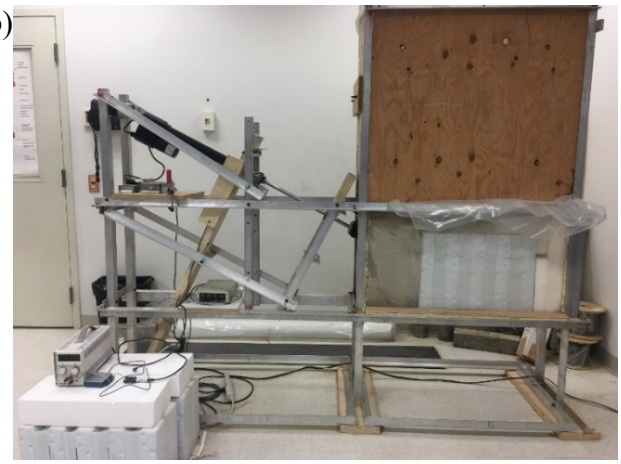

(c)

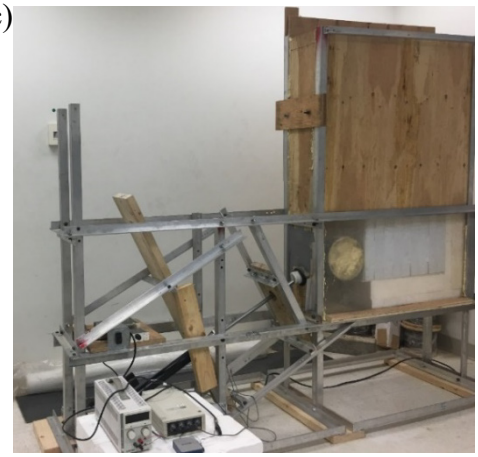

Figure 3- 6: Photograph of the experimental test setup for: a) Horizontal loading; b) Downward loading; c) Upward loading.

3.5.3 Instrumentation

Instrumentations used in the experimental program consist of a data acquisition system (DAQ), a load cell mounted on the linear electric actuator, draw wire sensors, as shown in Fig. 3-4. Using a D.C. controller and a rocket switch, the actuator displacement rate was set at a minimum speed of

0.1 mm/s. The speed of the D.C controller was calibrated through a series of 4 trial tests to achieve the minimum speed required to replicate a slow and steady ground movement while minimizing measurement errors. With this speed, each test loading was completed in approximately 30 min. The draw-wire sensors and load cells were calibrated to ensure reliable data acquisition. The load cell with a preinstalled strain gauges was mounted on the electric linear actuator. The actuator force, once sensed, deforms the strain gauges, which, in turn, converts the strains from the strain gauges into an electrical signal. The output of the electrical signal was further amplified using an instrumentation amplifier. The linear displacement of the loading system was achieved by attaching draw-wire sensors at the actuator tip using a thin metal string. The draw-wire sensor and the electric linear actuator were then connected to a D.C. power supply, which sends signals to the data acquisition system to record the measured force and displacements at every step of the experiment.

3.6 TEST RESULTS

The results of the test program, namely the observation of the overall response and force-displacement relationship, are presented here for each loading angle. The force-displacement response for each group in Table 3-1 was obtained by computing the average value of the forces in each group at a given displacement. The slope of the force-displacement curve represents the stiffness of the proposed SGB as the pipe displaces as a rigid body in the presence of soil backfill.

3.6.1 Horizontal Loading

The average force-displacement response for each group of horizontal loading is shown in Fig. 3-7. The curves indicate that the system behaviour is nonlinear; however, it can be approximately expressed via a bi-linear curve segment followed by an exponential hardening. The slope of these curves that features the force per unit length per unit width of the SGB is used to evaluate the system stiffness. Referring to Fig. 3-7, the stiffness across each group remained nearly identical until an

average force of 0.7 kN and a pipe displacement of 5.0 mm. However, as the test progressed, the system stiffness reduced significantly due to the progressive collapse of voids, followed by the exponential hardening effect caused by the deformation of the geofoam blocks when all the voids have fully collapsed. As anticipated, other than the first initial stiffness at the beginning of the test, an average expected force of 2.0 kN was achieved within a corresponding average displacement of 225 mm after the voids have fully collapsed. More importantly, the curves of Fig. 3-7 indicate that changing the contact surfaces between the SGB and the sand fill does not have a noticeable effect on the force-displacement behaviour of the system.

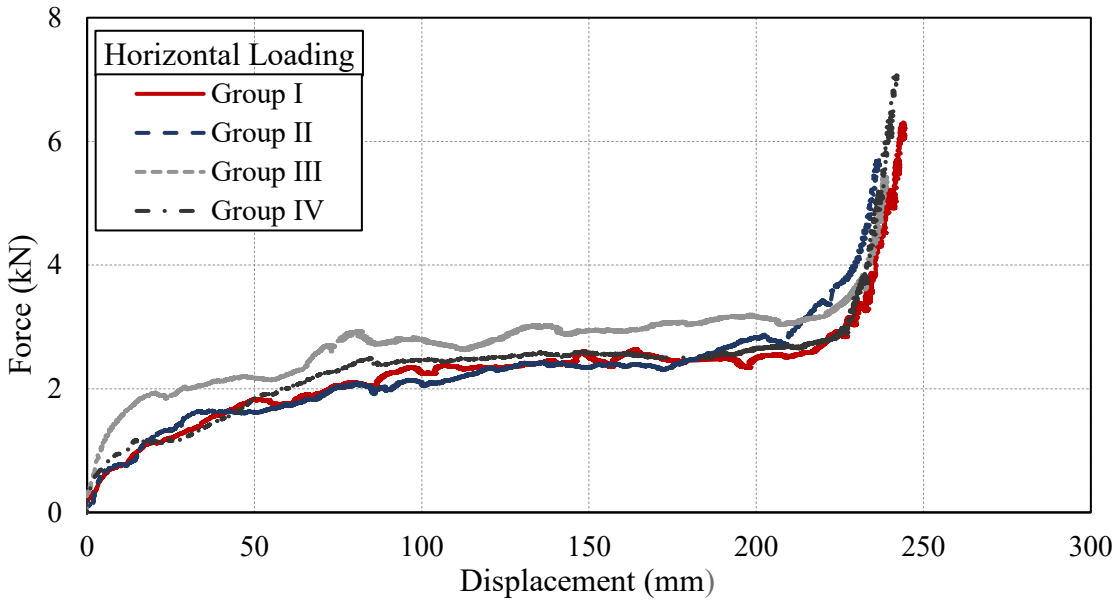

Figure 3- 7: Force – displacement response for horizontal loading (groups defined in Table 3-1).

Referring to Fig. 3-7, the results of Groups I and II tests show that the system compressed somewhat linearly to a lateral load of approximately 0.64 kN at 5.71 mm displacement and 0.66 kN at 5.84 mm displacement, respectively. However, those of Groups III and IV were recorded to occur at approximately 1.23 kN at 5.85 mm displacement and 0.76 kN at 5.33 mm displacement, respectively. Group III had the largest initial stiffness of 0.210 kN/mm, followed by Group IV with 0.143 kN/mm, then Group II with 0.113 kN/mm and finally Group I with 0.112 kN/mm. Groups I and II indicate

nearly identical initial stiffness and a continually increasing load that followed an initial linear part of the curve that stems from having the same contact surface area between the plastic sheets and the SGB used in both tests.

Beyond the initial linear region, the forces across each group increased at a rate of approximately 0.01 kN/mm. As shown in Fig. 3-7, Groups I, II and IV have almost identical force-displacement responses, indicating less dependency of the system response to the different cover arrangements examined here. However, Group III behaved slightly differently from the rest of the tests, which can be attributed to the rough contact surface area between the SGB and the geofoam layers. The highest peak force for each group was calculated by ignoring the final hardening region of the curves, as this region does not contribute to the intended response of the SGB. The peak force equal to 3.58 kN at 230 mm displacement was recorded for Group III. The peak force and the corresponding displacements experienced by Groups I, II and IV are 3.06 kN at 230 mm, 3.9 kN at 230 mm, and 3.3 kN at 230 mm, respectively.

The force-displacement responses of all four groups are shown in Figs. 3-8a to 8d. The results of the first three sets of Group I, as defined in Table 3-1, were considered inaccurate because the specimen did not uniformly deform as expected due to the inflow of sand particles into the voids. Minor discrepancies observed between the response of each group can be attributed to the imperfections in the SGB specimen, the differing contact surface of the cover configuration across each group, and the sands getting into the gap between the walls of the sand container and the SGB specimen as experienced in H7. The latter is not expected in the field applications since there would be no gap between the installed SGB.

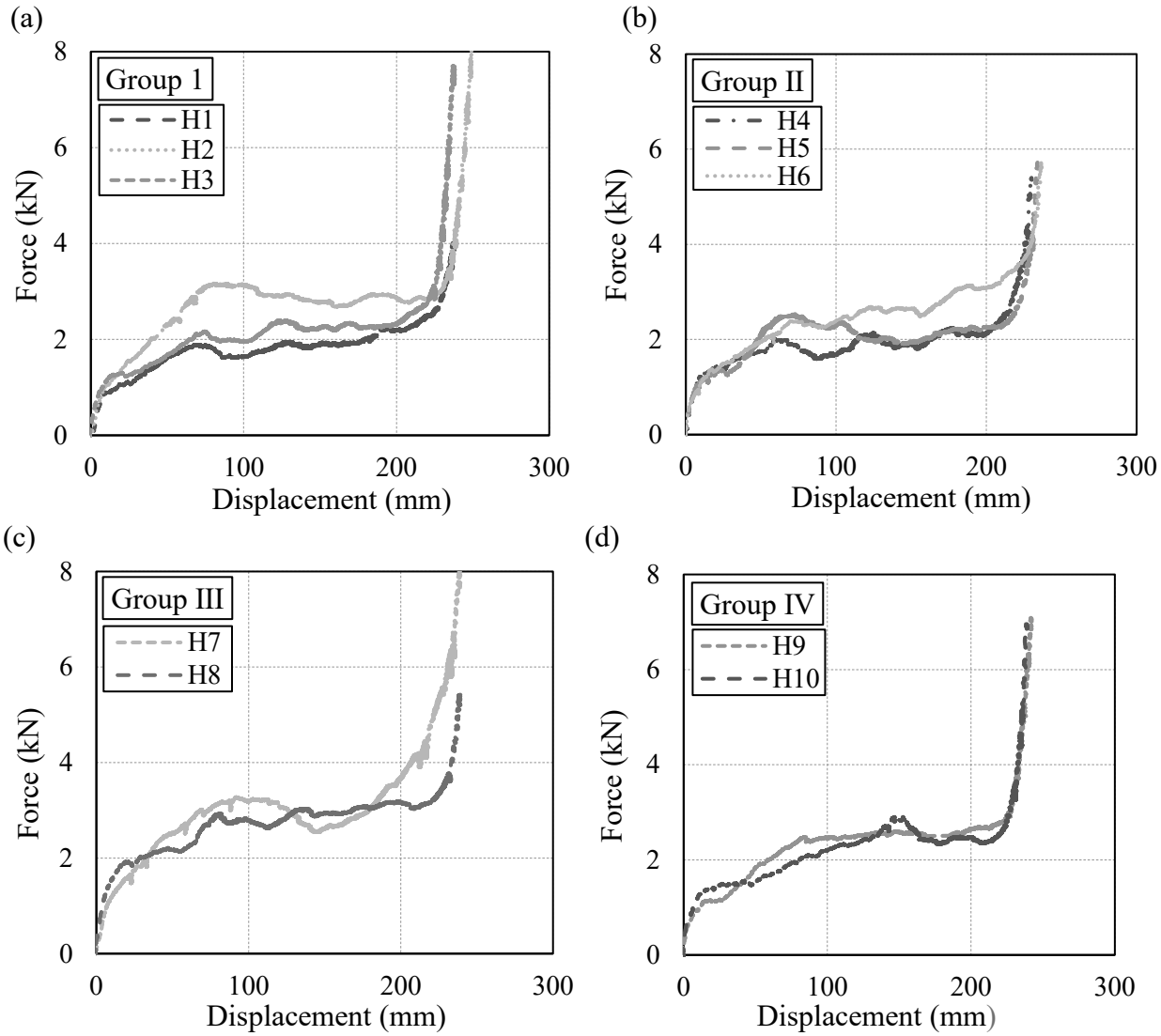

Figure 3- 8: Force – displacement response of individual groups of the horizontal loading case: a) Group I; b) Group II; c) Group III; d) Group IV.

The evaluation of the SGB response under the horizontal loading condition suggests that the proposed SGB can favourably be used as a proper remediation technique for pipeline networks. Furthermore, the observed force-displacement response can be simulated using a trilinear curve involving the initial stiff region, a nearly linear region representing the stepwise collapse of the voids and the final hardening region. Such simplification can be used as an efficient tool by the

pipeline designer to reproduce the relationship between the SGB force and displacement when developing the numerical model of the system. Moreover, the force-displacement relationship can be used to select an appropriate set of geofoams and voids in order to accommodate the expected lateral displacement of the pipe through a progressive collapse of the voids and not the failure of the geofoam blocks.

3.6.2 Downward Loading

The force-displacement responses of the tests involving the downward loading condition are shown in Fig. 3-9. The curves show that the system possesses a nonlinear behaviour that can be approximately reproduced via multiple linear segments. The average initial stiffness between the Groups is 0.05 kN/mm recorded at an average force of 0.95 kN and a displacement of 17.9 mm. As the SGB displaces against the pipe, a stepwise collapse of the voids was observed in both tests with gradually increasing force as the voids collapse. Similar to horizontal loading cases, the response approaches to exponentially increasing force due to the hardening effect caused by the deformation of the geofoam blocks when all the voids have fully collapsed.

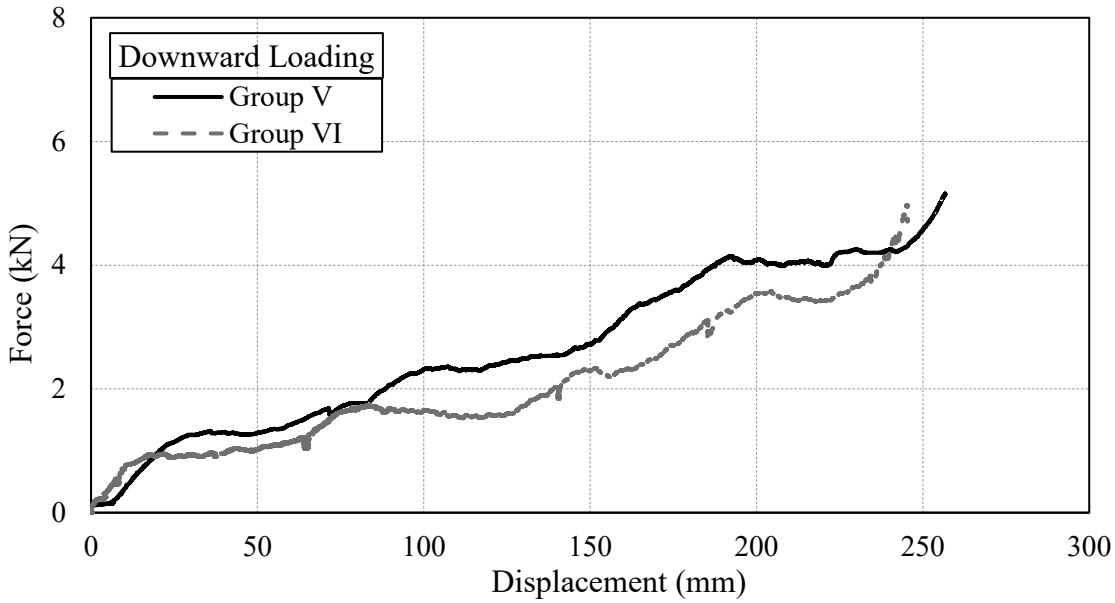

Figure 3- 9: Force – displacement response for downward loading (groups defined in Table 3-1).

The comparison between the two groups in Fig. 3-9 shows that the system response follows a nearly similar pattern with Group V, having a slightly higher force than Group VI. Group V reached a peak force of 4.2 kN at a corresponding displacement of 237 mm, while 3.9 kN at 236 mm displacement was recorded for Group VI.

The average reaction force in the downward loading tests increased by approximately 19% compared to that observed in their horizontal loading counterparts. This increase in the reaction force is attributed to the variation in the backfill weight of the soil, and more importantly, the reaction force developed between the pipe and horizontal plane that is translated to an additional force acting in the direction of the applied load. This suggests that when there is a downward ground movement in a field condition, a high reaction force is expected due to the horizontal component of the force resisted by the ground surface acting against the pipe.

Figure 3-10 shows the force-displacement response for each group of specimens (see Table 3-1) tested in the downward condition. The reasons for discrepancies observed in each group are identical to those described for the horizontal loading tests. Similar to the horizontal loading tests, a simplified trilinear model matching the nonlinear force-displacement response reported here can be used by the engineer for analyzing the effect of downslope movement on a pipeline network upgraded by the proposed SGB.

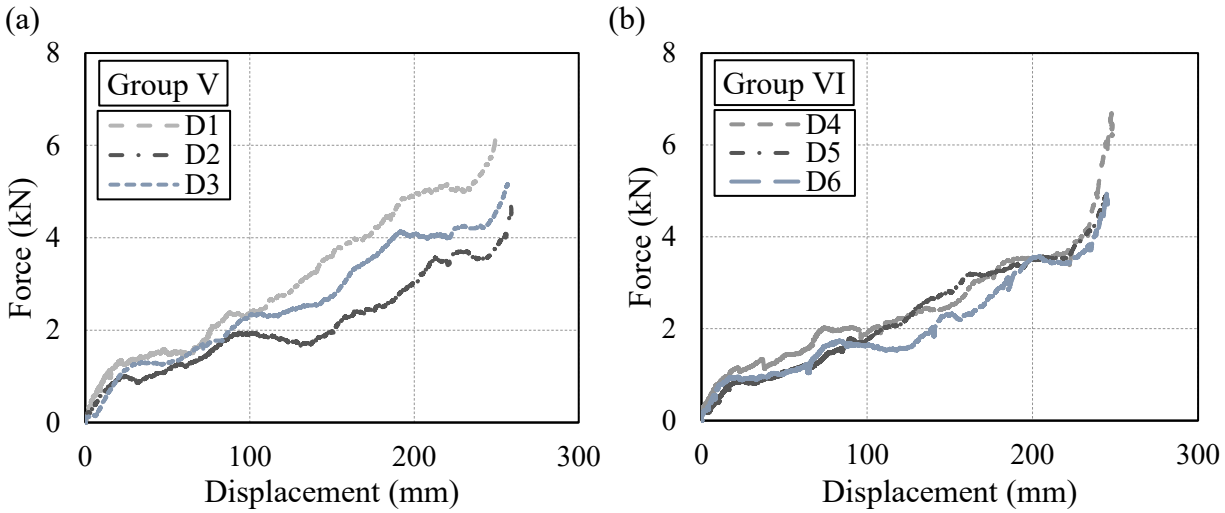

Figure 3- 10: Force – displacement responses for the individual groups of downward loading tests: a) Group V; b) Group VI.

3.6.3 Upward Loading

The force-displacement responses for the upward loading tests are shown in Fig. 3-11. After an initial stiffness of 1.23 kN/mm, a relatively low stiffness while the voids collapse was observed, followed by the exponential hardening effect contributed by the geofoam blocks after all the voids have fully collapsed. A peak force of 2.89 kN at 221 mm displacement was recorded for Group VII, while Group VIII specimens experienced, on average, a peak force of 2.7 kN with a corresponding displacement of 217 mm.

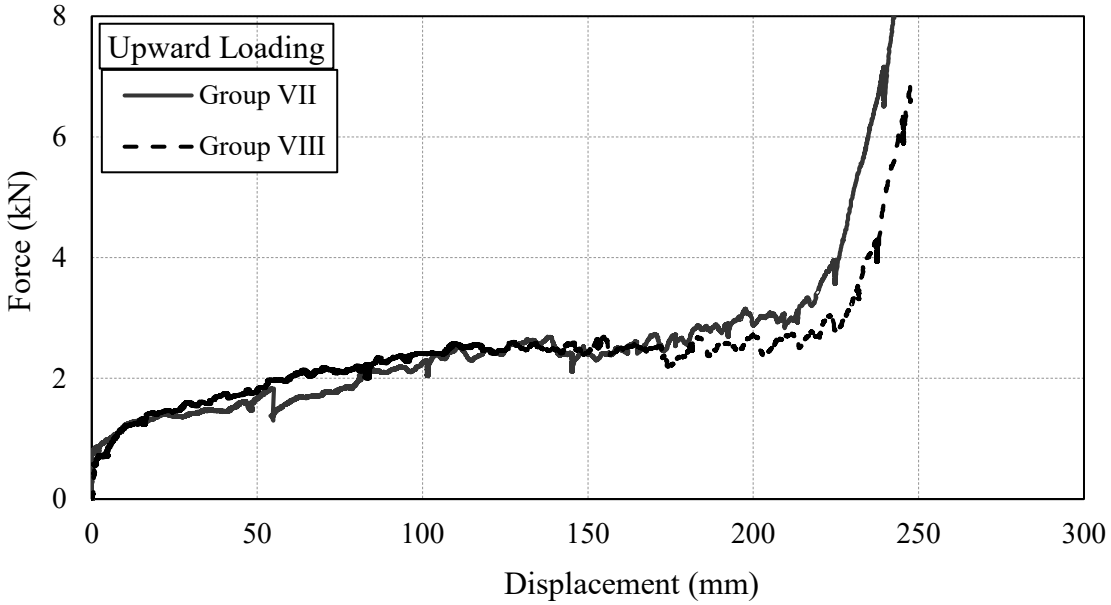

Figure 3- 11: Force – displacement response for downward loading (groups defined in Table 3-1).

Figure 3-12 shows the response for each group of the upward loading case (see Table 3-1). Similar to the previous loading angles, the discrepancies observed in each group are attributed to imperfections in the SGB and irregularities in the height of the geofoam blocks from test to test, and the sands getting into the gap between the walls of the sand container and the SGB.

The response of the SGB under the upward loading condition was observed to be approximately similar to their horizontal counterparts as no effect on the reaction force was contributed by the ground surface of the test setup as seen in the downward loading case, and the SGB still resisted the horizontal component of the applied force at a given displacement. Moreover, the results indicate that a simplified trilinear force-displacement curve can be employed by the engineer for analyzing the effect of upslope movement on a pipeline network, e.g., running across a steep mountainous region.

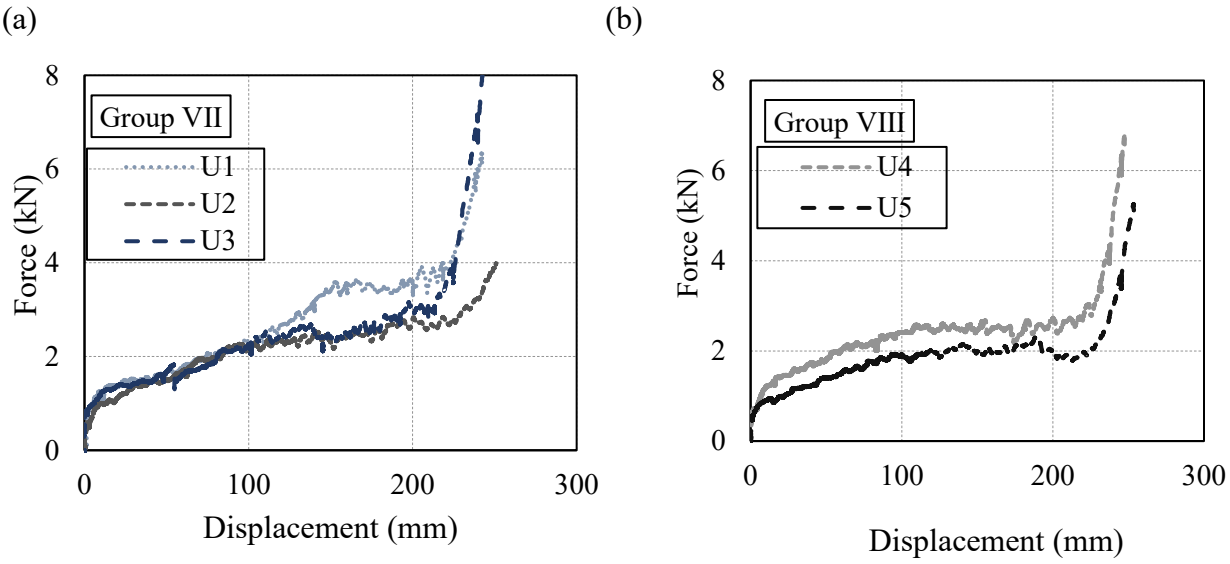

Figure 3- 12: Force-displacement responses for the individual groups of upward loading tests; a) Group VII, b) Group VIII

Overall, the response observed across each case of loading angle indicates that the system would have a nearly identical response for pipelines moving across a lateral and an upslope ground movement. In contrast, pipelines subjected to downslope ground movements may experience a continuous increase in reaction force with increased soil displacement. Additionally, for the sake of design, the designer should account for the loading angle of the ground displacement when selecting the SGB since a pure lateral pipe displacement is rarely seen in practice; more so, the loading angle would affect the amplitude of the reaction force to be experienced by the pipeline. It is also worthy to note that the mitigation measure evaluated in this study only applies to pipelines undergoing lateral and oblique ground displacement.

3.7 SPRING-BASED ANALYTICAL MODEL

3.7.1 System Description

A simplified spring-based model was developed to analytically predict the response of the pipe-SGB-soil assembly. The model can be used by the pipeline engineer to predict the anticipated

displacement accommodated by the SGB when the pipe is subjected to lateral ground deformation, determine the force attracted by the pipe as it laterally displaces, gain insight into the force – displacement response of the assembly for any given geometrical configuration of the SGB and identify the parameters affecting the response of the assembly. The proposed model was validated using the experimental data from the cross-sectional tests.

3.7.2 Model Formulation

3.7.2.1 Assumptions

The proposed model features a set of relatively stiff elastic-perfectly plastic translational strings to represent geofoams and a set of relatively flexible elastic-perfectly plastic springs simulating intermediate voids that act in series, as shown in Fig. 3-13. The key mechanical assumptions adopted here are as follows:

a) Elastic-perfectly plastic springs with significantly large elastic stiffness are used to simulate friction between the soil backfill and the SGB.
b) The load is transferred from the pipe to the support (Fig. 3-13) through friction generated between the soil and the SGB. The interface frictional forces developed between the soil and the SGB (Fig. 3-3) are a function of the contact surfaces and the weight of the soil backfill.
c) A void is assumed to collapse when the frictional forces developed between the moving end of the SGB adjacent to the pipe and the void are reached. Thus, a stepwise response is expected as each void moving towards the fixed end collapses.
d) The stiffness of the void block in the elastic region is considered 10% of that of the adjacent geofoam block. It should be noted that this assumption is not expected to affect the anticipated response of the SGB, given that friction governs the force generated in the assembly. The geofoam blocks are assumed to act as a set of relatively rigid elastic-perfectly plastic springs

with negligible internal deformation that are capable of transferring the loads to the adjacent voids, which are modelled using a set of relatively flexible elastic-perfectly plastic springs while moving as a rigid body in the direction of the applied displacement.

e) The contribution from the geofoam deformation, which is insignificant compared to the void displacement, is neglected in the model.

f) The frictional forces between the SGB-soil interfaces are accounted for by multiplying the overlying soil pressure on the SGB by the coefficient of friction $\mu = 0.64$ as recommended by (Horvath et al. 2004)

g) The minimal effect of the encased corrugated plastic sheets on the frictional forces developed is neglected.

h) The hardening zone of the force-displacement response (Fig. 3-7) that stems from the limited internal deformation of the geofoam block after the voids had collapsed is not considered for simplicity and the fact that the hardening region is not a controlling parameter in design.

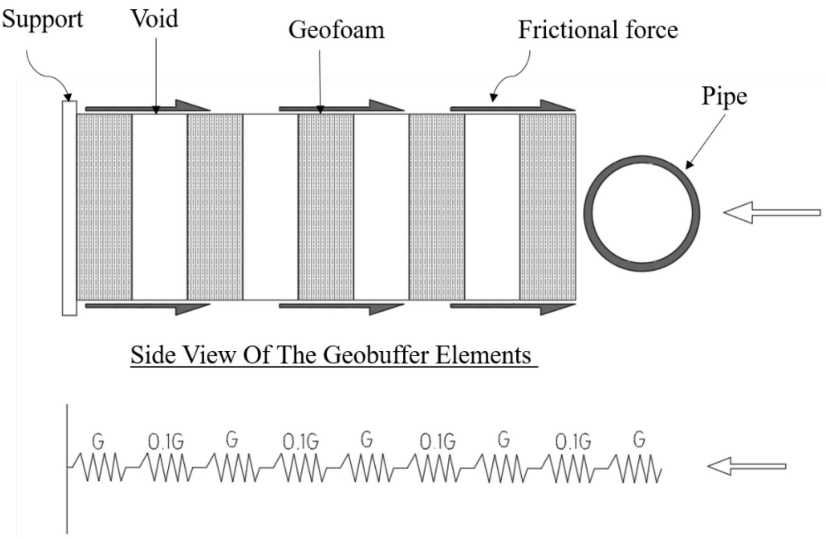

Figure 3- 13: Spring-based analytical model (*G* represents the elastic stiffness of geofoam springs).

3.7.2.2 Mathematical Formulation

The effective frictional force F_f due to the soil backfill atop of the SGB can be computed as follows:

$$F_f = \mu F_N \qquad \text{where} \quad F_N = \rho w h \qquad (1)$$

where F_N is the normal force acting atop of the SGB, ρ is the soil density, w is the width of the SGB, and h is the depth of trench cover.

As the SGB element displaces against the pipe, the frictional force F_i, which is generated between the soil and a set of geofoam and void blocks, can be obtained as:

$$F_{f,i} = F_N x_i \qquad (2)$$

in which x_i is the summation of the thicknesses of the set of geofoam and void blocks that has displaced, which led to the development of the frictional force within their thicknesses. The frictional force developed at the end of the first step (i =1) as the first void collapses and the first geofoam adjacent to the pipe displaces is then denoted by $F_{f,1}$.

Similar frictional forces are expected to develop as the lateral displacement increases while the SGB deforms further. The force generated by friction in the next step $F_{f,2}$ should be added to the force obtained in the first step $F_{f,1}$ to obtain the resultant or total force $F_{f,e}$ when the second set of geofoam block and void is engaged:

$$F_{f,e} = F_{f,1} + F_{f,2} \qquad \text{where } F_{f,2} = F_N x_2 \qquad (3)$$

where x_2 is the summation of the thicknesses of the second set of geofoam and void elements, as shown in Fig. 3-13. A similar approach is taken until all the void elements have entirely collapsed. This condition represents the complete collapse mechanism of the proposed SGB, which may not necessarily be achieved in an actual loading condition because significantly large ground movement may be required to achieve this condition. Nonetheless, it provides the force capacity and respective displacement that the SGB can offer.

The proposed analytical model was verified using the experimental test data presented in this paper. For this purpose, the force-displacement response of the pipe-SGB-soil assembly predicted by the model was compared to those obtained for the specimens tested under the horizontal loading condition (Fig. 3-7). The comparison is shown in Fig. 3-14. As shown, the prediction by the analytical model proposed here is in good agreement with the test data obtained from Groups I, II and IV. The amplitude of the force is slightly over-predicted with an average percentage error of 13%, which can be attributed to the experimental errors and assumptions made in the development of the analytical model. The predictive model for Group III tests was obtained using a higher coefficient of friction $\mu = 0.75$ to account for the rough contact surface between the SGB and the geofoam layers used in Group III tests (Table 3-1). As shown, a good match was observed between the prediction and test results, which suggests that a proper estimate of the coefficient of friction between the contact surfaces shall be used in the design.

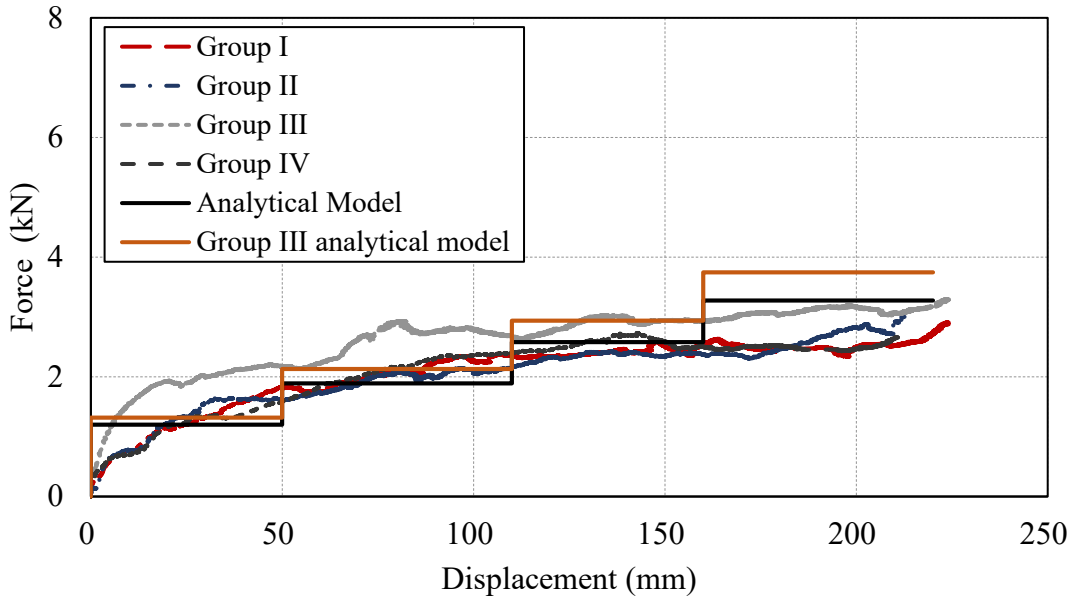

Figure 3- 14: Comparison of the force – displacement response for horizontal loading case: analytical model prediction vs. test data.

It is significant to note that the proposed analytical model is intended to provide the engineer with an estimate of the force and displacement response of the pipe-SGB-soil assembly to configure the SGB for an anticipated ground deformation and is expected to be used in conjunction with a detailed numerical model (e.g., finite element analysis method) in design.

The proposed analytical model can be applied in angled loadings with the exception that the horizontal component developed between the pipe and horizontal plane in the downward loading condition should be accounted for in the calculation of the force resisted by the pipe.

3.8 EVALUATION OF THE GEOMETRICAL PROPERTIES OF THE SGB

A parametric investigation was carried out to evaluate the factors affecting the behaviour of the pipe-SGB-soil assembly. For this purpose, the number and the thickness of the geofoam layers were varied. Each layer of a geofoam includes a geofoam block and void. A range of 9 to 13 geofoam layers and varying thicknesses 55 mm, 110 mm, and 165 mm were examined.

3.8.1 Influence of number of Geofoam layers

The SGB with a geofoam thickness of 55 mm was used to study the effect of the number of geofoam layers. Fig. 3-15a compares the effect of the number of geofoam layers on the force-displacement response of the pipe-SGB-soil assembly. The maximum force and corresponding displacement for each case are also provided. As shown, a minimal change was observed in the force amplitude when increasing in the number of geofoam layers, suggesting that the number of geofoam layers did not affect the dissipated force at a given displacement (i.e., anticipated ground deformation) before the complete collapse. The results of this evaluation confirmed that the number of layers could be adjusted along the length of the pipe to achieve the desired displacement anticipated during the ground movement with a sufficient margin of safety.

3.8.2 Influence of thickness of Geofoam layers

The thickness of the geofoam layers was varied at a range of 55 – 165 mm while keeping the number of layers at a constant value of 9. Fig. 3-15b compares the effect of the thickness of the geofoam layers on the force-displacement response of the subassembly. An increase in the thickness of geofoam layers increases the amplitude of frictional forces that need to be overcome, and as a result, a higher force is developed in the assembly before all the voids have completely collapsed. Moreover, the geofoam with thicker blocks can sustain a larger displacement demand, e.g., ground deformation, which can be beneficial for the pipes subjected to large lateral ground movements. However, the force developed at a given displacement does not follow the trend observed for the maximum displacement, which suggests that an optimized layer thickness should be selected by the engineer for an anticipated pipe lateral displacement. It should be noted that the selection of the layer thickness may be limited by the available EPS geofoam and manufacturing capabilities.

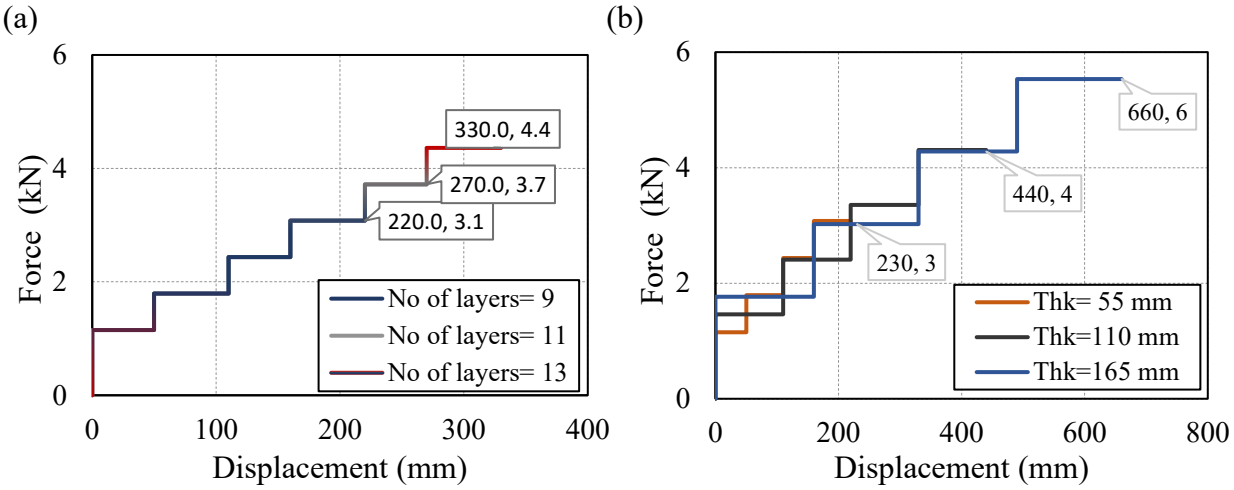

Figure 3- 15: a) Influence of the number of geofoam layers; b) Influence of thickness of geofoam layers (Thk denotes the SGB layer thickness).

3.9 CONCLUSIONS

The occurrence of ground-induced actions on buried steel pipeline networks has posed a significant threat to the structural integrity of these infrastructures. These potential damages can be curbed by

installing special geomaterial blocks (SGB) consisting of a set of expanded polystyrene geofoam and polypropylene squared plastic boxes adjacent to the pipe. This technique takes advantage of the orthotropic mechanical property of the SGB, which significantly limits the induced stresses and strains in the pipe when subjected to ground deformation induced from multiple mechanisms while allowing the pipe to move along its cross-sectional plane. An experimental test program was developed to examine the interaction between the pipe, the SGB and soil, the influence of the loading angle and the SGB cover configuration. A simplified spring-based analytical model was also proposed to predict the force-displacement response of the pipe-SGB-soil assembly. The key findings of this study can be summarized as follows:

- A novel remediation technique, which involves altering the boundary condition of buried pipelines with the adjacently installed SGB, consisting of a set of expanded polystyrene geofoam and polypropylene squared plastic boxes, was proposed to improve the safety and structural integrity of buried steel pipelines subjected to ground deformation. The proposed technique was validated using experimental cross-sectional testing.
- The interaction between the pipe, soil and the SGB, along with the interface frictional forces developed between the SGB and overlaying soil pressure, were identified using the experimental tests.
- The experimental test results confirmed that the cover configuration has minimal impact on the force induced in the pipe-SGB-soil assembly unless a rough contact surface (e.g., the SGB interacting with the geofoam) was used.
- The results obtained from the tests showed that the response of the proposed mitigation technique is affected by the loading angle. The reaction force is increased in downward loading due to the horizontal component of the force developed between the pipe and the

horizontal plane on which the pipe rests. In contrast, an approximately similar response was observed in both horizontal and upward loading conditions.

- The force-displacement response of the pipe-SGB-soil assembly can be simulated using a trilinear curve involving the initial stiff region, a nearly linear region representing the stepwise collapse of the voids and the final hardening region. This relationship can be used as an efficient tool by the pipeline designer to configure the SGB for an anticipated ground deformation and to develop the numerical model of the system.
- A simplified spring-based analytical model was proposed to predict the force-displacement response of the pipe-SGB-soil assembly. The proposed analytical model well predicted the force-displacement response of the assembly, displacement tolerated by the SGB before the voids have collapse and the force attracted by the pipe.
- The parametric study performed using the proposed analytical model showed that increasing the number of geofoam and void blocks does not appreciably affect the system response. However, thicker geofoam and void blocks can accommodate greater displacements while maintaining the flexibility of the system.
- The proposed spring-based analytical model can serve as an efficient design tool to estimate the force and displacement response of the pipe-SGB-soil assembly in order to configure the SGB for an anticipated ground deformation and identify the parameters affecting the response of the assembly. The model should be used in conjunction with a detailed numerical model in design.

Future studies should further investigate using large-scale laboratory testing and advanced numerical simulations the adequacy and efficiency of the proposed mitigation technique.

3.10 Acknowledgment

Financial support provided by the Natural Sciences and Engineering Research Council (NSERC) of Canada is acknowledged. The authors would like to acknowledge the financial support and in-kind contributions of donating test specimens by ALFA Upgrades. The authors wish to thank Prof. Mustafa Gul of the University of Alberta for providing laboratory space to conduct the experimental work and Dr. Onyekachi Ndubuaku for his input throughout the project.

4. LARGE-SCALE LABORATORY TESTING AND NUMERICAL MODELLING

4.1 Abstract

This paper presents a laboratory testing program and numerical modelling technique to examine the efficiency of a new remediation technique used to improve buried pipelines' safety and structural integrity when subjected to lateral ground movements. This technique involves the installation of special geomaterial blocks (SGB) adjacent to a pipeline to reduce the stresses and strains induced in the pipe when subjected to permanent ground deformations. The proposed element involves a set of Expanded Polystyrene (EPS) geofoams and lightweight polypropylene squared plastic boxes designed to act as voids between the EPS geofoam blocks. The SGB is oriented such that its orthotropic mechanical property allows the pipe to move laterally without developing significant reactions. A full-scale experimental test program developed to evaluate the beneficial effects of the SGB on the pipe response when subjected to lateral and oblique displacements is presented first, followed by a finite element model proposed to numerically simulate the pipe-SGB-soil interaction under lateral soil displacement. The numerical model is validated using the data obtained from the experimental tests. The results of laboratory testing and numerical simulations confirm the efficiency of the proposed remediation technique in improving the structural integrity of buried pipelines. Furthermore, by choosing the appropriate spring stiffness representation of the SGB, the proposed beam model is able to predict the global lateral load-deformation response of the system accurately; finally, this model can be used in practice to predict the response of the buried pipelines equipped with the SGB.

Keywords: Buried pipelines, Ground deformation, Geomaterial, Laboratory testing, Computer simulation.

4.2 INTRODUCTION

Buried steel pipelines used to transport oil and gas traverse long-distance areas susceptible to ground deformations. Ground-induced actions are considered a significant cause of failure in pipeline networks. The ground movement that takes place in the form of landslides, moving slopes, earthquake-induced faulting, urban excavation, soil liquefaction, or excessive ground settlement can result in significant damage to buried pipelines, leading to detrimental societal, environmental, and economic effects (Ariman et al. 1987, Fathi et al. 2018, O'Rourke and Stewart 2000, Vazouras et al. 2012, Rofooei et al. 2012, Sim et al. 2012). For instance, the water supply and gas distribution system in Los Angeles damaged during the 1994 Northridge earthquake caused severe gas explosions and simultaneous flooding along the San Fernando valley (Schiff and Hills 1995). The data published by the National Energy Board (NEB 2011) indicated that geotechnical loads caused approximately 7% of pipeline incidents in Canada from 1991 to 2009. In 2013, Enbridge, Canada, reported a heavy rainfall that triggered ground movement at a slope near the Cheecham Alberta pipeline's right-of-way, which led to approximately 1,300 barrels of light synthetic crude oil leaking from the damaged pipeline, causing a temporary suspension of service and large financial losses (Enbridge 2013).

When ground deformation occurs, portions of the pipeline network are subjected to a thrust deformation pattern accompanied by high stresses and strains, often beyond the pipe limit state (Fathi et al. 2018, Vazouras et al. 2012). In particular, high tensile stresses near girth welds may lead to pipe fracture, whereas high compressive stresses can result in wrinkling or local buckling of the pipe wall, which in some cases may trigger global instability of the pipeline. It is, therefore, crucial to identify the potential hazards causing permanent ground deformation and mitigate the detrimental effects of such deformation on pipelines to avoid failures and their consequences.

4.2 EXISTING MITIGATION METHODS

Due to the hazardous nature of buried pipelines, pertinent efforts have been ongoing to develop effective remediation techniques for protecting pipelines against the consequences of ground deformation. Several methods have been proposed and implemented to mitigate the effects of ground movement on buried pipelines and enhance their performance. The key mitigation techniques are summarized here.

Slope stabilization techniques have been employed as one of the practical ways of curbing the effects of downhill creep or landslides. This measure involves various techniques such as excavation and regrading of slope geometry, managing the groundwater through drainage systems and reinforcing the slope (Saftner et al. 2017). However, slope stabilization techniques may be uneconomical and typically exceed the pipe's right-of-way. O'Rourke and Liu (1999) proposed the use of stronger material and larger pipe wall thickness to improve the performance of buried steel pipelines when the longitudinal pipe strain dominates the pipe's response. Periodic excavation and backfilling of pipe (i.e., stress relief) under slow but steady ground movements seems beneficial for pipes installed on slopes with downhill creep; however, with the remoteness of some transmission lines, this method may not offer the best economic approach and may also damage the existing pipe during the excavation process (Lockey and Young 2012).

Wide trenches with soft backfill enable the pipe to distribute the applied displacements to a longer distance by reducing the backfill resistance against the movement. However, the variations in the geomechanical properties of the soil medium and the embedment conditions of the pipe may increase the backfill resistance against the movement. Furthermore, the need for larger trench excavation and transportation of the desired backfill material may significantly increase the costs associated with constructing pipelines in remote sites (Honegger et al. 2010).

Dredged materials such as sand have widely been employed for backfilling pipelines as a cost-efficient solution to alleviate ground-induced effects. However, the stiffness of the material used as the backfill can influence the efficiency of the method, aggravating the pipeline response when subjected to large ground movements (Paulin 1998).

The benefits of using geotextile and geogrid reinforcement in reducing the effects of soil loads on buried pipelines were investigated in the past. Moghaddas and Khalaj (2008) used geogrid reinforced sand to protect buried pipelines against traffic loads through a series of laboratory tests on small-diameter High-Density Polyethylene (HDPE) pipes. The results showed an approximately 56% reduction in the vertical pipe deformation and a 65% reduction in the soil surface settlement compared to tests conducted with unreinforced soil. Palmeira and Andrade (2010) performed a series of small-scale tests using a combination of geotextile and geogrid reinforced soil to protect buried Polyvinyl Chloride (PVC) pipelines against accidental damages. The tests confirmed that reinforced sand could result in an approximately 40% reduction in the pipe strains compared to the unreinforced sandbed.

Expanded polystyrene (EPS) geofoams were used as a lightweight cover to protect the pipe against applied loads, which resulted in reducing the horizontal force on the pipe by 50% compared with the case where a standard sand cover is used (Yoshizaki and Sakanoue 2003). Moreover, it was found that the resistance of pipe elbows, when subjected to ground displacement, is significantly improved as long as EPS geofoam backfill is placed around the pipe elbow. Choo et al. (2007) experimentally evaluated the benefits of using EPS geofoam as a lightweight cover material in reducing stresses on high-density polyethylene (HDPE) pipe subjected to permanent ground deformation. This study found that the transverse lateral force at the soil-pipe interface can be reduced by 80%, and the reduction is a function of the orientation of the pipe with respect to the

fault line. The reduction in the lateral force led to a 45 to 60% reduction in the pipe bending strain compared to the system without EPS remediation. However, the remediation technique was less effective in reducing the pipe axial strain.

More recently, the benefits of using EPS geofoam blocks as a lightweight cover and a compressible inclusion for pipes undergoing vertical and horizontal ground movements were evaluated using a series of field and laboratory tests (Lingwall et al. 2012, Bartlett and Lingwall 2014). This study confirmed that the geofoam cover could reduce the peak vertical uplift force to 136 kN at a displacement of 136 mm compared to the native soil backfill test where the pipe experienced an uplift force of 520 kN at a displacement of 70 mm. However, the test results showed that using geofoam blocks as a compressible inclusion results in a higher resistance for pipes undergoing large horizontal displacement compared to traditional sand backfill.

Other than mitigation techniques that involve changing the pipe properties or altering soil-pipe interaction, rerouting pipelines and periodic pipe monitoring have been proposed to overcome the detrimental effects of ground deformation. Rerouting pipelines by avoiding areas with possible geohazards can significantly reduce the risks associated with ground deformation; however, deviation from the desirable path may result in a longer pipeline, leading to higher construction costs and potential issues with the pipeline right-of-way (Sancio et al. 2020). Periodic pipe monitoring involves installing force-displacement measurement devices such as fibre optic cables on pipelines to monitor pipe profiles and ground movements (Honegger et al. 2010). Nonetheless, this technique only identifies the potential hazards and requires a mitigation technique to eliminate existing hazards.

To address high construction or upgrade costs and achieve a more efficient remediation technique for buried pipelines undergoing ground deformation, a novel mitigation technique has recently been studied by the authors (Ilozumba et al. 2021). This method involves the installation of special

geomaterial blocks (SGB) consisting of a set of expanded polystyrene (EPS) geofoam and polypropylene squared plastic boxes designed to act as voids between the EPS geofoam blocks. Unlike the past techniques using EPS geofoams, where the ESP geofoam serves as a compressible inclusion and a lightweight cover, the SGB, which are analogous to car fender when subjected to the displacement, alters the boundary conditions of buried pipelines. The lower horizontal translational stiffness of the SGB compared to the backfill material would enable the pipe to endure large lateral displacements by distributing the applied deformation over a longer length while attracting a minimal lateral force. As a result, the maximum pipe curvature and axial elongation can significantly be reduced, leading to lower longitudinal strain demands and making the pipe less prone to subsequent buckling or weld rupture. A series of cross-sectional tests were carried out by the authors (Ilozumba et al. 2021) to assess the local response of the pipe-SGB-soil assembly when subjected to lateral and oblique ground displacements, evaluate the influential effects, including the loading angle and the interface frictional force developed between the SGB and sand, on the efficiency of the proposed SGB, and verify the adequacy of the simplified analytical procedure proposed to predict the force-displacement response of the pipe-SGB-soil assembly. However, this mitigation technique has not yet been validated using full-scale laboratory testing under lateral loading representing ground deformation, and no numerical modelling method yet exists to simulate the response of the enhanced pipeline network when the adjacent soil induces lateral movement on the pipe.

This study aims to first experimentally validate the novel mitigation technique introduced to improve the structural integrity of buried pipelines subjected to ground deformation, then propose a numerical simulation technique to reproduce the pipe-SGB-soil interaction when the pipe is subjected to ground movements. The laboratory test setup and the testing procedure are first presented, followed by the results of the six full-scale tests on non-pressurized steel pipes with an outside diameter of 8.62

inches and a length of 6.0 m (19.7 feet). The tests were carried out under lateral and oblique soil loading conditions. A numerical modelling technique based on the finite element method is then proposed to reproduce the response of the pipe-SGB-soil subassembly. The model is calibrated using the experimental data obtained from the tests. The proposed numerical model is finally used to evaluate the response of the pipe with and without the SGB.

4.3 LABORATORY TESTING

A full-scale test program was developed to test the application of the SGB. In particular, laboratory testing was used to measure the force attracted by the pipe when the SGB are installed adjacent to the pipe as it is displaced by the lateral soil displacement. The test program was conducted at C-FER Technologies in Edmonton, Alberta.

4.4.1 Test setup and procedure

A schematic representation of a deflected pipe subjected to lateral soil displacement is shown in Fig.4-1a. In this study, the deflected curvature of the pipe represented with a fixed end (Fig. 4-1b) was simplified and used to design the test specimen as a pinned-end member such that there would be minimum pipe deformation and no lateral resistance arising from the pipe. In this way, emphasis is placed only on the influence of the SGB on the pipe response when subjected to the lateral displacement. This simplified pipe deformation is shown in Fig. 4-1c.

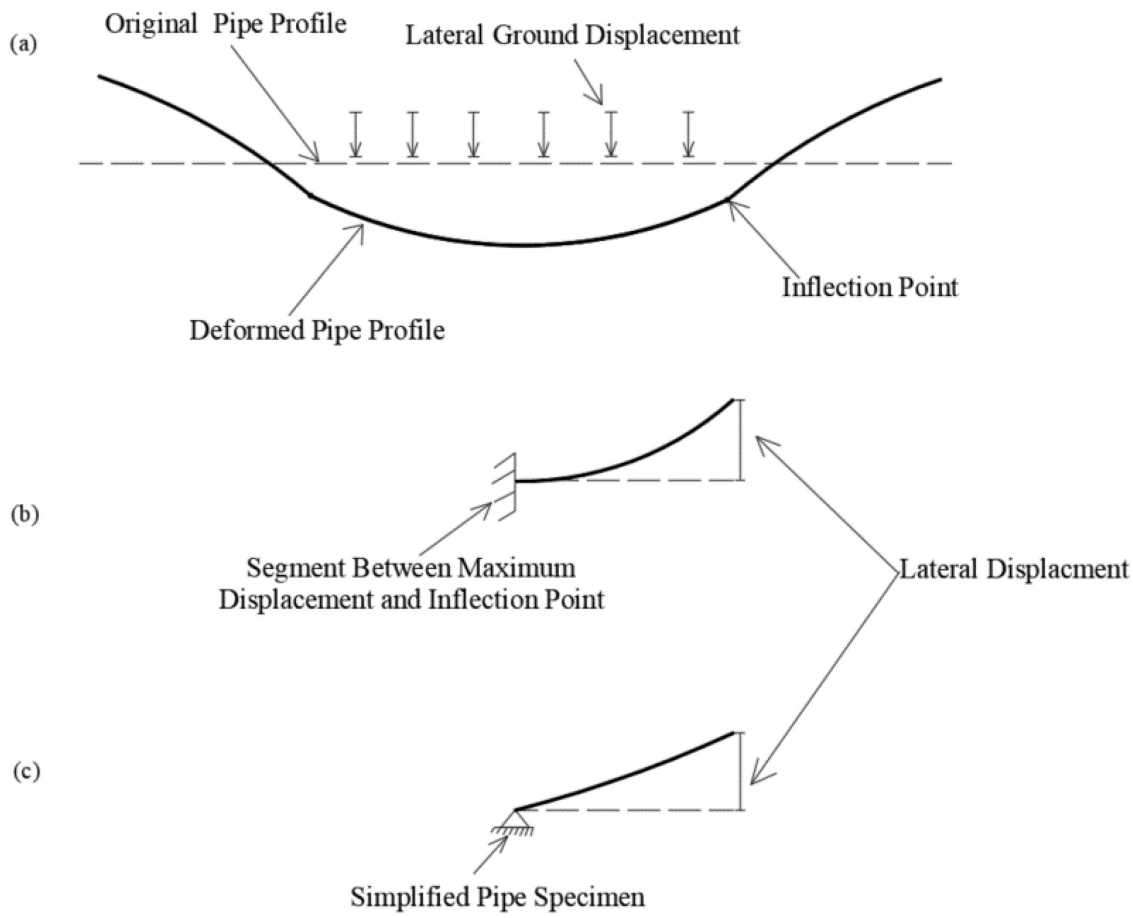

Figure 4- 1: a) Deformation profile of a pipeline subjected to lateral soil displacement; b) Pipeline segment between the maximum deflection and the inflection point; c) Simplified model to achieve the lateral displacement expected in the pipeline (soil reactions not shown).

The experimental test setup designed to achieve the deformation profile of Fig. 4-1c is shown in Fig. 4-2. The test setup consists of a wooden sandbox, geofoam blocks, Meccano columns, a hydraulic actuator and fixtures. The sandbox and its connections were designed following the guidelines of the engineering design in wood, CSA O86 (CSA 2014). The fixtures of the pipe end connections were designed as per the Canadian steel design standard CSA S16 (CSA 2019).

(a)

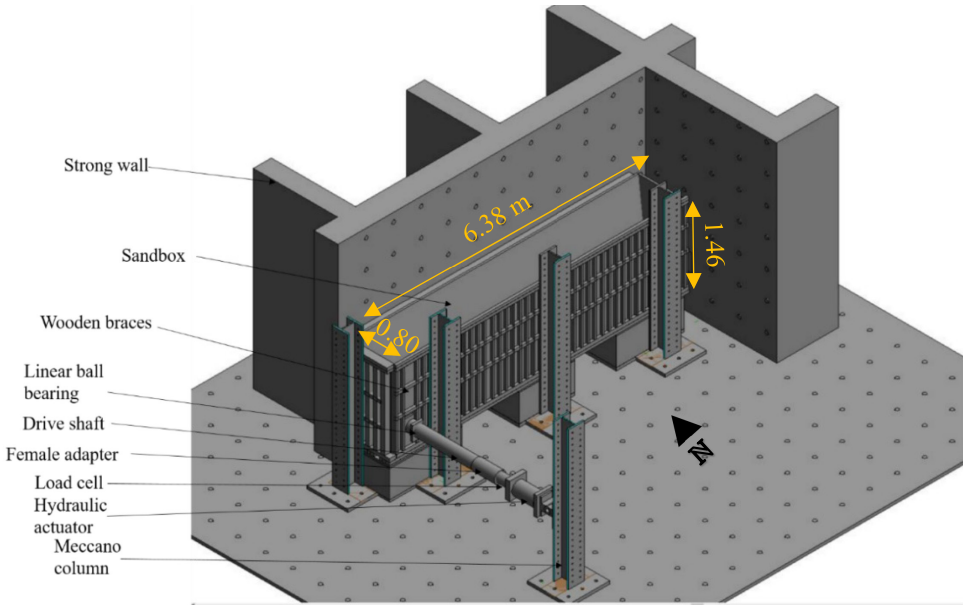

(b)

Figure 4- 2: Experimental test setup: a) 3-D representation; b) Photograph (Horizontal loading shown).

The sandbox is placed on three sets of geofoam blocks spaced at approximately 1.1 m intervals (Fig. 4-2b). The sandbox is oriented such that the strong wall of the laboratory can provide support along two sides (north and east) of the sandbox, while the other two sides are supported using

wooden braces connected to four Meccano columns. The east end of the pipe (Fig. 4-2b) is pinned using the connection shown in Fig.4-3a. The other end of the pipe, where it is loaded, is attached to a drive shaft using a collar via a slotted pinned connection to transfer only lateral force to the pipe without generating axial loading. A hydraulic actuator capable of producing up to 1150 kN push force with a total stroke length of 812 mm is mounted on the Meccano column placed at the west of the test setup (Fig. 4-2a). A tension-compression load cell with a capacity of 1000 kN is attached to the end of the actuator to measure the applied load. The load is transmitted to the pipe specimen through a 500 mm-long drive shaft, with one of its ends connected to the load cell and the other end connected to the pipe end fixture through a linear ball bearing. The tail end of the pipe on the east side of the setup is welded to a cap plate and a pivot bracket. The pivot bracket is connected to a double-sided pivot bracket, which is connected to a hinge support on the strong wall (Fig. 4-3a). The double-sided pivot bracket allows shear transfer to the supporting wall.

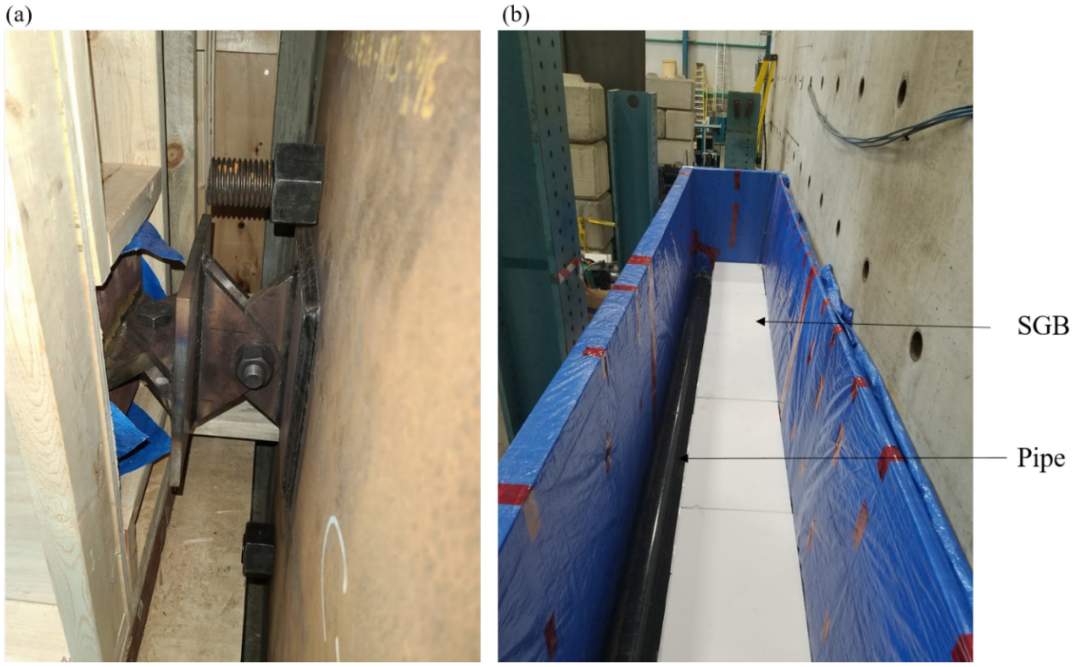

Figure 4- 3: a) Pipe end support condition (east end); b) Inside view of sandbox after the installation of the SGB.

A total of six full-scale laboratory tests were conducted. For each test, the 6-m pipe specimen was first placed in the sandbox. Twenty-seven sets of the SGB were then installed adjacent to the pipe as shown in Fig. 4-3b and backfilled. The centerline of the pipe rests 360 mm above the bottom of the box, producing a backfill height-to-pipe diameter of H/D = 5. Once the SGB were installed, polyethylene plastic sheets were placed around the SGB to prevent sands from getting between the SGB specimens. Approximately 8.0 m^3 volume of 5mm dried sand with a density of γ = 1551 kg/m^3 was then dumped through the top of the sandbox using the overhead crane without compaction to fill the sandbox with dimensions of 6.38 × 0.8 × 1.46 m (Fig.4-2a). The sand was uniformly spread using a shovel, levelled around the box, and emptied after each test. Fig. 4-4 shows the inside view of the test setup at the end of the test after the sand was emptied.

The pipe specimen used in the test program is a 219 mm- (8.62 in) diameter steel pipe with a nominal wall thickness of 8.2 mm and a resulting diameter-to-wall thickness D/t = 27. The material of the pipe conforms to G40.21 M350W (Surya 2020) with the yield and tensile strength of 310 MPa and 450 MPa, respectively. The test setup was designed such that the pipe remains elastic under the applied displacement as the SGB deform (see Fig. 4-1c).

(a) (b)

Figure 4- 4: a) Test assembly at the end of the test; b) Deformed SGB at the end of the test.

The sand backfill is classified as poorly-graded sand with a specific gravity of 2.65. The coefficient of uniformity, coefficient of curvature and the effective grain size of the sand are recorded to be 2.5, 3.3 and 0.2, respectively.

Two samples of the SGB used in this test program are shown in Fig. 4-5. The SGB comprises a set of EPS geofoams and lightweight polypropylene squared plastic boxes encased in corrugated plastic sheets and designed to act as voids between the geofoams blocks. For simplicity, the squared plastic boxes are referred to as voids throughout this paper. The SGB with four and five voids are shown in Figs. 4-5a and 5b, respectively. The EPS geofoam blocks are low-density lightweight plastic cellular geosynthetic material often used in geotechnical engineering for ground fill applications where lightweight fill material is required to reduce stresses on underlying soils. It also acts as a compressible inclusion as well as a thermal insulator. The EPS geofoams are designated with their density in kg/m^3. For instance, EPS46 represents an EPS geofoam with a nominal density of 46 kg/m^3. The standard density of EPS geofoams ranges between 11 and 46 kg/m^3. In this study, EPS39 was used to design the SGB.

The SGB has an orthotropic mechanical property, which provides higher stiffness in the vertical plane of geofoam layers. At the same time, it is relatively flexible in the direction perpendicular to the plane of geofoam layers. The geomaterials are to be placed adjacent to the buried pipe (Fig. 4-3b) such that their compressible axis is oriented against the pipe to allow the pipe to laterally move without developing significant reactions while resisting the weight from the soil overburden pressures acting on the top surface of the geomaterial. The thickness of the voids and geofoams are to be selected and verified, taking into account the passive pressure of the soil backfill.

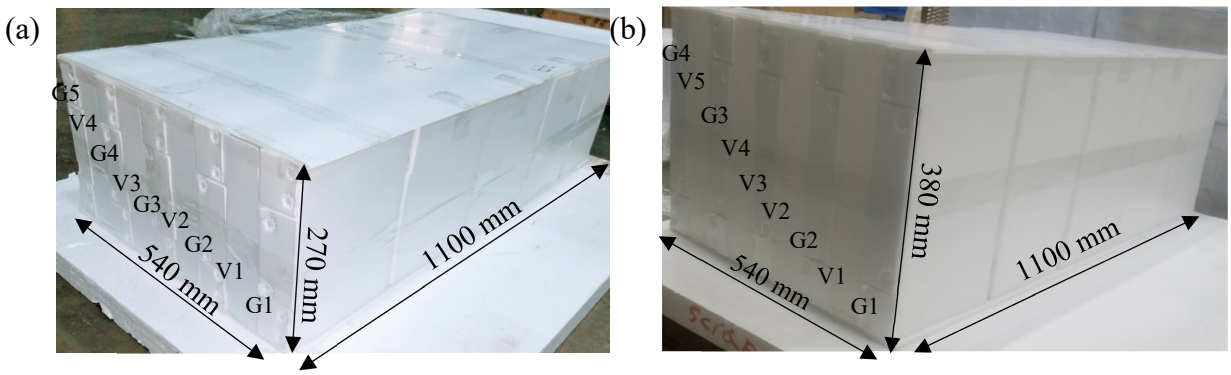

Figure 4- 5: Special Geomaterial Blocks (SGB) with a) 4 voids; b) 5 voids (G=Geofoam; V=Void).

4.4.2 Experimental test matrix

The full-scale laboratory tests were conducted by varying the number of voids and the loading angle with respect to the horizontal plane passing through the pipe centerline. Table 4-1 shows the experimental test matrix. In this table, 90 degrees indicates horizontal loading, while 27 and -27 degrees represent downward and upward loading, respectively. The angle of inclination of the hydraulic actuator was changed to achieve the loading angle anticipated in each test, Figs. 4-2b. 4-6a and 6b show the test setup constructed to perform 27 and -27 degrees loading cases, respectively. For each loading case, two tests were performed to evaluate the effect of the increased number of the SGB voids (4 voids vs. 5 voids). As shown in Fig. 4-5, the SGB components are symmetrically placed with respect to the mid-length of 540mm-dimension of the block; the middle geofoam in the specimen with five voids is replaced with a void creating three voids being placed next to each other. The increased number of voids is hypothesized to allow distributing the displacement applied to the pipe within a longer distance while further reducing the force attracted by the pipe. The cover configuration for the SGB used in all six tests is a set of corrugated plastic sheets and a geofoam block placed atop of the SGB and used to uniformly distribute the soil pressure on the SGB as the pipe pushes towards the SGB. The taller SGB was used in the inclined

loading tests with a height of 380 mm (Table 4-1) to ensure that the SGB accommodates the vertical displacement produced by inclined loading.

Table 4- 1: Experimental test matrix.

Specimen	Loading Angle	Loading Condition	SGB Dimensions mm	Number of Voids
F-90-H1	90^0	H1	1100 × 540 × 270	4
F-90-H2		H2		5
F-27-D1	27^0	D1	1100 × 540 × 380	4
F-27-D2		D2		5
F-27-U1	-27^0	U1	1100× 540 × 380	4
F-27-U2		U2		5

H = Horizontal loading; D = Downward loading; U = Upward loading

To perform the test, the pipe was pushed in the displacement-controlled mode against the SGB into the sandbox using the hydraulic actuator until a minimum target displacement of 300 mm was achieved in the direction of the application of loading.

(a) (b)

Figure 4- 6: Experimental test setup: a) Downward loading; b) Upward loading.

4.4.3 Instrumentation

Instrumentation used to measure the local response of the SGB, as well as the global response of the pipe specimen, consists of a tension-compression load cell, a computer-controlled data acquisition system (DAQ), a cable transducer, a breakout unit, and a DC power supply. A hydraulic intensifier controlled the working principles of the actuator, and the displacement rate of the actuator was set at a minimum speed of 4 mm per minute, which resulted in a test duration of approximately 90 minutes. The load cell with preinstalled strain gauges was connected at the end of the actuator and to a DAQ unit. The linear displacement of the pipe was measured using a cable transducer attached to the loading end of the pipe. Using a breakout unit, the transducer was connected to a DC power supply which sends signals to the DAQ to record the measured force and displacement at every step of loading. Moreover, analogue sensors were installed in the voids of the first two SGB (SGB1 and SGB2 shown in Fig. 4-4b) placed at the tip of the pipe. They were designed to get activated when a void completely collapsed in order to monitor the progressive collapse of the voids in these critical SGB as they experience the greatest deformation compared to the rest of the pipe.

4.4 RESULTS

The results obtained from the laboratory test program, including the load-displacement relationship and observation of the overall response, are presented in this section for each loading angle.

4.4.1 Horizontal Loading

The load-displacement responses for the horizontal loading tests are shown in Fig. 4-7. The response shows a continually increasing load following an initial linear region until it reaches a hardening region at the end of the test. The initial linear region that ends at an average force of 8.3 kN and a pipe displacement of 15 mm is caused by the resistance contributed by the encased walls of the SGB and the friction that should be overcome until the first void collapses. As the test

progressed, the stiffness in both tests reduced significantly due to the progressive collapse and flexibility of the voids, followed by the exponential hardening effect caused by the deformation of the geofoam blocks when all the voids have fully collapsed. This response indicates that the system possesses a nonlinear behaviour that can approximately be expressed via a trilinear curve, as proposed by Ilozumba et al. (2021). As shown in Fig. 4-7, the initial stiffness in both tests remained approximately identical. As anticipated, both tests followed a nearly similar pattern, with F-90-H1 having a slightly higher force than F-90-H2, which is attributed to lesser voids in F-90-H1 that make the system less flexible to lateral pipe displacement.

The peak force was calculated when all the voids have fully collapsed by ignoring the hardening region of the curves (i.e., the point at which there is a sudden increase in the reaction force), as this region does not contribute to the intended response of the system. Before the hardening region, F-90-H1 reached a peak force of 26 kN at a displacement of 223 mm, while F-90-H2 recorded 26 kN at 260 mm. The comparison of forces between the two tests at a displacement of 223 mm shows that F-90-H2 experiences 4% lower force compared to F-90-H1, which shows that an increase in the number of voids results in a more flexible system, i.e., it allows the pipe to mobilize lesser force at a given displacement while accommodating the applied displacement and resisting the overburden soil pressure. The SGB pattern with five voids (F-90-H2) can be used in practice when reducing the force reaction on the pipe is critical, e.g., vintage pipelines having a reduced force resistance.

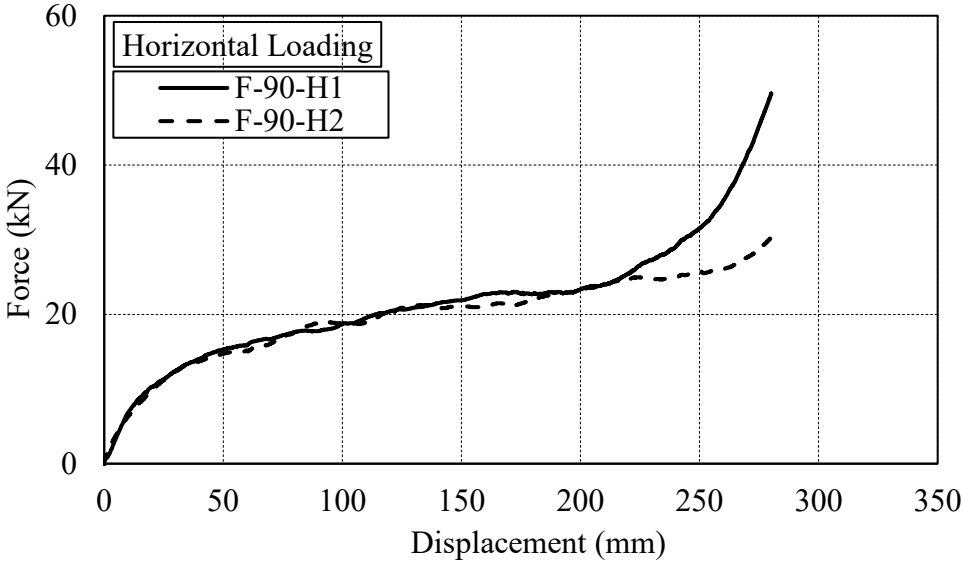

Figure 4- 7: Force – displacement response for horizontal loading (F-90-H1: specimen with four voids; F-90-H2: specimen with five voids).

The behaviour of the critical SGB placed at the tip of the pipe (Fig. 4-4b) is shown in Fig. 4-8 for F-90-H1. These results were obtained from the DAQ unit when the installed sensors got activated during the test. Note that the collapse of the second void in the SGB2 (Fig. 4-8) was excluded because the installed sensor failed during the test. As shown in Fig. 4-8, the first void (i.e., closer to the pipe) in the SGB1 is first engaged, followed by the same void in the SGB2 as the displacement increases, which led to the gradual increase in the force attracted by the pipe. As the displacement increases, the following voids in both the SGB collapse progressively, as shown in Fig.4-8.

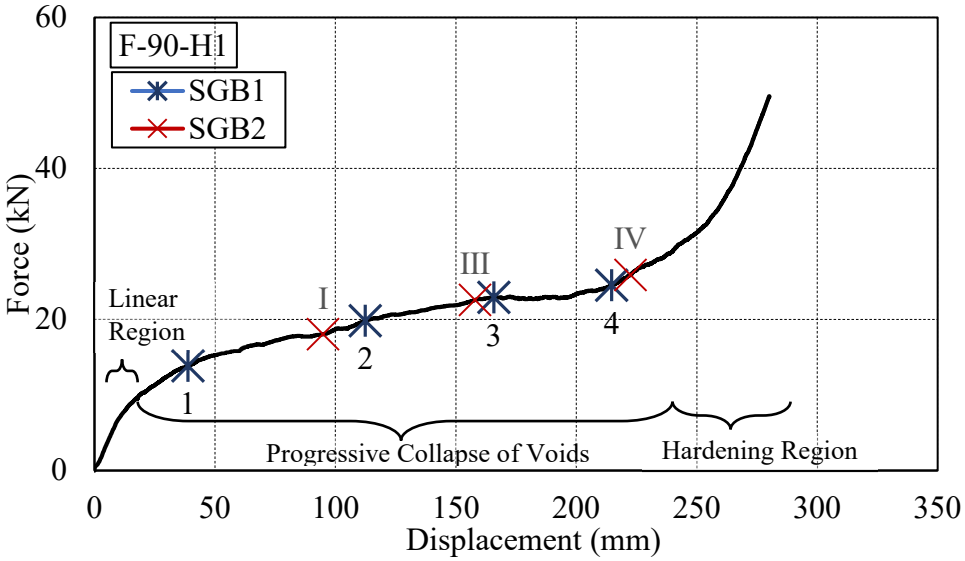

Figure 4- 8: Local response of the SGB in F-90-H1.

The load-displacement response obtained from the horizontal loading tests having H/D = 5 were compared to the results of the experiments performed by Trautmann and O'Rourke (1985) on the pipes undergoing lateral ground displacement without significant pipe contribution. These tests were carried out on only loose sand backfill with H/D ranging between 1.5 to 8 to demonstrate the beneficial effects of the SGB for pipes subjected to lateral displacement. The force-displacement response was converted to normalized force-dimensionless displacement to eliminate the effects of the pipe length, pipe diameter, burial depth, and density of the sand backfill, allowing for direct comparison with the test results by Trautmann and O'Rourke (1985). The force was normalized by dividing the total load by the product of the total weight of the sand backfill, depth of embedment H, length of the pipe L, and the diameter of the pipe D. The pipe displacement was normalized by dividing the measured displacement Y by the diameter of the pipe D.

Neglecting the hardening region of F-90-H1 and F-90-H2 (Fig. 4-7), the force-displacement response of the specimens tested in this study follows the same pattern as that of the loose sand reported by Trautmann and O'Rourke (1985). The results obtained from the pipe with the adjacent

SGB indicate that significantly lower forces are mobilized by the pipe when the SGB is installed compared to a traditional sand backfill, e.g., on average 86% less force at the maximum displacement. The comparison suggests that the SGB would sufficiently allow the pipe to accommodate longer horizontal displacement while maintaining a low force reaction.

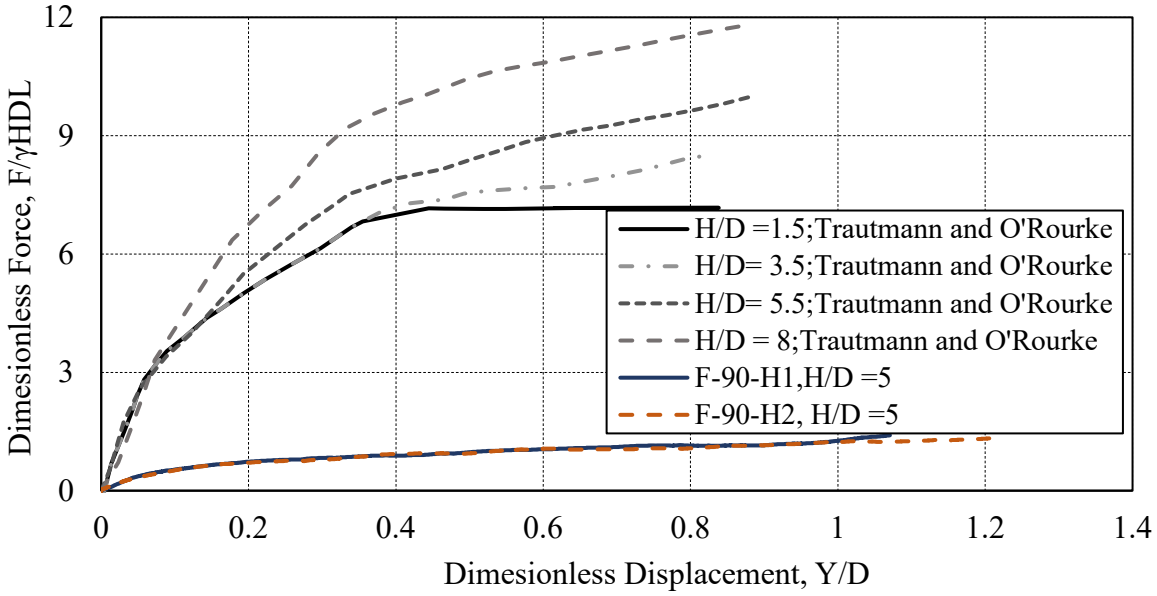

Figure 4- 9: Comparison of the normalized force – displacement response between the horizontal loading tests and those reported by Trautmann and O'Rourke (1985).

4.5.2 Downward loading

The force-displacement responses for downward loading tests are shown in Fig. 4-10. The initial stiffness of the two specimens, on average, is 0.6 kN/mm recorded at a force of 12.7 kN and a displacement of 44 mm. As shown, both specimens followed a nearly similar pattern, although F-27-D1 experienced a slightly higher force than F-27-D2. F-27-D1 reached a peak force of 39 kN at 288 mm displacement before the hardening region, while a peak force of 38 kN at a displacement of 323 mm was recorded for F-27-D2. The difference in the peak force between the two tests reached 16% at the displacement of 288 mm.

Referring to Fig. 4-10, it can be seen that an increased number of voids (5 vs. 4) reduces the resistance of the pipe when subjected to a given displacement or accommodates a larger displacement while achieving almost the same force reaction (291 vs. 328 mm at a force equal to 40 kN). The comparison between the responses presented in Figs. 4-7 and 4-10 show that the force attracted by the pipe when loading downward increased on average by 8% at 223 mm displacement compared to the horizontal loading counterparts. In the downward loading condition, the reaction force includes the force resisted by the SGB plus the horizontal component of the force developed between the pipe and the soil underneath the pipe as the displacement is applied with a 27-degree angle toward the floor of the sandbox. Thus, the higher peak forces recorded in both tests compared to their horizontal loading counterparts are attributed to the reaction force developed between the pipe and horizontal plane that is translated to the force acting in the direction of the applied displacement. Similar to the horizontal loading case, an approximate bilinear force-displacement response followed by an exponential hardening curve can represent the overall response of the system.

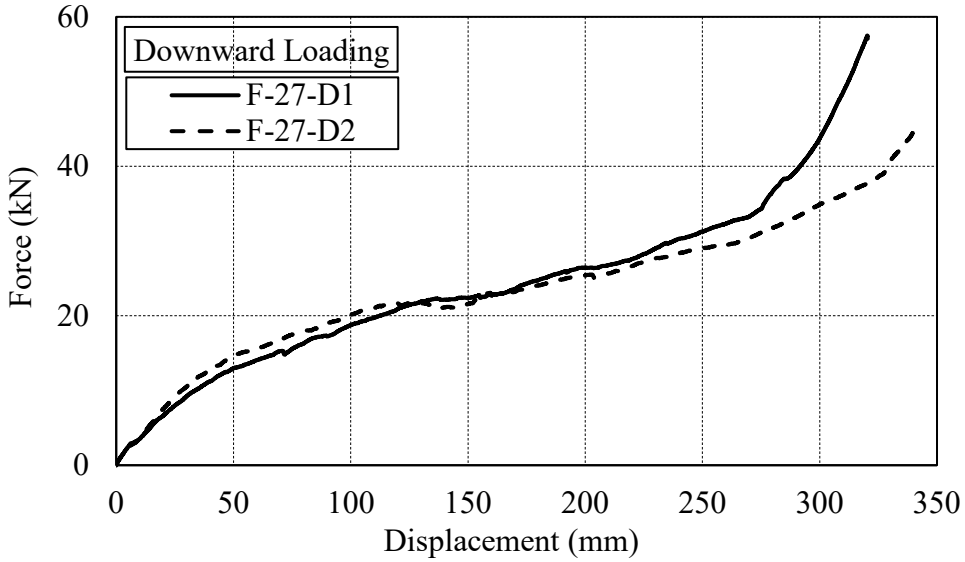

Figure 4- 10: Force – displacement response for downward loading (F-27-D1: specimen with four voids, F-27-D2: specimen with five voids).

Figure 4-11 shows the local response of the SGB1 and the SGB2 in F-27-D1. Note that the third void in the SGB2 specimen was excluded because the installed sensor failed during the test. The readings show a sequential collapse of the voids as the displacement is applied. Similar to the horizontal loading condition, the voids in the SGB1 are first engaged, progressively followed by the voids in the SGB2 as the displacement increased. Unlike the horizontal loading counterpart, there is a significant disparity between the readings reported in this test which may be attributed to misalignment during the installation of the sensors.

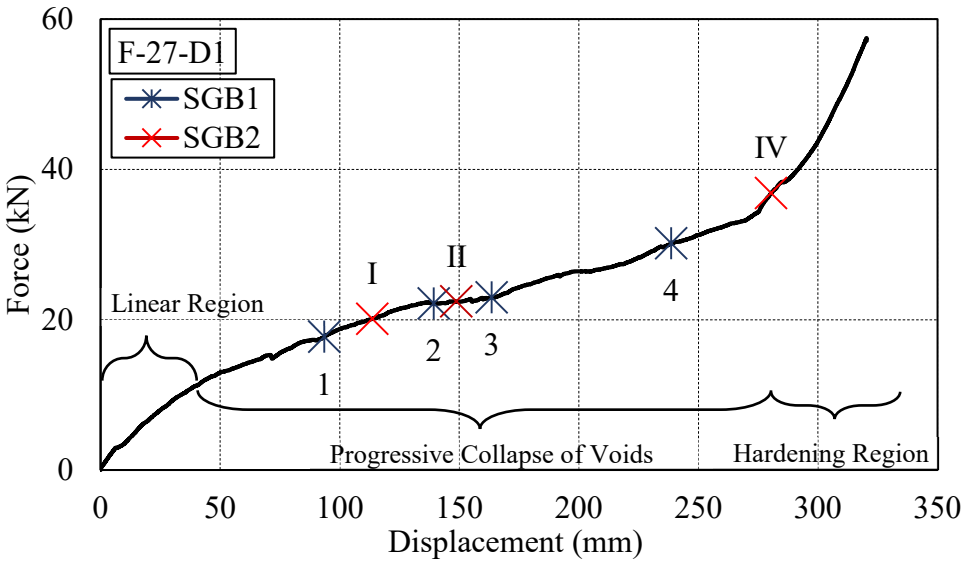

Figure 4- 11: Local response of the SGB in F-27-D1.

4.5.3 Upward loading

The force-displacement responses for the tests involving upward loading are depicted in Fig. 4-12. Both tests have an average initial stiffness of 0.5 kN/mm, which occurred at a force of 8 kN and a corresponding displacement of 15.8 mm. After this point, a relatively low stiffness while the voids collapse was observed, followed by the exponential hardening effect contributed by internal deformation of the geofoam blocks. The response can be reproduced by a bi-linear curve and a hardening region at the end of the test. A peak force of 34 kN at 270 mm was recorded for F-27-U1

(excluding the hardening region), while F-27-U2 experienced approximately a peak force of 29 kN with a corresponding displacement of 295 mm. The comparison between the forces attracted by two specimens (e.g., 23% at the displacement of 270 mm) indicates that the pipe resistance to ground displacement can significantly be reduced by increasing the number of voids in the SGB provided that the SGB can still carry the soil overburden.

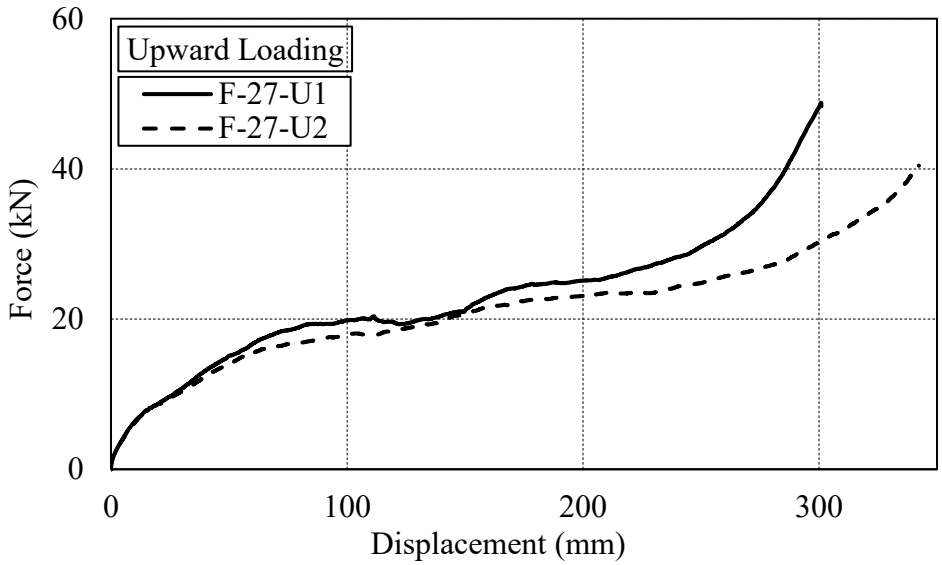

Figure 4- 12: Force – displacement response for upward loading (F-27-U1: specimen with four voids, F-27-U2: specimen with five voids).

Figure 4-13 shows the readings obtained when the sensors installed for F-27-U1 were activated during the test. As can be seen, the voids in both the SGB1 and the SGB2 collapsed nearly simultaneously under the lateral displacement, which confirms that both the SGB placed at the tip of the pipe (Fig. 4-4b) contributed to the overall load-carrying capacity of the system.

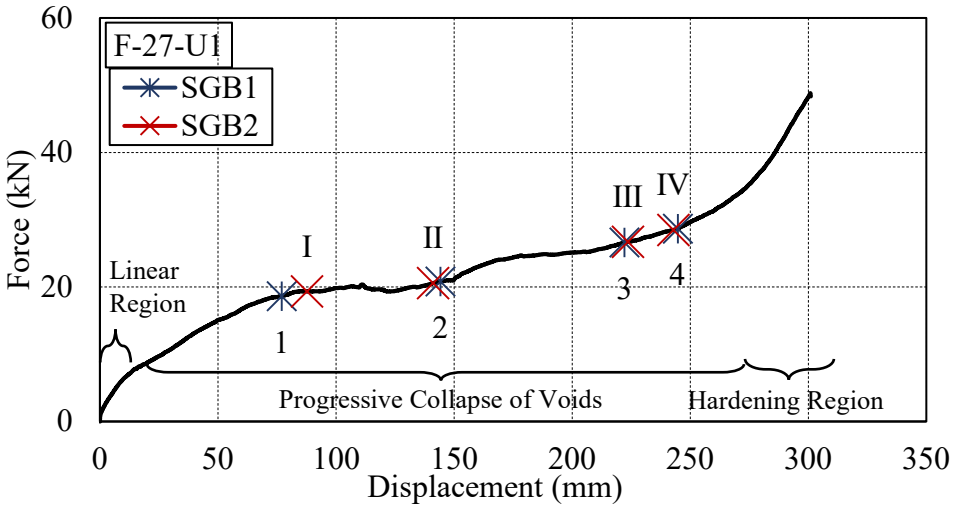

Figure 4- 13: Local response of the SGB in F-27-U1.

The response observed for the tests having the same number of voids (see Table 4-1) shows that the force-displacement relationship of the pipe-SGB-soil features an approximately similar bilinear response followed by an exponential hardening region due to the deformation of the geofoam after all the voids collapsed. Moreover, the tests with the increase in the number of voids in each loading condition produced the lowest peak force and maintained a relatively lower force for a considerable displacement, e.g., on average, 9% lower force at the maximum displacement is mobilized when five voids are used instead of 4 voids. In practice, a set of the SGB with an appropriate number of voids should be adjusted along the pipe length depending on the amplitude and angle of anticipated ground deformation such that the desired displacement is achieved while maintaining a reaction force lower than the pipe limit states with a sufficient safety margin.

4.6 NUMERICAL MODELLING OF PIPE-SGB-SOIL

4.6.1 Proposed model for pipe-SGB-soil

A simplified yet accurate numerical modelling technique is proposed in this study to simulate the response of buried pipelines improved using the proposed special geomaterial blocks when subjected to lateral ground deformation. Two models are shown in Figs. 4-14 and 4-15. The first model is to

be used to replicate the field condition (Fig. 4-14) where the symmetrical force-displacement response assigned to the soil spring reproduces the effect of the soil on both sides of the pipe and the unsymmetrical force-displacement response assigned to the soil-SGB spring is intended to simulate the soil response placed on one side the pipe, and that of the SGB installed on the opposite side. In both force-displacement responses, the soil and the SGB only work when they are subjected to compression. The second model shown in Fig. 4-15 is used to replicate the experimental test performed in this study. The SGB may be required on both sides of the pipe for the former model, depending on the source of ground movement (see Fig. 3-2). To save construction costs, however, it is proposed that the engineer evaluates the direction of the ground deformation and preferably place the SGB on one side of the pipe following the anticipated direction of ground movement, as was the case in this study in which the displacement is applied only in one direction, and the SGB or the soil is placed on one side of the pipe. Although the boundary conditions in both the model of Fig. 4-15 and the experimental test specimen of this study were simplified to eliminate the effect of material nonlinearity in the pipe, the modelling technique presented here can also apply to the pipe undergoing plastic behaviour or pressurized pipes.

As shown in Fig. 4-15, the body of the pipe is modelled using beam-type elements with pinned end conditions. Discrete nonlinear springs are used to reproduce the stiffness and passive resistance of the soil surrounding the pipe and the lateral stiffness and strength of the SGB as obtained from the experiments. A schematic representation of the force-displacement response adopted for the nonlinear springs for the cases with and without the SGB is shown in Fig. 4-15.

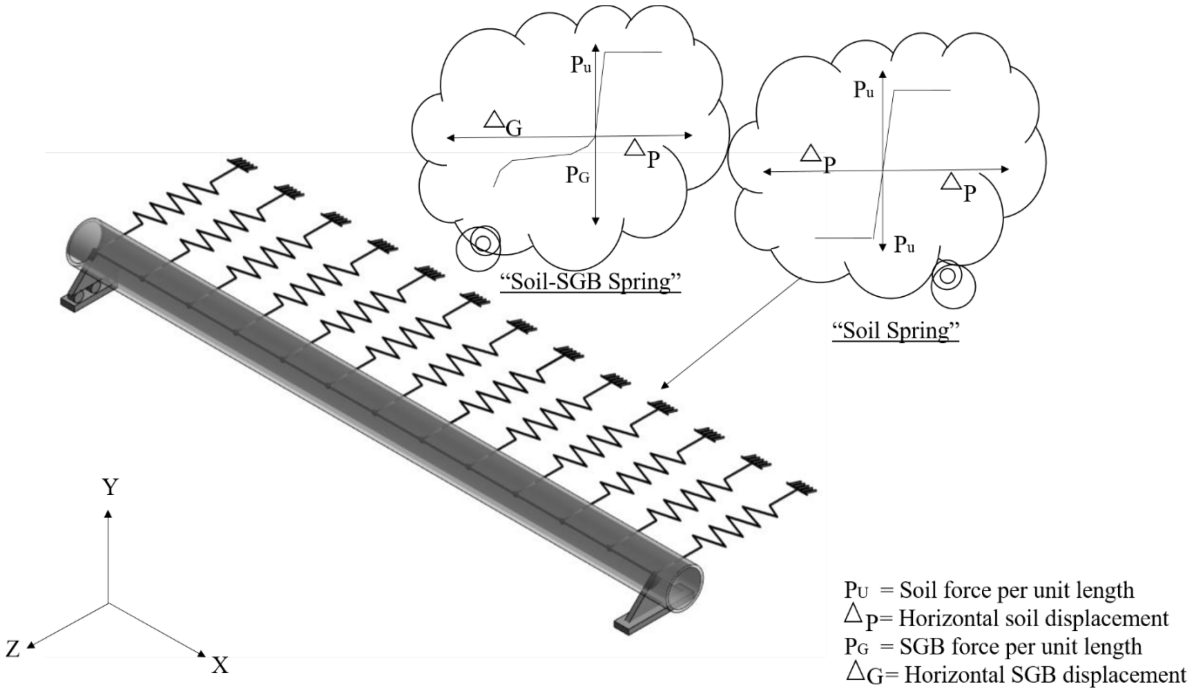

Figure 4- 14: Proposed pipe-SGB-soil numerical model for the field condition.

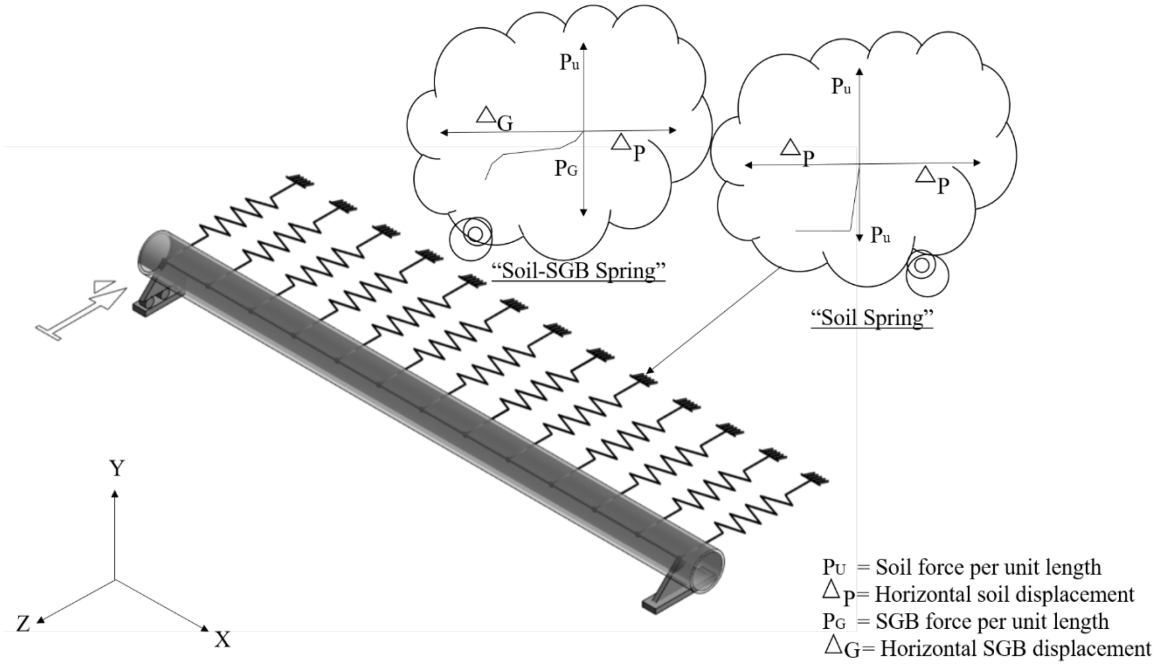

Figure 4- 15:Proposed pipe-SGB-soil numerical model for the experimental test.

The force-displacement relationship for the lateral soil springs is adopted following ASCE guidelines for the design of buried steel pipe (ASCE 2001), assuming sandy soil:

$P_u = N_{qh}\gamma HD$

(4-1)

where N_{qh} is the horizontal bearing capacity factor equal to 9.

The force-displacement relationship for the SGB can be defined using the measurements collected from the cross-sectional test data available in (Ilozumba et al. 2021). Fig. 4-16a shows a sample force-displacement response for a single SGB specimen. This response is smoothed out and used to define the lateral force-displacement relationship of the soil-SGB spring in the proposed model of Fig. 4-15, as shown in Fig. 4-17a. The exponential hardening region in Fig.4-16a, where the slope becomes nearly 90 degrees, is excluded from the force-displacement response of the SGB assigned to the spring (Fig. 4-17a) to avoid convergence issues in the numerical model. Moreover, the force values in Fig. 4-17a are scaled to represent the force developed by the respective spring with a given spacing.

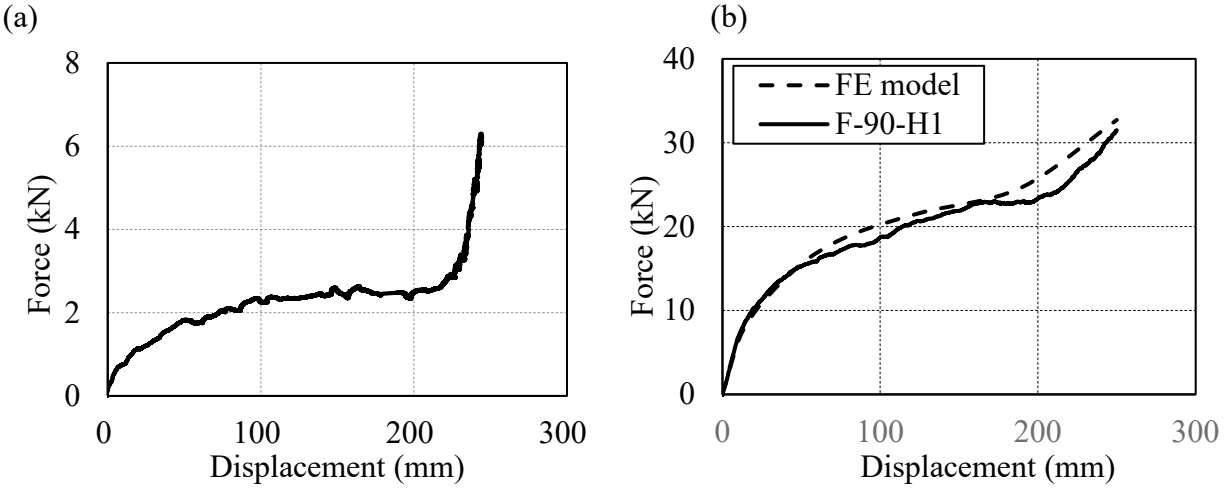

Figure 4- 16: a) Typical force – displacement response of a single SGB; b) Comparison of the prediction from the finite element model and data from Test F-90-H1.

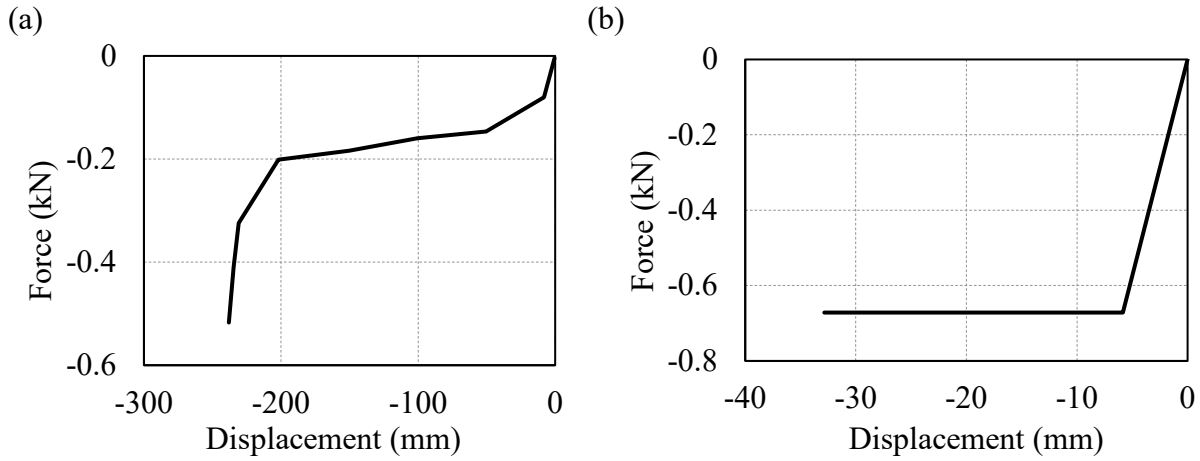

Figure 4- 17: a) Force – displacement relationship of the soil-SGB spring; b) Force – displacement relationship of the soil spring.

4.6.2 Finite element model development

The proposed modelling technique was used to simulate the pipe specimen experimentally tested in this study. The numerical model was developed in the Abaqus finite element program (Dassault Systèmes 2011). The pipe is modelled using a two-node linear beam element (PIPE31) from the Abaqus library (Hibbitt et al. 2014). The element formulation follows Timoshenko's beam theory (Timoshenko and Gere 2009), which accounts for transverse shear deformation in addition to flexural deformation. The 6.0 m length of the pipe is uniformly discretized using PIPE31 elements with a mesh size of 0.02 m. The pipe is modelled as a non-pressurized steel pipe with an outside diameter (OD) of 219 mm, a wall thickness of 8.2 mm and yield stress of 310 MPa. The nonlinear elastic behaviour of the pipe material is modelled using the Ramberg-Osgood material model with the constants n = 22 and r = 0.5, where n and r represent the strain-hardening exponent and the yield offset parameter, respectively (Ramberg and Osgood 1943). The surrounding soil and the SGB are modelled using a set of discrete nonlinear spring elements with two nodes, SPRING2 from the Abaqus library. The springs with the force-displacement relationship of Fig. 4-17a are

connected to the pipe at each node, i.e., at every 0.02 m. As shown in Fig.4-17a, the negative force response features the SGB.

All three translational degrees-of-freedom (DOFs) of the spring ends are restrained, as shown in Fig.4-15. The tail end of the pipe is restrained in all translational DOFs, while only the translational DOF in Y-axis is fixed at the opposite end of the pipe. The lateral displacement with an amplitude of 0.25 m is applied along Z-axis at the roller end to simulate the actuator-induced lateral displacement.

4.6.3 Validation of the proposed model

The model developed for buried pipes equipped with the SGB was validated using the results obtained from the experimental test data presented in this study. For this purpose, the force-displacement response predicted by the numerical model was compared to that obtained for the specimen tested under the horizontal loading condition (F-90-H1), as shown in Fig 4-16b. As shown, the prediction by the finite element model proposed here is in excellent agreement with the data obtained from the laboratory experiment. The amplitude of the force is slightly over-predicted with a percentage error of 4%, which is attributed to the proposed model assumptions, namely, the force-displacement response of the SGB and the soil. The good match observed between the model prediction and test result suggests that the finite element model proposed here can be used to efficiently simulate the remediation technique involving the SGB.

4.6.4 Evaluation of the pipe performance

The finite element model of Fig. 4-15 was used to evaluate the efficiency of the application of the SGB when the pipe is undergoing ground deformation, and particularly, how the SGB improves the pipe resistance to the lateral soil displacement. For this purpose, two finite element models, one with the SGB and the second one without them, were created. The former involves the springs

with the force-displacement response defined in Fig. 4-17a, and the latter simulates the pipe with the surrounding soil without the SGB and encompasses the springs with the force-displacement response of the soil alone, as shown in Fig. 4-17b. The force-displacement responses predicted by these two models are shown in Fig. 4-18. Comparing the peak forces obtained from two cases at a lateral displacement of 200 mm, 100 kN vs. 25 kN indicates that the SGB appreciably reduces the horizontal force mobilized by the pipe as the lateral displacement is applied to the pipe. This result reaffirms the beneficial effects of the application of the SGB as an efficient mitigation technique for buried steel pipelines undergoing ground movements.

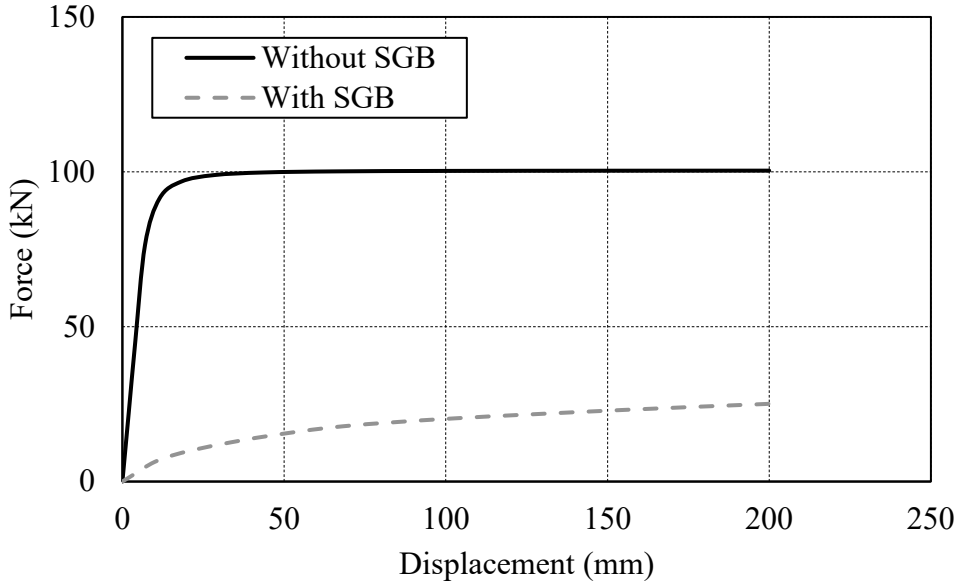

Figure 4- 18: Force – displacement response of the pipe specimen with and without the SGB.

4.7 CONCLUSIONS

This research is intended to evaluate using laboratory testing the mitigation technique involving the installation of special geomaterial blocks (SGB) to improve the structural integrity of buried steel pipelines subjected to ground deformation. A series of the SGB is placed adjacent to the pipe to alter its boundary conditions. The system exploits the orthotropic mechanical property of these SGB,

which allows the pipe to move freely along its cross-sectional plane, thereby reducing the induced stresses and strains in the pipeline system when subjected to ground deformation. Moreover, a numerical modelling technique is proposed to simulate the response of the pipeline with the SGB when the adjacent soil induces lateral movement on the pipe. The key findings of this study are summarized as follows:

- The full-scale experimental test program developed in this study confirms the efficiency of the application of the SGB adjacent to buried steel pipelines in reducing the lateral resistance of pipe to soil displacement.
- The results obtained from the experimental tests show that increasing the number of the SGB voids (4 vs. 5) appreciably allows the pipe to mobilize a lower boundary reaction when subjected to the ground displacement. The tests with an increased number of the SGB voids in the three loading cases mobilized on average a 9% lower force at the maximum displacement compared to the tests with four voids.
- The force-displacement response of the pipe-SGB-soil assembly can be represented using a trilinear curve involving the initial stiff region, a nearly linear region representing the stepwise collapse of the voids in multiple SGB, and the final hardening region caused by the deformation of the geofoam blocks when all the voids have fully collapsed.
- The comparison between the normalized test results (sand only) reported by Trautmann and O'Rourke (1985) and those of the full-scale experimental test under horizontal loading confirms that at maximum displacement, the pipe equipped with the SGB attracts on average 86% less force at a given displacement.
- The test results confirmed that the loading angle affects the response of the proposed system. Comparing the forces between the horizontal and inclined loading cases at a displacement of

223 mm (i.e., the maximum displacement corresponding to the mobilized peak force of the horizontal test consisting of four voids) shows that the force in the pipe with adjacent four voids-SGB is increased by 7.7 and 2.7% in the downward and upward loading, respectively. In contrast, when five voids-SGB are used to alter the pipe boundary condition, an 8% increase in the reaction force was observed in the downward loading case, while a nearly similar force was achieved in both horizontal and upward loading conditions.

- The numerical modelling technique proposed here, which consists of beam-type elements to simulate the pipe and nonlinear springs simulating soil and the SGB force-displacement response, can appropriately predict the response of the pipe equipped with the SGB, affirming that the pipeline engineers can use the technique to model buried pipelines undergoing lateral soil displacement.
- The comparison between the results obtained from the numerical simulation of the pipe without the SGB and those of the pipe with the adjacent SGB, on average 75% reduction in force, confirms the beneficial effects of using the SGB as an efficient mitigation technique for buried pipelines undergoing ground movements.

The proposed modelling technique could be used in future to evaluate the influence of material properties and geometry of the pipe, diameter-to-wall thickness ratio, backfill and in-situ soil properties, and the geometry of the SGB on the efficiency of the mitigation technique. Additionally, future experimental test programs could investigate pressured pipes, pipes undergoing plastic deformation and pipes in field conditions.

4.8 ACKNOWLEDGMENT

This study is based on work supported by the Natural Sciences and Engineering Research Council (NSERC) of Canada. The financial support is greatly acknowledged. The authors would also like to

acknowledge the financial support and in-kind contributions of donating test specimens by ALFA Upgrades Inc. The authors wish to thank Dr. Onyekachi Ndubuaku for his input throughout the project. The authors sincerely thank the technical staff at the I.F. Morrison Structures Laboratory of the University of Alberta for their valuable advice and assistance during the test program. The authors wish to thank C-FER Technologies for providing the opportunity to use their structural testing facilities.

5. CONCLUSIONS AND RECOMMENDATIONS FOR FUTURE STUDIES

This chapter summarizes the key findings, scientific and engineering contributions, limitations of this M.Sc. thesis and recommends future research directions.

5.1 SUMMARY

This research introduces a new remediation technique for alleviating the effects of ground deformation on the safety and structural integrity of buried steel pipelines. The technique consists of the installation of special geomaterial blocks (SGB), comprising a set of expanded polystyrene (EPS) geofoam, polypropylene squared plastic boxes (i.e., voids) encased in corrugated plastic sheets, and a stiff shell adjacent to the pipe before backfill. The beneficial effects of this technique in limiting the induced stresses and strains on the pipe subjected to ground movements are evaluated.

An in-depth review of the literature reveals that existing mitigation techniques may not necessarily provide a more efficient and cost-effective solution for solving pipeline incidents triggered by ground movements. Various field observations of onshore pipelines, especially those buried in unstable slopes or areas susceptible to ground deformation, e.g., landslides, have indicated that the loads induced by these ground motions often result in large circumferential and axial strains in the pipe, which may result in high compressive and tensile stresses, thus causing pipe wall local buckling or wrinkling. This violation in the pipe's integrity may cause the release of the pipe products to the environment and substantial economic losses or even fatalities. This research program developed a state-of-the-art remediation technique using adjacent-installed special geomaterial blocks (SGB) that target economic and efficient means of improving the stability response of buried pipelines when subjected to large lateral deformations caused by severe ground

movements such as landslides, earthquake, fault rupture or unstable slopes. This study took advantage of the SGB's orthotropic mechanical property, which efficiently controls the ground-induced stresses and strains in steel pipelines while accommodating lateral pipe displacement along its cross-sectional plane. In other words, the lower lateral stiffness of the SGB enables the pipeline to endure large lateral displacements by distributing its deformation over a longer length.

The first phase of this research program focused on understanding the local response of pipe-SGB-soil assembly, which consists of a typical cross-section of a steel pipe and the SGB, gain insight into the beneficial effects of using the SGB adjacent to the pipe and quantifies the potential dominant effects of the SGB response through a series of laboratory cross-sectional tests. This phase also focused on the development of a simplified analytical model intended to serve as a tool for pipeline engineers to predict the anticipated displacement dissipated by the mitigation technique when the pipe is subjected to lateral movement and also obtain the force–displacement response of the assembly for any given geometrical configuration of the SGB. Accordingly, 25 cross-sectional tests were undertaken under the lateral and oblique ground displacements and the various SGB cover configurations placed between the soil, pipe, and the SGB. The results obtained in these tests were compared and discussed for each group of the SGB cover configurations. They were also used to validate the simplified spring-based analytical model proposed in this study. In the second phase of this work, six full-scale laboratory tests were carried out on non-pressurized 8-inch-diameter 6-meter long steel pipes to validate the new mitigation technique proposed to improve the performance of buried pipelines subjected to ground deformation, to investigate the effect of an increased number of voids in the SGB hypothesized to allow distributing the pipe displacement within a longer length and to study the influence of loading angle on the performance of the proposed mitigation technique. A numerical simulation technique was also developed in this

phase to reproduce the pipe-SGB-soil interaction when a pipe equipped with the SGB blocks is subjected to ground movement. The model input parameters for the SGB were obtained from the cross-sectional tests, and the model was validated against the full-scale test data.

5.2 MAIN SCIENTIFIC AND ENGINEERING CONTRIBUTIONS

The main contributions of this M.Sc. research study are as follows:

- a new remediation technique, which involves altering the pipe boundary condition by special geofoam blocks, is proposed to mitigate the detrimental effects of ground motions.
- The force-displacement response of the SGB is determined through a series of cross-sectional.
- The efficiency of the proposed mitigation technique is verified using full-scale laboratory testing.
- The force-displacement behaviour of the pipe equipped with the adjacent SGB are determined using full-scale laboratory testing.
- A simple spring-based analytical model is proposed and validated to serve as a predictive tool for evaluating pipe-SGB-soil assembly response and predicting the displacement accommodated by the SGB.
- An accurate yet efficient numerical modelling approach is developed to predict the response of buried steel pipelines equipped with the SGB.
- Design recommendations for the improvement of buried steel pipelines using the SGB are proposed as part of the above-mentioned contributions.

5.3 CONCLUSIONS

The main conclusions drawn from the two laboratory test programs, analytical and finite element predictions performed in this study are summarized as follows:

- The results from the cross-sectional tests confirmed the adequacy of the proposed remediation technique to limit the damage to buried pipelines subjected to ground deformation, the interaction between the pipe, soil and the SGB, and the interface frictional forces developed between the SGB and overlaying soil pressure.
- The cross-sectional tests confirmed that the cover configuration has minimal impact on the force induced in the pipe-SGB-soil assembly unless a rough contact surface (e.g., the SGB interacting with the geofoam) is used.
- The cross-sectional test results indicated that the loading angle (i.e., between the applied displacement and the horizontal plane crossing pipe centreline) affects the response of the pipe-SGB-soil assembly. The force attracted by the pipe increases in downward loading, while an approximately similar force response is observed in both horizontal and upward loading conditions.
- The force – displacement relationship per unit width of the SGB is idealized using a trilinear curve, representing the initial linear region with the highest stiffness, the relatively low stiffness region due to progressive collapse of the voids and the hardening region caused by the deformation of the geofoam blocks when all the voids have fully collapsed. This curve is used to represent the SGB behaviour assigned to a set of nonlinear springs in the numerical model of the pipe.

- The proposed spring-based analytical model well predicted the force – displacement response of the assembly, anticipated displacement accommodated by the SGB before the voids have collapsed, and the effect of influential geometric parameters affecting the SGB response.
- The parametric study performed using the proposed analytical model showed that increasing the number of geofoam and void blocks does not appreciably affect the system response. However, thicker geofoam and void blocks can accommodate greater displacements while maintaining the flexibility of the system.
- The full-scale experimental test program developed in this study confirms the efficiency of the application of the SGB adjacent to buried pipelines in reducing the lateral force resistance of pipe to soil displacement, effectively reducing stress and strain in the pipe.
- The results obtained from the full-scale experimental tests show that increasing the number of the SGB voids (4 vs. 5) appreciably allows the pipe to mobilize a lower boundary reaction when moving relative to the ground displacement. The tests with an increased number of the SGB voids mobilized on average a 9% lower force at the maximum displacement compared to the tests with 4 voids. This finding was predicted by the analytical approach proposed here.
- The force-displacement response of the pipe-SGB-soil assembly as obtained from the full-scale experimental testing can be represented using a trilinear curve involving the initial stiff region, a nearly linear region representing the stepwise collapse of the voids in the multiple SGB and the final hardening region.
- The comparison between the normalized test results (sand only) reported by Trautmann and O'Rourke (1985) and those of the full-scale experimental test under horizontal loading confirms that at maximum displacement, the pipe equipped with the SGB attracts on average 86% less force at a given displacement.

- The results from the full-scale experimental tests suggest that the loading angle affects the response of the proposed system. Comparing the forces between the horizontal and inclined loading cases at a displacement of 223 mm (i.e., the maximum displacement corresponding to the mobilized peak force of the horizontal test consisting of 4 voids) shows that the force in the pipe with adjacent 4 voids-SGB is increased by 7.7 and 2.7% in the downward and upward loading, respectively. In contrast, when 5 voids-SGB are used to alter the pipe boundary condition, an 8% increase in the reaction force was observed in the downward loading case, while a nearly similar force was achieved in both horizontal and upward loading conditions.
- The numerical modelling technique proposed here, which consists of beam type elements simulating the pipe and nonlinear springs simulating soil and the SGB force-displacement response, can appropriately predict the response of the pipe equipped with the SGB, affirming that the pipeline engineers can employ the modelling technique to simulate buried pipelines undergoing the lateral soil displacement.
- The comparison between the results obtained from the numerical simulation of the pipe without the SGB and those of the pipe with the SGB installed adjacent to the pipe showed a 75% reduction in the force when the SGB is used, affirming the beneficial effects of using the SGB as an efficient mitigation technique for buried pipelines undergoing ground movements.

5.4 LIMITATIONS

The following limitations should be considered when interpreting or generalizing the results presented in this M.Sc. thesis:

- The backfill soil used in the study does not necessarily account for an actual condition anticipated in the field.

- This study only considers a geofoam and void thickness of 55 mm; the results cannot be extrapolated for other thicknesses of the geofoam and void without laboratory testing or detailed numerical analysis.
- The beneficial effects of the SGB on 8 inch-diameter pipe were examined here; the results cannot directly be applied to larger pipes that are typically used in the oil and gas industry.
- The mechanical properties of geofoams and the SGB as a whole were excluded in this study as the response of the pipe-SGB-soil assembly is dominated by friction between the soil and the SGB.
- The numerical model proposed here does not account for the effect of the uplift or bearing and the longitudinal response of the soil. Moreover, the numerical model is independent of the mechanical properties of the geofoam.

5.5 RECOMMENDATIONS FOR FUTURE STUDIES

This research has laid the foundation for understanding the response of buried steel pipelines with the adjacent SGB when subjected to lateral ground-induced actions. The following research directions are recommended for future related research works:

- Experimental fieldwork should be carried out to better understand the behaviour of the pipe equipped with the SGB in actual field conditions.
- This research is only intended for pipelines undergoing lateral ground deformation. Pertinent efforts should be carried out to inculcate the benefits of using the technique for pipelines undergoing vertical displacement due to ground movements, e.g., fault movement.
- A more detailed numerical model taking into account the effects of various loading conditions expected in buried pipelines such as bending, axial and torsional loads should be developed

to evaluate the performance, stresses and strain demands of the pipeline network equipped with the SGB.

- Parametric numerical simulations should be performed to evaluate the performance of various pipe geometrical properties and field conditions on the performance of the pipe with the adjacent SGB and determine the parameters affecting the response of the assembly.
- The beneficial effects of using the SGB on pressurized pipelines should be investigated.
- The geometry and material of the geofoams in the SGB should further be enhanced by efficiently placing the voids and geofoams to accommodate the lateral displacement while resisting the backfill weight. The results from the full-scale testing performed here confirm the possibility of refining the proposed SGB in future.
- Weathering effects due to freezing and thawing on the performance of the SGB placed adjacent to buried pipes should be investigated.
- Practical considerations associated with deploying and installing the SGB in the field should be studied.

REFERENCE

Aabøe, R. (1996). “40 years of experience with the use of EPS Geofoam blocks in road construction.” 14.

Abaqus. (2011). Users’manual. Simulia, Providence,RI,USA,.

ABS. (2006). Guide for Building and Classing Subsea Pipeline Systems. American Bureau of Shipping.

Agbo, S. (2020). “A Novel Tool For Predicting The Tensile Strain Capacity Of Welded Onshore Vintage Pipelines.”

Agbo, S., Lin, M., Ameli, I., Imanpour, A., Duan, D.-M., Cheng, J. J. R., and Adeeb, S. (2019). “Experimental evaluation of the effect of the internal pressure and flaw size on the tensile strain capacity of welded X42 vintage pipelines.” International Journal of Pressure Vessels and Piping, 173, 55–67.

American Society of Civil Engineers. (2001). Guidelines for the Design Of Buried Steel Pipe. In American Society of Civil Engineers.

Andersson-Sköld, Y., Bergman, R., Johansson, M., Persson, E., and Nyberg, L. (2013). “Landslide risk management—A brief overview and example from Sweden of current situation and climate change.” International Journal of Disaster Risk Reduction, 3, 44–61.

Anshel J. Schiff and Los Altos Hills. (1995). Northridge Earthquake: Lifeline Performance and Post-Earthquake Response.

API RP 1111. (2015). Design, construction, operation, and maintenance of offshore hydrocarbon pipelines.

Ariman, T., Lee, B. J., and Chen, Q. (1987). “Failure of Buried Pipelines Under Large Ground Deformations.” Developments in Geotechnical Engineering, Elsevier, 63–75.

ASTM D6817. (2013). Standard specification for rigid cellular polystyrene geofoam.

Athanasopoulos, G.A., Pelekis, P.C., and Xenaki, V.C. 1999. Dynamic Properties of EPS Geofoam: An Experimental Investigation. Geosynthetics International, **6**(3): 171–194. doi:10.1680/gein.6.0149.

Bartlett, S. F, Lingwall, B, Trandafir, A. C, and Lawton, E. C. 2012. Protection of Steel Pipelines from Permanent Ground Deformation Using EPS Geofoam. Seismic Resilience of Natural Gas Systems: Improving Performance, 34, 5.,.

Bartlett, S.F., and Lingwall, B.N. 2014. Protection of Pipelines and Buried Structures Using EPS Geofoam. In Ground Improvement and Geosynthetics. American Society of Civil Engineers, Shanghai, China. pp. 547–556.

Bartlett, S.F., Lingwall, B.N., and Vaslestad, J. 2015. Methods of protecting buried pipelines and culverts in transportation infrastructure using EPS geofoam. Geotextiles and Geomembranes, **43**(5): 450–461. doi:10.1016/j.geotexmem.2015.04.019.

Beju, Y.Z., and Mandal, J.N. 2017. Expanded Polystyrene (EPS) Geofoam: Preliminary Characteristic Evaluation. Procedia Engineering, **189**: 239–246. doi:10.1016/j.proeng.2017.05.038.

Cheng, X., Ma, C., Huang, R., Huang, S., and Yang, W. 2019. Failure mode analysis of X80 buried steel pipeline under oblique-reverse fault. Soil Dynamics and Earthquake Engineering, **125**: 105723. doi:10.1016/j.soildyn.2019.105723.

Choo, Y. W., Abdoun, T. H., O'Rourke, M. J., and Ha, D. (2007). "Remediation for buried pipeline systems under permanent ground deformation." Soil Dynamics and Earthquake Engineering, 27(12), 1043–1055.

Cruden, D. M and Varnes, D. J. (1996). Landslides: investigation and mitigation. Chapter 3-Landslide types and processes. Transportation research board special report, (247).

CSA S16-19. (2019). Design of steel structures.

CSA O86-14. (2014). Engineering design in wood.

CSA S157-17. (2017). Strength design in aluminum. Canadian Standards Association (CSA).

CSA Z662. (2019). Oil and gas pipeline systems. Sixth Edition; Update No 1; January 2019.

D. Hibbitt, B. Karlsson, and P. Sorensen. (2014). ABAQUS Standard User's and Reference Manuals. Version 6.14.

D. Negussey. (2006). "Modulus of Subgrade Reaction For EPS Geofoam."

David Saftner, Carlos Carranza-Torres, and Mitchell Nelson. (2017). Slope Stabilization Guide for Minnesota Local Government Engineers. Manual, Minnesota Local Road Research Board Minnesota Department of Transportation, 18.

DNV-OS-F101. 2010. Submarine pipeline systems. Det Norske Veritas, DNV, Oslo, Norway.

EGIG. 2013. 9th Report of the European Gas Pipeline Incident Data Group.

Enbridge. 2013. Addendum to Enbridge's 2013 Corporate Social Responsibility Report (with a focus on 2013 data).

EPS Industry Alliance. 2012. Innovative Applications of EPS Geofoam. https://www.epsindustry.org/.

Farhadi, B., and Wong, R.C.K. 2014. Numerical Modeling of Pipe-Soil Interaction Under Transverse Direction. In Volume 1: Design and Construction; Environment; Pipeline Automation

and Measurement. American Society of Mechanical Engineers, Calgary, Alberta, Canada. p. V001T03A021.

Fathi, A., and Cheng, J.J.R. 2011. Effect of Cross-sectional Strain Distribution on the Critical Buckling Strain of Energy Pipelines. : 7.

Fathi, A., Ndubuaku, O., and Adeeb, S. 2018. Using Controlled Global Buckling to Improve Buried Pipelines Performance Under Large Compressive Ground Displacements. In Volume 2: Pipeline Safety Management Systems; Project Management, Design, Construction, and Environmental Issues; Strain Based Design; Risk and Reliability; Northern Offshore and Production Pipelines. American Society of Mechanical Engineers, Calgary, Alberta, Canada. p. V002T06A010.

Ferreira, N.J. 2016. Risk to Buried Gas Pipelines in Landslide Areas.

Government of Canada. 2018. Statistical summary: Pipeline transportation occurrences in 2018.

Gioielli, P.C., Minnaar, K., Macia, M.L., and Kan, W.C. 2007. Large-Scale Testing Methodology to Measure the Influence of Pressure on Tensile Strain Capacity of a Pipeline. : 5.

Gresnigt, A. M. 1986. Plastic design of buried steel pipelines in settlement areas. Heron (Delft), 31(4), 1-113.,.

Han, B., Wang, Z., Zhao, H., Jing, H., and Wu, Z. 2012. Strain-based design for buried pipelines subjected to landslides. Petroleum Science, **9**(2): 236–241. doi:10.1007/s12182-012-0204-y.

Hazarika, H. 2006. Stress–strain modeling of EPS geofoam for large-strain applications. Geotextiles and Geomembranes, **24**(2): 79–90. doi:10.1016/j.geotexmem.2005.11.003.

Highland, L., & Bobrowsky, P. T. 2008. The landslide handbook: a guide to understanding landslides (p. 129). Reston: US Geological Survey.

Honegger, D.G., Hart, J.D., Phillips, R., Popelar, C., and Gailing, R.W. 2010. Recent PRCI Guidelines for Pipelines Exposed to Landslide and Ground Subsidence Hazards. In 2010 8th International Pipeline Conference, Volume 2. ASMEDC, Calgary, Alberta, Canada. pp. 71–80.

Horvath, J. 1997. The compressible inclusion function of EPS geofoam. Geotextiles and Geomembranes, **15**(1–3): 77–120. doi:10.1016/S0266-1144(97)00008-3.

Ilozumba, E, Imanpour, A., Adeeb, S., and Fathi A. (2021). “Novel Remediation For Buried Pipelines Underground Deformation: Cross-Sectional Testing And Analytical Approach.” Journal of Pipeline Systems - Engineering and Practice.

Kan, W.C., Weir, M., Zhang, M.M., Lillig, D.B., Barbas, S.T., Macia, M.L., and Biery, N.E. 2018. Strain-Based Pipelines: Design Consideration Overview. In The Eighteenth International Offshore and Polar engineering Conference. International Society of Offshore and Polar Engineers.,.

Karamitros, D.K., Bouckovalas, G.D., and Kouretzis, G.P. 2007. Stress analysis of buried steel pipelines at strike-slip fault crossings. Soil Dynamics and Earthquake Engineering, **27**(3): 200–211. doi:10.1016/j.soildyn.2006.08.001.

Kennedy, R. P., Chow, A. M, and Williamson, R. A. 1977. Fault movement effects on a buried oil pipeline. Transportation engineering journal of the American Society of Civil Engineers, 103(5), 617-633.

Koji Yoshizaki and Takashi Sakanoue. 2003. Experimental study on Soil-Pipeline Interaction Using EPS Backfill. Pipelines 2003, ASCE, Baltimore, MD, 1126-1134,.

Lam, C. 2015. Statistical analyses of historical pipeline incident data with application to the risk assessment of onshore natural gas transmission pipelines.

Lee, K.,. 2012. presentation at API-AGA Joint Committee meeting on Oil & Gas Pipeline Welding Practices.

Leinala, T. J. 1999. Computer modelling of landslides. Doctoral dissertation, University of toronto.

Lingwall, B., and Bartlett, S. 2014. Full-Scale Testing of an EPS Geofoam Cover System to Protect Pipelines at Locations of Lateral Soil Displacement. In Pipelines 2014. American Society of Civil Engineers, Portland, Oregon. pp. 605–615.

Lingwall, B.N. 2011. Development of an expanded polystyrene geofoam cover system for pipelines at fault crossings. dissertation, The University of Utah.

Liu, B., Liu, X.J., and Zhang, H. 2009. Strain-based design criteria of pipelines. Journal of Loss Prevention in the Process Industries, **22**(6): 884–888. doi:10.1016/j.jlp.2009.07.010.

Liu, M., Wang, Y.-Y., and Yu, Z. 2008. Response of Pipelines Under Fault Crossing. : 4.

Lockey, A., and Young, A. 2012. Predicting Pipeline Performance in Geohazard Areas Using ILI Mapping Techniques. In Volume 2: Pipeline Integrity Management. American Society of Mechanical Engineers, Calgary, Alberta, Canada. pp. 491–499.

Macia, M.L., Kibey, S.A., Arslan, H., Bardi, F., Ford, S.J., Kan, W.C., Cook, M.F., and Newbury, B. 2010. Approaches to Qualify Strain-Based Design Pipelines. In 2010 8th International Pipeline Conference, Volume 4. ASMEDC, Calgary, Alberta, Canada. pp. 365–374.

Mahdavi, H., Kenny, S., Phillips, R., and Popescu, R. 2008. Influence of Geotechnical Loads on Local Buckling Behavior of Buried Pipelines. In 2008 7th International Pipeline Conference, Volume 3. ASME, Calgary, Alberta, Canada. pp. 543–551.

MacPherson, A. 2016. July pipeline spill near North Battleford caused by "ground movement," says Husky Energy in report. thestarphoenix,.

Mahdavi, H., Kenny, S., Phillips, R., and Popescu, R. 2008. Influence of Geotechnical Loads on Local Buckling Behavior of Buried Pipelines. In 2008 7th International Pipeline Conference, Volume 3. ASME, Calgary, Alberta, Canada. pp. 543–551.

Melissianos, V.E., Lignos, X.A., Bachas, K.K., and Gantes, C.J. 2017. Experimental investigation of pipes with flexible joints under fault rupture. Journal of Constructional Steel Research, **128**: 633–648. doi:10.1016/j.jcsr.2016.09.026.

Moghaddas Tafreshi, S. N., and Khalaj, O. (2008). "Laboratory tests of small-diameter HDPE pipes buried in reinforced sand under repeated-load." Geotextiles and Geomembranes, 26(2), 145–163.

Mokhtari, M., and Nia, A.A. 2014. Using FRP Wraps to Reinforce Buried Steel Pipelines Subjected to Permanent Ground Deformations: A Feasibility Study. In Volume 1: Design and Construction; Environment; Pipeline Automation and Measurement. American Society of Mechanical Engineers, Calgary, Alberta, Canada. p. V001T03A028.

Ndubuaku, O. H. (2019). "A New Material Characterization Approach for Evaluating the Deformational Capacity of Onshore Pipelines." ERA, <http://era.library.ualberta.ca/items/994bee38-1fb3-4b1c-8117-b3cf3820cb2b> (Apr. 9, 2021).

Ndubuaku, O., Martens, M., Cheng, J., and Adeeb, S. (2019). "Integrating the Shape Constants of a Novel Material Stress-Strain Characterization Model for Parametric Numerical Analysis of the Deformational Capacity of High-Strength X80-Grade Steel Pipelines." Applied Sciences, 9(2), 322.

NEB. (2011). Focus On 2000-2009 Safety And Environment. National Energy Board.

Newmark, N. M and Hall, W. J. 1975. Pipeline design to resist large fault displacement.pdf. In Proceedings of US national conference on earthquake engineering (Vol. 1975, pp. 416-425,.

Nyman, D. J., Cluff, L. S., and W. J.,. 2006. Observations and lessons learned from three decades of seismic hazard mitigation for major oil and gas pipeline projects. In Proceedings of 8th US National Conference on Earthquake Engineering, San Francisco. Earthquake Engineering Research Institute, EERI, Oakland.

O'Rourke, M. J and Liu, X. 1999. Response of buried pipelines subject to earthquake effects. (p. 260). New York: Mceer.,.

Palmeira, E. M., and Andrade, H. K. P. A. (2010). "Protection of buried pipes against accidental damage using geosynthetics." Geosynthetics International, 17(4), 228–241.

Paulin, M. J. (1998). "An investigation into pipelines subjected to lateral soil loading (Doctoral dissertation, Memorial University of Newfoundland)."

Ramberg W and Osgood W. (1943). “Description of Stress-Strain Curves by Three Parameters.” Technical Note, No. 902, National Advisory Committee for Aeronautics, 28p.

Rofooei, F. R., Jalali, H. H., Attari, N. K. A., and Alavi, M. (2012). “Full-Scale Laboratory Testing of Buried Pipelines Subjected to Permanent Ground Displacement Caused by Reverse Faulting.” 10.

Rukovansky, M., Greenwood, J.H., and Major, G. 1985. Maintaining a Natural Gas Pipeline in Active Landslides. ASCE. pp. 438–448.

S. A. Karamanos, A. M. Gresnigt, and E. Dama. 2007. Failure of Locally Buckled Pipelines. J. Press. Vessel Technol. 129 (2007) 272. doi:10.1115/1.2716431.,.

S. Horvath, D. Stark, and D Arellano. 2004. Geofoam Applications in the Design and Construction of Highway Embankments. Transportation Research Board, Washington, D.C.

Sancio, R.B., Rice, A.H., Audibert, J., Morgan, D., and Rattray, J. 2020. Guidelines for managing geohazards affecting the engineering and construction of new oil and natural gas pipelines. In Pipeline Integrity Management Under Geohazard Conditions (PIMG). Edited by M.M. Salama, Y.-Y. Wang, D. West, A. Mckenzie-Johnson, A. B A-Rahman, G. Wu, J.P. Tronskar, J. Hart, and B.J. Leira. ASME Press. p. 0.

Sheeley, M., Negussey, D., Assistant, R., Center, G. R., and University, S. (2001). “An Investigation of Geofoam Interface Strength Behavior.” 12.

Sim, W. W., Towhata, I., Yamada, S., and Moinet, G. J.-M. (2012). “Shaking table tests modelling small diameter pipes crossing a vertical fault.” Soil Dynamics and Earthquake Engineering, 35, 59–71.

Surya. (2020). Manufacturer’s test certificate. Surya Roshni Limited.

Varnes, D. J. 1978. Slope movement types and processes. Special report. Special report, 176, 11-33.

Timoshenko, Stephen P. and James M. Gere. (2009). Theory of elastic stability. Courier Corporation.

Trautmann, C. H., and O’Rourke, T. D. (1985). “Lateral Force-Displacement Response of Buried Pipe.” Journal of Geotechnical Engineering, 111(9), 1077–1092.

Varnes, D. J. (1978). Slope movement types and processes. Special report. Special report, 176, 11-33.

Vazouras, P., Karamanos, S. A., and Dakoulas, P. (2012). “Mechanical behavior of buried steel pipes crossing active strike-slip faults.” Soil Dynamics and Earthquake Engineering, 41, 164–180.

Wang, L.R.-L., and Yeh, Y.-H. 1985. A refined seismic analysis and design of buried pipeline for fault movement. Earthquake Engineering & Structural Dynamics, **13**(1): 75–96. doi:10.1002/eqe.4290130109.

Wang, X., Shuai, J., Ye, Y., and Zuo, S. 2008. Investigating the Effects of Mining Subsidence on Buried Pipeline Using Finite Element Modeling. In 2008 7th International Pipeline Conference, Volume 3. ASME, Calgary, Alberta, Canada. pp. 601–606.

Wang, Y.-Y., Liu, M., Horsley, D., Salama, M., and Sen, M. 2014. Overall Framework of Strain-Based Design and Assessment of Pipelines. In Volume 4: Production Pipelines and Flowlines; Project Management; Facilities Integrity Management; Operations and Maintenance; Pipelining in Northern and Offshore Environments; Strain-Based Design; Standards and Regulations. American Society of Mechanical Engineers, Calgary, Alberta, Canada. p. V004T11A023.

West, D. O., M. M. Salama, Y.-Y. Wang, and McKenzie-Johnson. 2020. Ground movement hazards (landslides, subsidence) and pipelines: an overview. Pipeline Integrity Management Under Geohazard Conditions (PIMG) (p. 0). ASME Press.

West, D.O. 2020. Ground movement hazards (landslides, subsidence) and pipelines: an overview. In Pipeline Integrity Management Under Geohazard Conditions (PIMG). Edited by M.M. Salama, Y.-Y. Wang, D. West, A. McKenzie-Johnson, A. B A-Rahman, G. Wu, J.P. Tronskar, J. Hart, and B.J. Leira. ASME Press. p. 0.

Yong-Yi Wang, Bo Wang, and Kunal Kotian. 2017. Management of Ground Movement Hazards for Pipelines. final Report,Center for Reliable Energy Systems,.

Yong-Yi Wang, Bo Wang, and Kunal Kotian. 2017. Management of Ground Movement Hazards for Pipelines. Center for Reliable Energy Systems (CRES).

Zhang, S.-Z., Li, S.-Y., Chen, S.-N., Wu, Z.-Z., Wang, R.-J., and Duo, Y.-Q. 2017. Stress analysis on large-diameter buried gas pipelines under catastrophic landslides. Petroleum Science, **14**(3): 579–585. doi:10.1007/s12182-017-0177-y.

Zhao, L., Cui, C., and Li, X. 2010. Response analysis of buried pipelines crossing fault due to overlying soil rupture. Earthquake Science, **23**(1): 111–116. doi:10.1007/s11589-009-0072-8.